

UC Berkeley

UC Berkeley Electronic Theses and Dissertations

Title

Development of a Breast Cancer Stem Cell Model and the Inhibitory Regulation of Small Molecule Phytochemicals on Various Stages of Human Breast Cancer Cells

Permalink

<https://escholarship.org/uc/item/0fw3v9x3>

Author

Tin, Antony Shen

Publication Date

2013

Peer reviewed|Thesis/dissertation

**Development of a Breast Cancer Stem Cell Model and the
Inhibitory Regulation of Small Molecule Phytochemicals
on Various Stages of Human Breast Cancer Cells**

By

Antony S. Tin II

A dissertation submitted in partial satisfaction of the
Requirements for the degree of

Doctor of Philosophy

In

Endocrinology

In the

Graduate Division

Of the

University of California, Berkeley

Committee in charge:

Professor Gary L. Firestone, Chair
Professor Jen-Chywan (Wally) Wang
Professor Iswar K. Hariharan

Spring 2013

ABSTRACT

Development of a Breast Cancer Stem Cell Model and the Inhibitory Regulation of Small Molecule Phytochemicals on Various Stages of Human Breast Cancer Cells

By

Antony S. Tin II

Doctor of Philosophy in Endocrinology

University of California, Berkeley

Professor Gary L Firestone, Chair

The development of clinical breast cancer is a multistep process that manifests itself as a disease with various distinct phenotypes. At present, it is believed that a neoplastically-transformed cell undergoes many heterogeneous changes and mutations before evolving into a tumorous or invasive breast cancer. Due to the heterogeneity of breast cancer, a single therapeutic strategy is rarely completely effective for all patients. Current therapeutic options such as hormone antagonists, radiation and chemotherapy have many deleterious side effects which demonstrates a need for a more efficacious therapy alternative that can not only target varying phenotypes but also ameliorates harsh side effects. In addition, it is essential to identify compounds that can slow the promotion of the disease from preneoplastic lesions to invasive breast cancer. This thesis details the generation of a novel breast cancer stem cell model and the molecular mechanism of two small molecule phytochemicals, indole-3-carbinol (I3C), and artemisinin, target breast cancer stem cells and luminal A, estrogen sensitive breast cancer, respectively. We show that ectopic expression of HER2, a member of the epidermal growth factor receptor family, in MCF-10AT preneoplastic mammary epithelial cells induces a phenotype with the molecular markers of breast cancer stem cells expression: CD44⁺/CD24⁻/ALDH-1⁺ with highly expressing levels of stem cell marker, nucleostemin. These cells are capable of forming tumorspheres in 3-D cultures, indicative of a population highly enriched with stem cells. Furthermore, as few as 30,000 cells are able to form viable mammary tumors in athymic mouse xenograft models. In breast cancer stem cells, I3C induces apoptosis by selectively targeting nucleostemin and activating the p53 apoptotic pathway. I3C induces the proteolytic degradation of Akt1 and thereby functionally inactivates MDM2. Loss of MDM2 phosphorylation and its subsequent inactivation frees p53 to induce apoptosis. Coupled with the activation of nucleostemin by I3C, nucleostemin sequesters MDM2 away from p53 further enhancing the apoptotic effect. Knockdown of nucleostemin prevents the I3C apoptotic effects, suggesting the selective role of I3C on breast cancer stem cells. Also, expressing constitutively active Akt1 or a dominant negative form of p53 overrides the I3C induced apoptotic effect, highlighting the specific Akt1/MDM2/p53 pathway modulated by I3C. The preclinical results implicate I3C as a novel anti-cancer agent that can selectively

target cancer stem cells especially given that I3C also increases MDM2-nucleostemin interactions and can reduce tumors volumes *in vivo*. We also show that artemisinin, derived from the sweet wormwood, *Artemisia annua*, ablates key G1 cell cycle regulators to induce growth arrest in luminal A, estrogen sensitive breast cancer as well as inhibit *in vivo* xenograft growth in athymic mice. Artemisinin is selective towards malignant cells, such as the MCF-7 breast cancer cell line since it is ineffective in arresting growth in nontumorigenic breast cell lines. Artemisinin exposed MCF-7 cells displayed ablated levels of cyclin-dependent kinases 2 and 4 (CDK), cyclin E, cyclin D₁ as well as E2F1 at the protein and mRNA level. Promoter deletion mapping and subsequent chromatin immunoprecipitation analyses revealed that downregulation of E2F1 resulted in inhibition of CDK2 of promoter activity. Additionally, constitutive expression of E2F1 reversed the growth arrest, CDK2 and cyclin E downregulation induced by artemisinin.

ACKNOWLEDGEMENTS

I would like to thank Professor Gary Firestone for mentoring me on so many different levels throughout my tenure in graduate school. I will never forget that you took me in without hesitation after Professor Timiras passed away and willingly gave me a lab to call home. Gary, you have been more than a mentor to me, you have been a friend and a guide who has always encouraged me to think critically. You have provided me with the perfect balance of independence, while still given me direction and support. I am still learning valuable lessons from you about research and life and am looking forward to using all the skills you have taught me for the rest of academic and professional career. Thank you for always being there for me.

I would especially like to thank my loving family for always supporting me and being there through everything. Daddy, you have always encouraged me to pursue my dreams and have given me the world. You showed me the true meaning of life and exposed me to so many different things. I can honestly say you provided me with all the creature comforts in life. After all the talks and advice you have given me, I am just starting to appreciate and understand the meaning of it all. Mommy, there are no words to express how much I love you and just knowing how much you believe in me has helped me get to where I am today. Ever since I was a baby, you have taught me to stand up for myself and cared for me in a way nobody else ever could. I know you always put me first and I cannot begin to express the way I feel for your tireless efforts. Pearl, I want to especially thank you for always calling me and being there for me on a moments notice. You have been my emotional support and have given me so much perspective by teaching me the bigger picture in life. I cannot imagine having a better older sister knowing how you paved the way for me in all aspects of my life. I want to say thank you from the bottom of my heart and I cannot stop thinking about how you used to save me your notes from high school so I could use it two years later or making sure that I kept my social life in check during college and helping me in my professional life after graduate school. You are the strongest person I know and knowing that you are there for me helps me sleep at night. You truly are an amazing person and I will never forget that. Julia, I want to thank you for taking care of me and raising me as your own son. I will always be your son and will always remember all things you did when raising me to keep me happy like take me to IHOP on my birthday and making me cucumbers to eat and our walks at lake Chabot.

Shyam – I can't express how much I appreciate everything you have done for me. Without you, I literally would not know what to do. You gave me my projects that have led me to my thesis and PhD and it all started because of you. I know I will use all the skills you have taught me and despite the nonstop drama, I wanted to thank you for being the voice inside my head telling me what to do but also keeping me sane and motivated to work.

Kevin – You are the one that got me through grad school. I can never thank you enough for keeping me sane from team estrogen! I will never forget the time you helped me with all the PCRs right before the poster session or the crazy “adventures” at Granlibakken. It was great being with you in lab from the very start and you are one of the most thoughtful

people I know. I am so grateful to be able to call you my friend knowing you always have my back. I don't know what to do now that I am leaving and won't have you around to help me with all my math questions.

Kalvin – We started together and now we are ending together! You are my brother from another mother. After all those late nights complaining about the work Shyam put on us has finally paid off for the both of us. Thank you for all your help and tireless effort to make the Ishikawa and MCF-7 Art project come to fruition. You are truly an amazing person and I know that you will be rewarded in all your endeavors.

Anna – This is for you. You have been everything to me and to my life. I cannot imagine a world without you being there to support me mentally, emotionally, and physically. I will always think back to the first time I met you at USC and how I immediately knew that this would be the start of something epic. AT&T PARK. (ANNA TONY TIN PARK)! Without you, this thesis, my PhD would not be possible. You have played an integral part of my academic career and somehow everything always goes back to science. I will miss just getting a meal with you where we end up talking about the science behind every signaling pathway or how cells differentiate or what genes do what. I don't think anyone else knows me better than you and can relate to me the way you have. You really changed my life for the better and helped keep me motivated in all aspects of my life. Everything from exercising and doing a marathon and triathlon, to turning me into a kimchi connoisseur where I now love Korean food more than Chinese food...this would not have happened without you. You are the most amazing person that I have ever met and I want you to know that you are the smartest, most caring, and selfless person I know. I was so proud of you graduated with honors and then when you got accepted into graduate school. You are a winner and I know that you will succeed in anything you put your mind to and that your dedication and sincerity will get you very far in life. You deserve to have it all and I have no doubt that you will be rewarded for all your hard work. I want to thank you for staying by my side for so long and enduring all the late nights, inconsistencies, contradictions and difficulties that you handle with grace and poise.

In addition, I would also like to thank all the colleagues in the Firestone lab that has been some of my best of friends I have ever had. Besides all the help and input, you guys kept my life fun and I will never forget all our happy hour adventures and lunches. You were all sources of my inspiration.

This work is dedicated to my uncle

Pang Pen Sheng

From the fond memories of playing with you in the park and riding the steam trains or hiking up the mountain to watch the view, I am constantly thinking about you. I miss you so much. You raised me as your own son and the unconditional love and support will forever inspire me. Thank you for always believing in me and even now still watching over me.

TABLE OF CONTENTS

List of Figures	v
General Introduction	vii
<u>Chapter I</u>	
Development of a novel model system to study breast cancer stem cells.....	1
Abstract	2
Introduction.....	3
Materials and Methods.....	5
Results.....	7
Discussion.....	30
References.....	32
<u>Chapter II</u>	
Essential role of nucleostemin in indole-3-carbinol anti-proliferative targeting of breast cancer stem cells.....	35
Abstract.....	36
Introduction.....	37
Materials and Methods.....	39
Results.....	42
Discussion.....	78
References.....	80
<u>Chapter III</u>	
Artemisinin antiproliferative response in human breast cancer cells requires the down-regulated expression of the E2F1 transcription factor and loss of E2F1-target cell cycle genes.....	82
Abstract.....	83
Introduction.....	84
Materials and Methods.....	86
Results.....	90
Discussion.....	125
References.....	127
<u>Chapter IV</u>	
Conclusion and Future Directions.....	131
Conclusion and Future Directions.....	132

LIST OF FIGURES

General Introduction Figures

Figure 1:	Classical model of tumor progression.....	ix
Figure 2:	The cancer stem cell model.....	xii
Figure 3:	Phosphotyrosine interactome of the epidermal growth factor receptor kinase family.....	xvi
Figure 4:	The HER2 signaling pathway.....	xix
Figure 5:	Indole-3-Carbinol (I3C).....	xxii
Figure 6:	Postulated anticancer mechanism of action by artemisinin.....	xxvi

Chapter I Figures

Figure 7:	Characterization of CSC markers by HER2 overexpression in MCF-10AT cells.....	9
Figure 8:	Quantification of cell surface marker CD44 and CD24.....	12
Figure 9:	Quantification of ALDH-1 activity in 10AT-Her2 and 10AT-Neo cells.....	14
Figure 10:	Formation of tumorspheres by 10AT-Her2 cells <i>in vitro</i>	17
Figure 11:	Comparing 10AT-Her2 tumorsphere forming efficiency.....	29
Figure 12:	I3C inhibition of tumorsphere formation in 10AT-Her2 cells.....	22
Figure 13:	I3C and 1-benzyl-I3C selectively disrupts cancer stem cell tumorsphere formation	24
Figure 14:	Tumor-forming efficiency between 10AT-Her2 and 10AT-Neo cells	27
Figure 15:	I3C inhibition of 10AT-Her2 Tumor Xenografts.....	29

Chapter II Figures

Figure 16:	I3C inhibits 10AT-Her2 cell proliferation.....	44
Figure 17:	Flow cytometry analysis of the I3C induced apoptotic effects on 10AT-Her2 cells.....	46
Figure 18:	I3C induces PARP cleavage in 10AT-Her2 breast cancer stem cells.....	48
Figure 19:	I3C induced apoptotic response is mediated by p53.....	51
Figure 20:	I3C induces nucleostemin-mdm2 interactions in cancer stem cells.....	54
Figure 21:	I3C releases p53 from its E3 ligase, MDM2 in cancer stem cells.....	56
Figure 22:	I3C induced MDM2 translocation into the nucleus requires nucleostemin expression.....	59
Figure 23:	MDM2 translocates into the nucleus and colocalizes with nucleostemin foci upon I3C treatment.....	62
Figure 24:	Nucleostemin knockdown diminishes I3C induced release of p53 from MDM2.....	65
Figure 25:	Nucleostemin siRNA overrides the I3C induced apoptosis in cancer stem cells	67
Figure 26:	I3C downregulates Akt1 expression at the protein level	70

Figure 27:	I3C induces the ubiquitination and 26S proteasome degradation of Akt1.....	72
Figure 28:	Constitutively active Akt1 can partially override the I3C induced apoptotic response	75
Figure 29:	Constitutively active Akt1 alters I3C regulation on the molecular interactions between nucleostemin, MDM2, and p53.....	77

Chapter III Figures

Figure 30:	Artemisinin reduces MCF-7 cell number in culture.....	92
Figure 31:	Artemisinin inhibition of MCF-7 tumor xenografts.....	95
Figure 32:	Artemisinin induces a G1 cell cycle arrest in MCF-7 breast cancer Cells.....	98
Figure 33:	Dose response and time course of artemisinin induced G1 cell cycle arrest.....	100
Figure 34:	Flow cytometry analysis of artemisinin cell cycle effects in human breast cancer cell lines with distinct phenotypes.....	102
Figure 35:	Artemisinin ablates key G1 cell cycle regulators in a dose dependent manner	105
Figure 36:	Time dependent regulation of artemisinin on key G1 cell cycle regulators	108
Figure 37:	E2F1 protein downregulation by artemisinin occurs as early as 12 hours	110
Figure 38:	Artemisinin ablates transcript levels of G1 cell cycle regulators.....	113
Figure 39:	Artemisinin regulates CDK2 promoter activity.....	115
Figure 40:	Loss of the E2F1 signaling inhibits CDK2, Cyclin E, and E2F1 promoter activity	118
Figure 41:	Constitutive expression of E2F1 overrides artemisinin-mediated downregulation of cyclin E and CDK2.....	121
Figure 42:	Constitutive expression of E2F1 prevents artemisinin induced G1 cell cycle arrest	124

INTRODUCTION

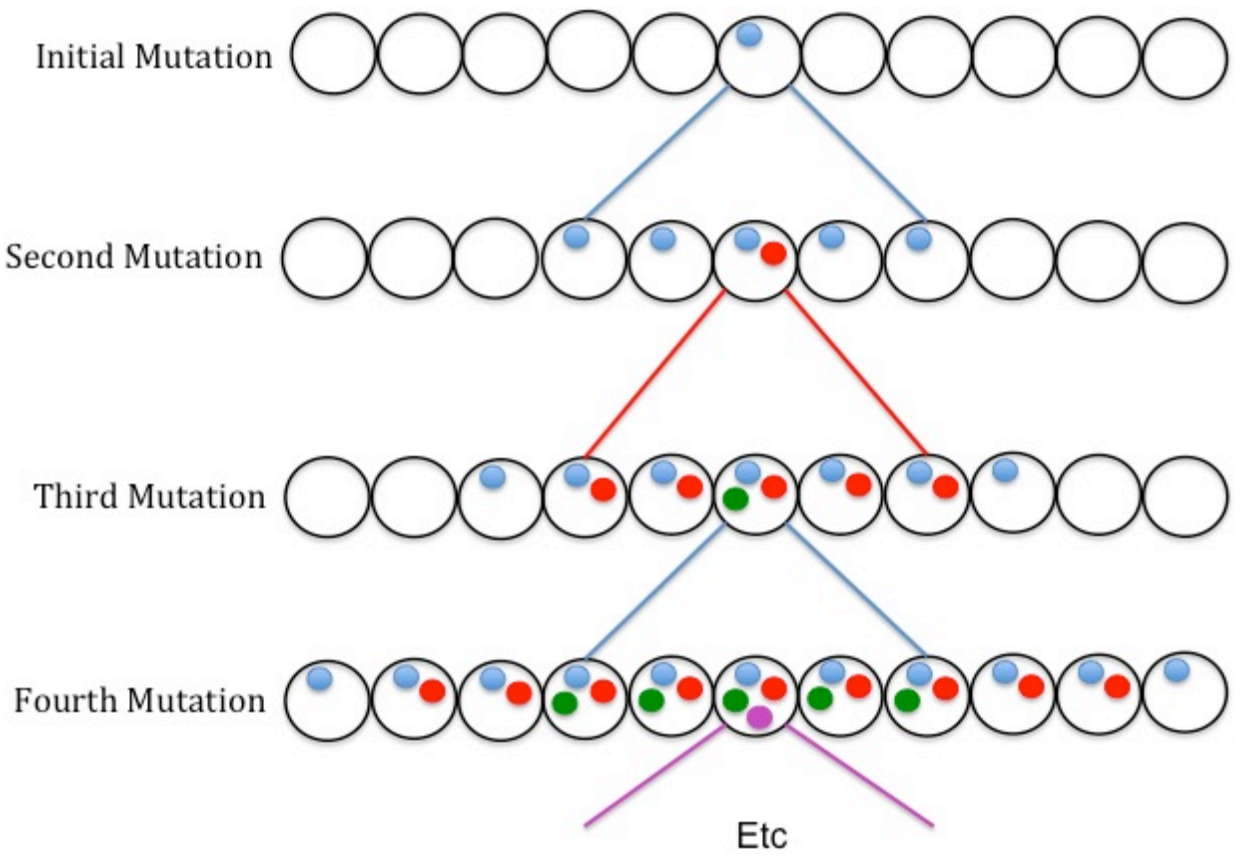
The Cancer Stem Cell Hypothesis

In the past decade, there has been a remarkable paradigm shift regarding the biological origins of cancer. The classical model of cancer is viewed as a multistep process and reflects numerous genetic modifications that drive the transformation of normal human cells into highly malignant tumors (1, 2). The prevailing hypothesis was that any cell that acquired multiple genetic mutations that conferred traits such as increased proliferative capacity and insensitivity of antigrowth signals could give rise to a tumor (Figure 1). Several lines of evidence support this notion where many types of cancers are diagnosed in an age-dependent incidence implicating four to seven rate-limiting events are necessary to drive tumorigenesis (3, 4). Furthermore, the cellular diversity of cancer has mostly been attributed to the genetic instability of its cells. As tumor cell populations grow, individual cells increasingly acquire random mutations, and their molecular fingerprint starts to diverge. By the time the tumor is detected, the cancer is heterogeneous and the millions of cells making up the cancer are distinctly different from one another (4).

Figure 1

Classical model of tumor progression.

Tumors arise as a result of multiple mutations acquired over time. With each successive mutation, the clonal population expands as it confers a proliferative advantage over neighboring cells. Mutations that inactivate inhibitory signals and upregulate proliferative inputs, allow the cells to invade and expand more rapidly compared to normal cells resulting in tumor formation.



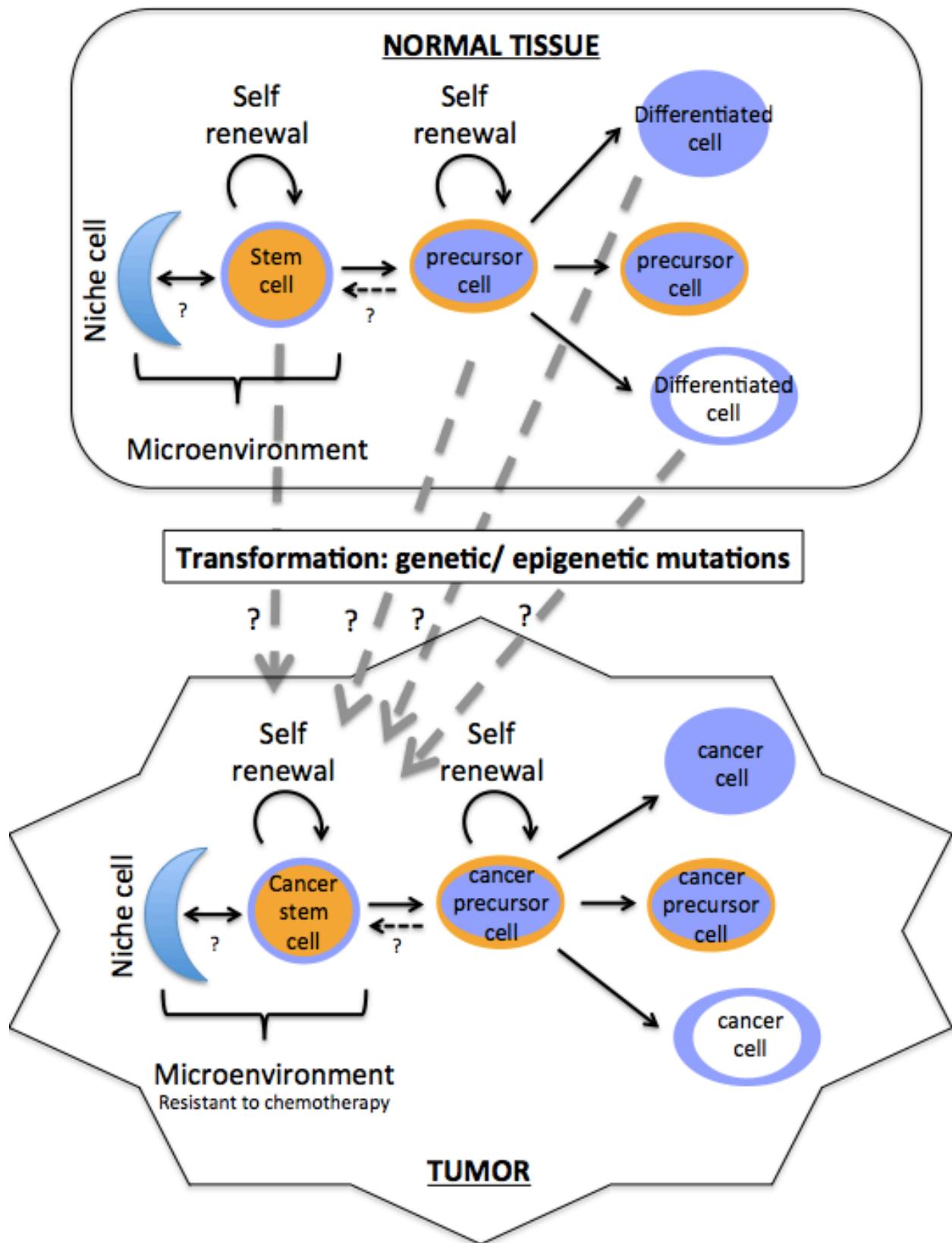
While the classic model of cancer biology has greatly progressed the understanding, diagnosing, and treating cancer, not all cancers types fit with its foundations of requiring multiple cellular mutations over time and in recent years a new model: the cancer stem cell hypothesis, has emerged (5). This new hypothesis is not mutually exclusive from the classical view of cancer initiation but it has challenged the very notions of tumorigenesis and its therapeutic implications. The cancer stem cell hypothesis posits that only a small subset of cells, termed tumor-initiating cells (TIC) or cancer stem cells (CSCs) is capable of giving rise to and maintaining tumors (6-8). Therefore all CSCs must display several characteristics: they must be capable of giving rise to a tumor, they must be capable of self renewal and maintain the population of tumorigenic cells, and they must be able to give rise to a heterogeneous population of cells composing of the entire tumor (Figure 2).

While, the basis of the cancer stem cell hypothesis has led to the recent scientific study and treatment of CSCs, the idea that cancer cells have properties reminiscent of stem cells is not a new theory. As early as the nineteenth century, Rudolph Virchow noted the similarities between fetal tissue and cancer cells with respect to their ability to proliferate and differentiate (9, 10). Although not necessarily derived from embryonic or adult stem cells, CSCs presumably result from result from a malignant transformation event that deregulates the self-renewal program of normal stem cells. Similarly, differentiated cells can under a transformative process acquiring the ability to self-renew. Further genetic or epigenetic alterations lead to CSCs, which retain key stem cell properties such as the ability to self renew, differentiate, and initiate carcinogenesis (11).

Figure 2

The cancer stem cell model.

Normal cells and tumors most likely consist of a small number of stem cells that can self-renew, have limitless replicative potential, and can give rise to differentiated cells. The cancer stem cell model postulates that tumors are organized in a cellular hierarchy with tumor-initiating cells, commonly known as cancer stem cells, at the apex.



In 1961, Southam and Brunschwig first demonstrated that individual cells within a tumor had differential tumor-forming ability. By harvesting recurrent cancer cells from patients and then autotransplanting the cells into different sites, they found that at least one million cells needed to be injected and this only worked at 50% efficiency. Later studies showed similar results for colony initiation *in vitro* (12, 13). This suggested that not all cancer cells could initiate a tumor and that tumors are organized in a cellular hierarchy with tumor-initiating cells at the apex.

Breast Cancer Stem Cells

Breast cancer is one of the most common malignancies in American women. Despite advances in early detection and adjuvant therapy, a substantial proportion of patients are diagnosed as advanced or metastatic disease at initial presentation or suffer a disease relapse (14, 15). Metastatic breast cancer is incurable and while chemotherapy obtains palliative effects, these effects are short lived in terms of overall survival. This therapeutic limitation is associated with intrinsic neoplastic heterogeneity (16). The identification of tumor heterogeneity has highlighted the need to appropriately define different phenotypes for individual patients to enable more tailored therapies. The molecular profiling studies in breast cancer divided it into six phenotypes: Luminal-A, Luminal-B, Basal-like, Normal-breast-like, HER2 enriched, and Claudin-low (17). These studies demonstrate that breast cancer is a heterogeneous disease with distinct morphology, responses to therapy, metastasis pattern, and patient prognosis. The cancer stem cell hypothesis could explain not only this tumor heterogeneity, but also the intrinsic or acquired resistance to conventional treatments in breast cancer, like radiation, chemotherapy, or hormone targeted therapies.

The cancer stem cell hypothesis proposes a model based on a hierarchical organization where neoplasia originates from the malignant transformation of adult stem cells through the deregulation of a normally tightly regulated self-renewal program. This model holds that a breast carcinoma may contain genetically and morphologically diverse populations of cells, including primitive stem cells, luminal or basal progenitor cells, also known as transient amplifying cells, and terminally differentiated cells. The isolation and characterization of CSCs remains a challenge, especially when dealing with breast CSCs. Cells defined by cell surface markers $CD44^{+}/CD24^{-}/lin^{-}$ represent a population of cells in human breast cancer that display cancer stem cell properties. As few as 200 $CD44^{+}/CD24^{-}/lin^{-}$ cells were able to form tumors in immunocompromised NOD/SCID mice. Breast CSCs also have the unique ability to survive and grow in serum-free, nonadherent conditions as suspension cultures, also referred to as tumorspheres. In contrast, differentiated tumor cells, which are anchorage-dependent and undergo anoikis in these conditions. Furthermore, aldehyde dehydrogenase 1 (ALDH-1), an enzyme involved in the intracellular oxidation of aldehydes for detoxification purposes, plays an early role in the differentiation of stem cells by oxidizing retinol into retinoic acid. Through an enzymatic ALDEFLUOR assay used to monitor ALDH-1 activity, ALDEFLUOR positive cells display CSC properties and are able to generate tumors in NOD/SCID mice. Utilizing cells testing positive by the three criteria: able to form suspensions in tumorspheres, have a $CD44^{+}/CD24^{-}/lin^{-}$, and ALDEFLUOR positive phenotype represents a population of cells highly enriched in breast cancer stem cells capable of initiating and maintaining tumors.

HER2 Receptor Signaling

The human epidermal growth factor receptor 2 (HER2 receptor) also known as Neu, Erb-B2, Cd340, or p185 is a receptor tyrosine kinase encoded by the ERBB2 gene. Her2 is a member of the epidermal growth factor receptor (EGFR/ErbB) family and is considered an orphan receptor because there is no known ligand and unlike the other members of the receptor family, the extracellular domain of HER2 remains constitutively in an activated conformation, ready for dimerization with other receptor family members. On the intracellular side, HER2 contains multiple interacting domains including: src homology 2 (SH2), phosphotyrosine-binding domain (PTB), src homology 2 domain containing (Shc), growth factor receptor-bound protein 2 (Grb2), protein-tyrosine phosphatase 2c (PtP-2c), and SH3 domain-binding glutamic acid-rich-like (SH3BGRL) (18). Interestingly, HER2 does not contain any PI3K-p85 interacting domains.

Given that the signaling function of the epidermal growth factor receptor family is triggered by the specificity of ligands for each receptor subtype, the potency of each signaling event is determined by positive and negative ligand effectors and the distinct combination of homo or hetero-dimeric partners. For example, a HER2 homodimers does not result in downstream signaling, while an activated HER2-HER3 heterodimer results in extensive transforming and mitogenic effects. Furthermore, each ligand plays an important role in determining which receptor combination dimerization occurs. HER2-HER4 heterodimerization can be enhanced by neuregulin-4 compared to EGF inducing HER2-HER3 or HER2-HER1 signaling. The various combinations of dimerization pairs as well as level of signal strength results in different receptor mediated events and ultimately different genetic and epigenetic outcomes (Figure 3).

Figure 3

Phosphotyrosine interactome of the epidermal growth factor receptor kinase family.

This figure is in reference to Schulze (2005). The kinase domain of the receptors is designated as an oval. Underlined and colored tyrosine residues mark identical sequence regions between different receptors; regions around colored residues show strong homology between receptors. Most interaction partners to tyrosine residues are found at the C-terminal end outside the kinase domain. HER2 has few interaction partners, of them Shc is the most common. The dimerization is indicated by HER1 dimer.

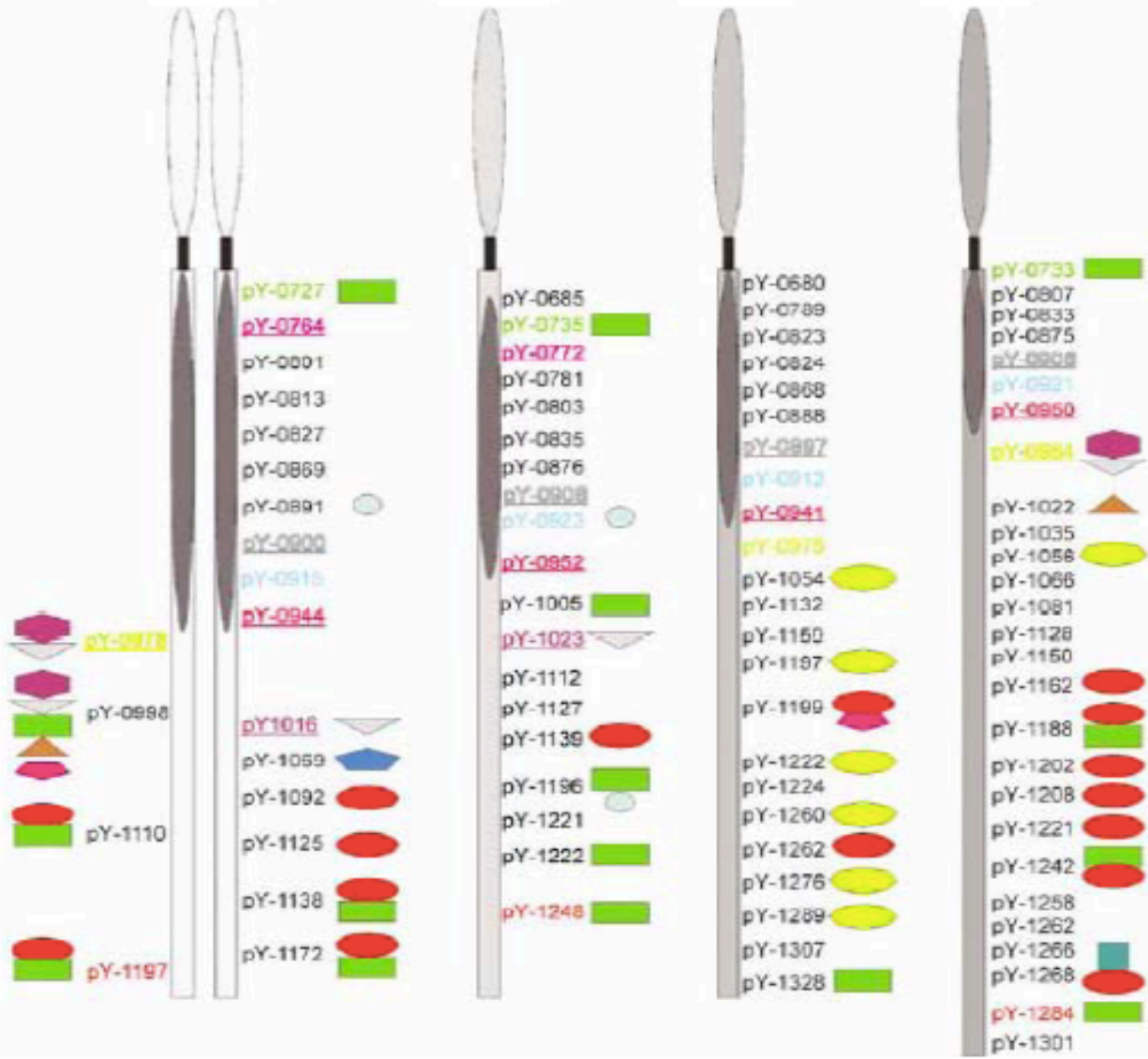


HER1

HER2

HER3

HER4



HER2 Receptor Signaling in Breast Cancer

The HER2 gene is amplified in 20-30% of all human breast cancers either through gene amplification or transcriptional deregulation and has been associated with aggressive metastatic disease (19). HER2 overexpressing breast cancers have a range of 25-50 copies of the HER2 gene and up to 40-1000 fold increase in HER2 protein expression resulting in up to 2 million receptors expressed at the tumor cell surface (20-23). The overexpression of HER2 in human mammary epithelial cells induces a proliferative advantage, transformed characteristics, tumorigenic growth, and antiapoptotic changes that mimic early stages of epithelial cell transformation (24). Its overexpression often results in spontaneous dimerization with other HER receptor family members leading to elevated or constitutively active downstream gene expression. Therefore, although HER2 amplified breast cancers appear to have a higher propensity for progression and worse prognosis compared with other breast cancer classified phenotypes, the amplification is an early event and defines a subtype of breast cancer not a later stage of it (25). Furthermore, gene expression profiling studies highlights that HER2 amplified breast cancers only maintain a unique molecular portrait and genetically represents a specific subset of the disease (15, 26).

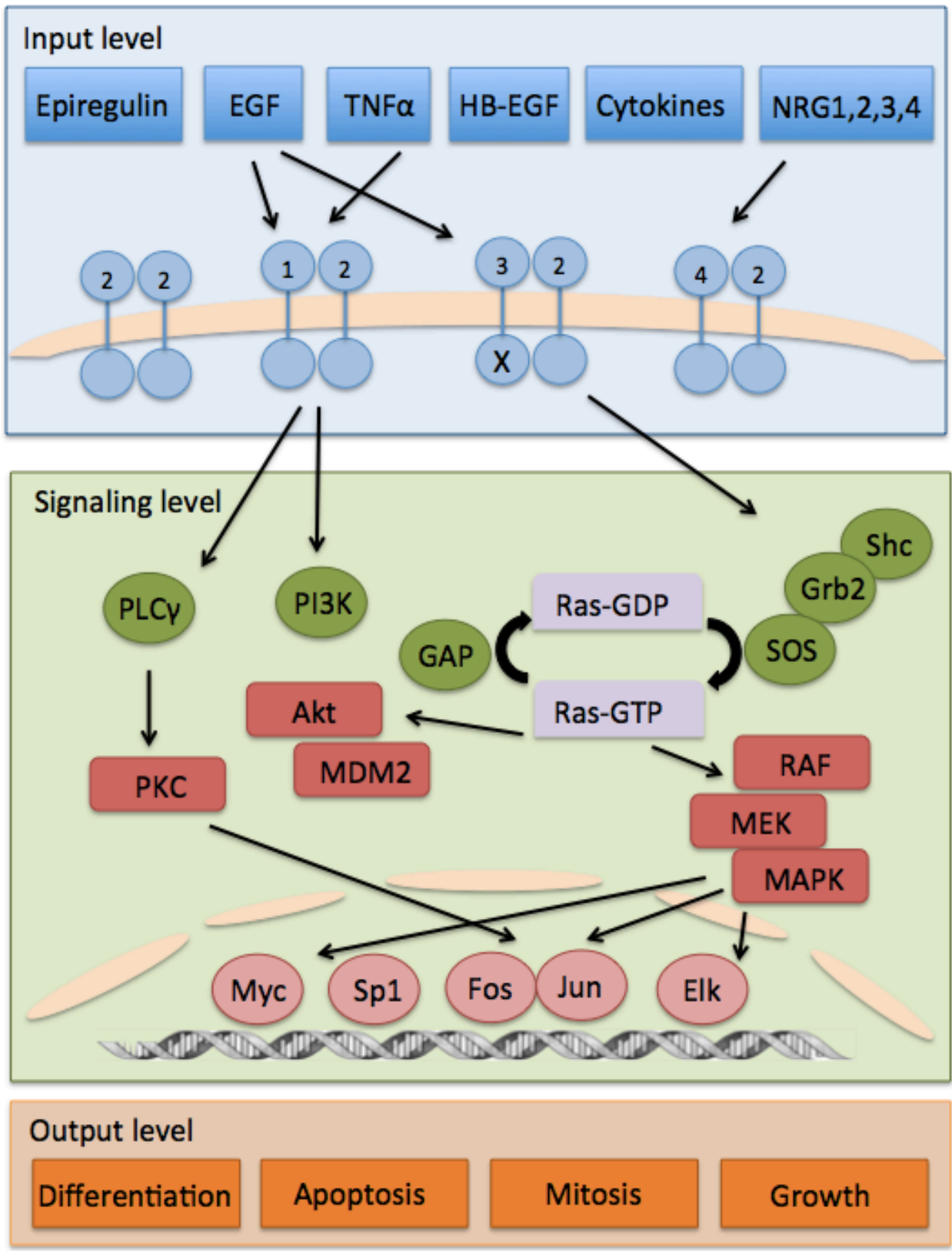
At the plasma membrane, overexpression of HER2 increases heterodimerization with HER1, HER3, and HER4. Overall, compared with other members of the HER family, HER2 is the least subject to inactivation and degradation (27). Upon forming heterodimerization signaling complexes, HER2 amplifies and prolongs signaling leading to genetic and epigenetic changes (Figure 4). Moreover, HER2 overexpression leads to significantly prolonged activation of downstream targets. For example, in cancer cells preferentially stimulated by HER2-HER1 heterodimers, MAPK and c-Jun activity increases dramatically (28). The unique cellular ramifications of HER2-HER3 heterodimers have been extensively studied and are well established. The main transformative effects of HER2 signaling is thought to be mediated by the cooperation with HER3 to the point where HER3 is often considered an obligate partner and necessary for HER2 induction of transformation (29, 30). The main contributing oncogenic pathway important in the HER2-HER3 heterodimer appears to be the activation of the phosphatidylinositol 3-kinase (PI3K)/ Akt pathway (29-31). While HER2 lacks binding sites necessary for the p85 subunit of PI3K to dock to the receptor, HER3 has seven specific phosphotyrosine motifs capable of PI3K binding (18). Growth factors and other ligands that activate the PI3K/Akt pathway by HER2 are mediated specifically through phosphorylation of HER3. Cell transformation by overexpressed HER2 is also associated with increased HER3 phosphorylation and activation of PI3K/Akt signaling.

At present, specifically targeting the HER2 receptor using antibodies such as Trastuzumab (Herceptin) has been an extremely effective initial treatment option for HER2 amplified breast cancers (32, 33). The efficiency of the HER2 targeted therapies may be explained by the role of HER2 in regulation of the cancer stem cell population (19, 20, 25). There is a significant correlation between expression of the stem cell marker ALDH-1 and HER2 (34, 35). Furthermore, HER2 overexpression in normal mammary epithelial cells or mammary carcinomas increases the proportion of stem cells and breast cancers with an increased proportion of CD44⁺/CD24⁻ cells.

Figure 4

The HER2 signaling pathway.

Various receptor ligands promote specific HER2 dimerization combinations. Except for HER2 homodimers, every other combination of HER2 dimerization results in specific signaling pathways to promote changes in gene transcription. As a result of distinct signaling and transcriptional changes, various outputs often promote growth and proliferation while preventing apoptosis and death.



Indole-3-carbinol and Breast Cancer








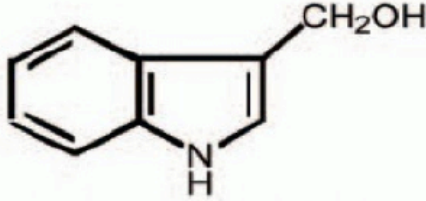






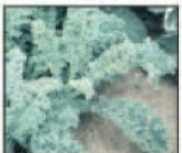

Indole-3-Carbinol (I3C) is a phytochemical found naturally in cruciferous vegetables of the brassica family such as kimchi, bok choy, broccoli, and brussel sprouts (Figure 6) (36). I3C is a promising chemo-preventative that growth arrests a variety of breast cancer and immortalized breast epithelial cells in culture (37). I3C has also been shown to be effective in preventing formation of many chemical carcinogen and virally induced cancers in other organs (38). Epidemiological evidence has shown that Asian diets where cruciferous vegetables intake is increased has decreased reproductive cancer incidence. This specific class of vegetable is very high in glucosinolates, a precursor to I3C.

When ingested, most of the I3C is converted by the stomach acid to a dimer, 3,3' Diindolylmethane (DIM) and other dimers and trimers. Both I3C and DIM cause growth arrest of various breast cancer cell lines, however, they have also been shown to have distinct effects in these cell lines (38). For instance, although both I3C and DIM induce a G1 cell cycle arrest, only I3C has been shown to transcriptionally downregulate cyclin dependent kinase 6 (CDK6) through modulation of specificity protein 1 (Sp1) activity in the luminal A subtype, estrogen sensitive MCF-7 breast cancer cell line (38). In vivo, I3C and DIM have both been shown to decrease the incidence and multiplicity of chemically induced breast cancers in mice and rats suggesting that I3C and DIM decrease proliferation and hence slow down the promotion of preneoplastic mammary cells to invasive mammary cancers in these animals (39).

Figure 5

Indole-3-Carbinol (I3C).

This figure is in reference to Aggarwal and Ichikawa (2005). I3C is produce by members of the family Cruciferae, and particularly members of the genus Brassica.

					
Watercress	Arugula	Kohlrabi	Rutabaga/Turnips	Daikon	Radishes
			 Indole-3-carbinol		
Cauliflower			<i>Indole-3-carbinol</i>		Chinese cabbage
					
Broccoli					Cabbage
					
Pok choy	Collard greens	Mustard greens	Kale	Brussels sprouts	

In addition to an overall effect of growth, I3C is able to specifically target key molecular markers in various types of breast cancer models. In MCF-7 breast cancer cells which represent a luminal A, estrogen sensitive breast cancer, I3C strongly downregulates transcript expression of the catalytic subunit in the human telomerase (hTERT) gene through inhibition of estrogen receptor alpha (ER α) (40). With regards to in estrogen responsive breast cancer, I3C is a potent inhibitor of ER α . By targeting aryl hydrocarbon receptor (AhR) I3C initiates the proteosomal degradation of ER α . Furthermore, I3C disrupts endogenous GATA3 transcription factor signaling from interacting with the ER α promoter further preventing transcription of the ER α gene (41). Given all the target genes of ER α , the inhibition of ER α signaling by I3C disrupts multiple proliferative pathways. One well-characterized downstream target of ER α , inhibited by I3C is Insulin-like Growth Factor Receptor-1 (IGF1R) and Insulin Receptor Substrate-1 (IRS1). I3C prevents binding of endogenous ER α to the ERE-Sp1 composite element within the promoter of IGF1R and IRS1. Thus as a result of the loss of ER α , multiple growth and proliferative signaling pathways are attenuated leading to the arrest or apoptosis of human breast cancer cells.

While ER α signaling and estrogen sensitivity is important in breast cancer given that 50-70% of all breast cancers begin as hormone responsive cancer, there is still a major class of breast cancers that do not respond to estrogen signaling (42, 43). I3C has been shown to growth arrest breast cancers that are unresponsive to estrogen signaling suggesting there are alternative pathways that are ER α independent sensitive to I3C. For example, in the MBA-MB-231 breast cancer cells that represent a triple negative, basal-like phenotype, I3C is able to induce a G1 cell cycle arrest and apoptosis in a process completely independent of ER α signaling. I3C has been shown to directly bind to the carboxyterminal domain and inhibit human neutrophil elastase (44). Elastase is the only direct target protein of I3C known to date. The binding of I3C leads to the inhibition of the elastase's intrinsic proteolytic activity and prevents the cleavage and processing of its target substrates such as CD40, a member of the tumor necrosis factor (TNF) receptor superfamily. In human breast cancers CD40 is often associated with TNF receptor-associated factors (TRAFs) and by inhibiting CD40 processing, the equilibrium of TRAFs associated with CD40 ultimately resulting in disruption of nuclear factor kappa-light-chain-enhancer of activated B cells (NF κ B) (45). Given that elastase is the only known direct target of I3C, it would suggest all antiproliferative I3C responses are mediated through the elastase pathway however, other direct I3C target proteins remains to be seen.

Preclinical testing of I3C against many breast cancer model systems has made it an attractive anticancer agent. At present I3C utilization is limited because specific prognostic biomarkers predictive for I3C responsive breast cancer is not well established. Despite this, a promising therapeutic strategy for I3C may be the use to prevent the invasion and metastasis of patients already diagnosed with breast. Regardless of the breast cancer subtype, I3C has been shown to regulate migration and metastasis by preventing an epithelial-to-mesenchymal transition (EMT). I3C has been shown to decrease expression of focal adhesion kinase (FAK), matrix metalloproteinase (MMP)-2 and -9 activity (46) in both hormone responsive and hormone unresponsive breast cancers. This suggests that besides selectively targeting breast cancer subtypes, I3C may also be a potent inhibitor preventing the spread and metastasis of human breast cancer to distant sites.

Artemisinin in Cancer

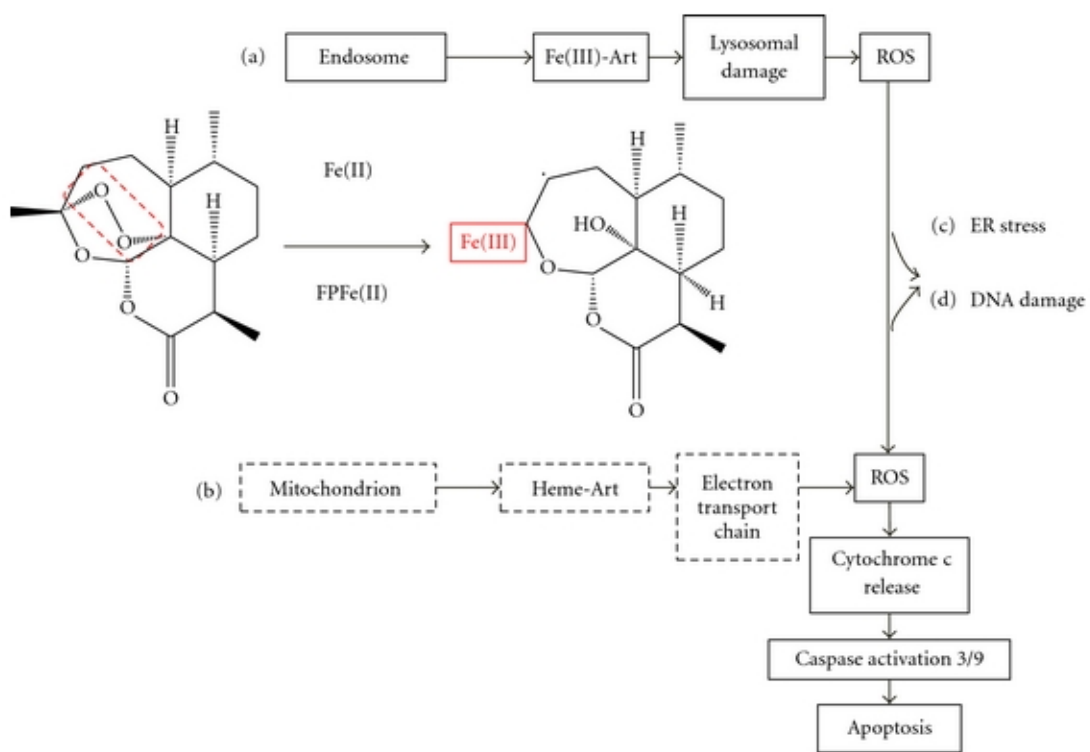
Artemisinin is a sesquiterpene lactone that was isolated from *Artemisia annua* (more commonly known as qinghaosu or sweet wormwood). Chinese medical practitioners have used artemisinin from plant extracts for over two thousand years to treat a variety of conditions such as fever and hemorrhoids and in the 1970s Chinese chemists isolated the compound and its derivatives as an effective treatment for malaria (47, 48). Nanomolar concentrations of artemisinin has been shown to be effective in killing malarial parasites, compared to mammalian cells where cytotoxic effects are observed in the micromolar range. In malaria, the cytotoxic effects of artemisinin are activated by the intraparacitic heme-iron, which catalyzes the endoperoxide bridge cleavage (47). The breakage of the endoperoxide bridge leads to release of hydroxyl free radicals and superoxide anions (47). These free radicals are able to damage food vacuole membranes and lead to autolysis of the malaria parasite (49, 50).

Cancer cells undergoing excessive proliferation often express elevated levels of the transferrin receptor, which is involved in iron transport. The levels of iron in these cancer cells are often significantly higher compared to normal cells (50). For example, breast cancer cells can have up to 15 times more iron than normal breast tissue (51). The excess iron creates an ideal environment for artemisinin to elicit the cytotoxic effects. This suggests that the toxicity of artemisinin may be selective and more effective in killing cancer cells (52) (Figure 6).

Figure 6

Postulated anticancer mechanism of action by artemisinin.

This figure is in reference to Crespo-Ortiz and Wei (2012). It has been postulated that bioactivation of artemisinin occurs in the endosome after pH-induced release of iron from internalized transferrin. Iron activated-artemisinin generates carbon-centered radicals that may mediate lysosomal disruption and generation of ROS resulting in mitochondrial damage, activation of caspases, and cell death. (b) Alternatively, it has been suggested that only specific activation of artemisinin by heme or heme-bound protein generates cytotoxic-carbon-centered radicals. In the mitochondrion, these adducts interfere with the electron transfer chain (ETC) by interacting with heme or heme-bound proteins leading to generation of ROS and apoptosis. (c) ROS harboring may induce ER stress and (d) genotoxicity.



While artemisinin may have some cytotoxic effects against cancer through free radical formation much in the same antimalarial mechanism postulated, in many reproductive cancer types artemisinin has been shown to selectively target cell cycle regulatory components to induce antiproliferative effects. This suggests that artemisinin may not just indiscriminately target iron reactive cells, but also selectively has intrinsic anticancer properties. In prostate and endometrial cancer cells, artemisinin has been shown to strongly inhibit cyclin dependent kinase 2 and 4 (CDK2 and CDK4) promoter activity (53). Furthermore, artemisinin selectively alters transcription factor activation and regulation such as Sp1, NFκB, and E2 transcription factor (E2F). While the direct mechanism of action of artemisinin remains unknown, given its ability to target so many different transcription factors regulating growth and proliferation, artemisinin may prove to be a potent anticancer agent.

REFERENCES

1. Hanahan D & Weinberg RA (2000) The hallmarks of cancer. *Cell* 100(1):57-70.
2. Hanahan D & Weinberg RA (2011) Hallmarks of cancer: the next generation. *Cell* 144(5):646-674.
3. Knudson AG, Jr. (1971) Mutation and cancer: statistical study of retinoblastoma. *Proceedings of the National Academy of Sciences of the United States of America* 68(4):820-823.
4. Nordling CO (1953) A new theory on cancer-inducing mechanism. *British journal of cancer* 7(1):68-72.
5. Wicha MS, Liu S, & Dontu G (2006) Cancer stem cells: an old idea--a paradigm shift. *Cancer research* 66(4):1883-1890; discussion 1895-1886.
6. Lawson JC, Blatch GL, & Edkins AL (2009) Cancer stem cells in breast cancer and metastasis. *Breast cancer research and treatment* 118(2):241-254.
7. Zhou BB, *et al.* (2009) Tumour-initiating cells: challenges and opportunities for anticancer drug discovery. *Nature reviews. Drug discovery* 8(10):806-823.
8. Pfeiffer MJ & Schalken JA (2010) Stem cell characteristics in prostate cancer cell lines. *European urology* 57(2):246-254.
9. Bignold LP, Coghlan BL, & Jersmann HP (2006) Hansemann, Boveri, chromosomes and the gametogenesis-related theories of tumours. *Cell biology international* 30(7):640-644.
10. Huntly BJ & Gilliland DG (2005) Leukaemia stem cells and the evolution of cancer-stem-cell research. *Nature reviews. Cancer* 5(4):311-321.
11. Charafe-Jauffret E, Ginestier C, & Birnbaum D (2009) Breast cancer stem cells: tools and models to rely on. *BMC cancer* 9:202.
12. Babcock VI & Southam CM (1961) Transplantable renal tumor of the rat. *Cancer research* 21:130-131.
13. Southam CM (1961) Applications of immunology to clinical cancer. Past attempts and future possibilities. *Cancer research* 21:1302-1316.
14. Cianfrocca M & Gradishar W (2009) New molecular classifications of breast cancer. *CA: a cancer journal for clinicians* 59(5):303-313.
15. Perou CM, *et al.* (2000) Molecular portraits of human breast tumours. *Nature* 406(6797):747-752.
16. Lu J, *et al.* (2009) Breast cancer metastasis: challenges and opportunities. *Cancer research* 69(12):4951-4953.
17. Prat A & Perou CM (2011) Deconstructing the molecular portraits of breast cancer. *Molecular oncology* 5(1):5-23.
18. Schulze WX, Deng L, & Mann M (2005) Phosphotyrosine interactome of the ErbB-receptor kinase family. *Molecular systems biology* 1:2005 0008.
19. Korkaya H, Paulson A, Iovino F, & Wicha MS (2008) HER2 regulates the mammary stem/progenitor cell population driving tumorigenesis and invasion. *Oncogene* 27(47):6120-6130.
20. Freudenberg JA, *et al.* (2009) The role of HER2 in early breast cancer metastasis and the origins of resistance to HER2-targeted therapies. *Experimental and molecular pathology* 87(1):1-11.

21. Venter DJ, Tuzi NL, Kumar S, & Gullick WJ (1987) Overexpression of the c-erbB-2 oncoprotein in human breast carcinomas: immunohistological assessment correlates with gene amplification. *Lancet* 2(8550):69-72.
22. Kallioniemi OP, *et al.* (1992) ERBB2 amplification in breast cancer analyzed by fluorescence in situ hybridization. *Proceedings of the National Academy of Sciences of the United States of America* 89(12):5321-5325.
23. Lohrisch C & Piccart M (2001) An overview of HER2. *Seminars in oncology* 28(6 Suppl 18):3-11.
24. Baselga J & Swain SM (2009) Novel anticancer targets: revisiting ERBB2 and discovering ERBB3. *Nature reviews. Cancer* 9(7):463-475.
25. Moasser MM (2007) The oncogene HER2: its signaling and transforming functions and its role in human cancer pathogenesis. *Oncogene* 26(45):6469-6487.
26. Weigelt B, *et al.* (2005) Molecular portraits and 70-gene prognosis signature are preserved throughout the metastatic process of breast cancer. *Cancer research* 65(20):9155-9158.
27. Lenferink AE, *et al.* (1998) Differential endocytic routing of homo- and heterodimeric ErbB tyrosine kinases confers signaling superiority to receptor heterodimers. *The EMBO journal* 17(12):3385-3397.
28. Karunagaran D, *et al.* (1996) ErbB-2 is a common auxiliary subunit of NDF and EGF receptors: implications for breast cancer. *The EMBO journal* 15(2):254-264.
29. Alimandi M, *et al.* (1995) Cooperative signaling of ErbB3 and ErbB2 in neoplastic transformation and human mammary carcinomas. *Oncogene* 10(9):1813-1821.
30. Holbro T, *et al.* (2003) The ErbB2/ErbB3 heterodimer functions as an oncogenic unit: ErbB2 requires ErbB3 to drive breast tumor cell proliferation. *Proceedings of the National Academy of Sciences of the United States of America* 100(15):8933-8938.
31. Tokunaga E, *et al.* (2006) Akt is frequently activated in HER2/neu-positive breast cancers and associated with poor prognosis among hormone-treated patients. *International journal of cancer. Journal international du cancer* 118(2):284-289.
32. Carter P, *et al.* (1992) Humanization of an anti-p185HER2 antibody for human cancer therapy. *Proceedings of the National Academy of Sciences of the United States of America* 89(10):4285-4289.
33. Izumi Y, Xu L, di Tomaso E, Fukumura D, & Jain RK (2002) Tumour biology: herceptin acts as an anti-angiogenic cocktail. *Nature* 416(6878):279-280.
34. Kang L, Guo Y, Zhang X, Meng J, & Wang ZY (2011) A positive cross-regulation of HER2 and ER-alpha36 controls ALDH1 positive breast cancer cells. *The Journal of steroid biochemistry and molecular biology* 127(3-5):262-268.
35. Ithimakin S, *et al.* (2013) HER2 Drives Luminal Breast Cancer Stem Cells in the Absence of HER2 Amplification: Implications for Efficacy of Adjuvant Trastuzumab. *Cancer research* 73(5):1635-1646.
36. Aggarwal BB & Ichikawa H (2005) Molecular targets and anticancer potential of indole-3-carbinol and its derivatives. *Cell Cycle* 4(9):1201-1215.
37. Cover CM, *et al.* (1998) Indole-3-carbinol inhibits the expression of cyclin-dependent kinase-6 and induces a G1 cell cycle arrest of human breast cancer cells independent of estrogen receptor signaling. *The Journal of biological chemistry* 273(7):3838-3847.

38. Firestone GL & Bjeldanes LF (2003) Indole-3-carbinol and 3-3'-diindolylmethane antiproliferative signaling pathways control cell-cycle gene transcription in human breast cancer cells by regulating promoter-Sp1 transcription factor interactions. *The Journal of nutrition* 133(7 Suppl):2448S-2455S.
39. Bradlow HL, Sepkovic DW, Telang NT, & Osborne MP (1995) Indole-3-carbinol. A novel approach to breast cancer prevention. *Annals of the New York Academy of Sciences* 768:180-200.
40. Marconett CN, *et al.* (2011) Indole-3-carbinol downregulation of telomerase gene expression requires the inhibition of estrogen receptor-alpha and Sp1 transcription factor interactions within the hTERT promoter and mediates the G1 cell cycle arrest of human breast cancer cells. *Carcinogenesis* 32(9):1315-1323.
41. Marconett CN, *et al.* (2010) Indole-3-carbinol triggers aryl hydrocarbon receptor-dependent estrogen receptor (ER)alpha protein degradation in breast cancer cells disrupting an ERalpha-GATA3 transcriptional cross-regulatory loop. *Molecular biology of the cell* 21(7):1166-1177.
42. Anderson WF, Chatterjee N, Ershler WB, & Brawley OW (2002) Estrogen receptor breast cancer phenotypes in the Surveillance, Epidemiology, and End Results database. *Breast cancer research and treatment* 76(1):27-36.
43. Bundred NJ (2001) Prognostic and predictive factors in breast cancer. *Cancer treatment reviews* 27(3):137-142.
44. Aronchik I, *et al.* (2012) Target protein interactions of indole-3-carbinol and the highly potent derivative 1-benzyl-I3C with the C-terminal domain of human elastase uncouples cell cycle arrest from apoptotic signaling. *Molecular carcinogenesis* 51(11):881-894.
45. Nguyen HH, *et al.* (2008) The dietary phytochemical indole-3-carbinol is a natural elastase enzymatic inhibitor that disrupts cyclin E protein processing. *Proceedings of the National Academy of Sciences of the United States of America* 105(50):19750-19755.
46. Ho JN, Jun W, Choue R, & Lee J (2013) I3C and ICZ inhibit migration by suppressing the EMT process and FAK expression in breast cancer cells. *Molecular medicine reports* 7(2):384-388.
47. Meshnick SR (2002) Artemisinin: mechanisms of action, resistance and toxicity. *International journal for parasitology* 32(13):1655-1660.
48. Duffy PE & Mutabingwa TK (2004) Drug combinations for malaria: time to ACT? *Lancet* 363(9402):3-4.
49. Meshnick SR (1994) The mode of action of antimalarial endoperoxides. *Transactions of the Royal Society of Tropical Medicine and Hygiene* 88 Suppl 1:S31-32.
50. Reizenstein P (1991) Iron, free radicals and cancer. *Medical oncology and tumor pharmacotherapy* 8(4):229-233.
51. Nicolini A, Ferrari P, Fallahi P, & Antonelli A (2012) An iron regulatory gene signature in breast cancer: more than a prognostic genetic profile? *Future Oncol* 8(2):131-134.
52. Crespo-Ortiz MP & Wei MQ (2012) Antitumor activity of artemisinin and its derivatives: from a well-known antimalarial agent to a potential anticancer drug. *Journal of biomedicine & biotechnology* 2012:247597.

53. Willoughby JA, Sr., *et al.* (2009) Artemisinin blocks prostate cancer growth and cell cycle progression by disrupting Sp1 interactions with the cyclin-dependent kinase-4 (CDK4) promoter and inhibiting CDK4 gene expression. *The Journal of biological chemistry* 284(4):2203-2213.

Chapter I

Development of a novel model system to study breast cancer stem cells

ABSTRACT

Signaling by the HER2 member of the EGF receptor gene family can be associated with an enhancement of stem/progenitor cell population levels in human breast cancer tumors. Expression of exogenous HER2 in the human MCF-10AT preneoplastic mammary epithelial cell line generated a novel breast cancer stem cell-like model system, 10AT-Her2 cells, that stably displays a CD44⁺/CD24⁻ phenotype with high levels of the stem cell marker nucleostemin, a nuclear GTPase, and active aldehyde dehydrogenase-1 (ALDH-1). 10AT-Her2 cells also exhibit the stem cell properties of forming tumorspheres in suspension cultures at limiting cell dilutions and greater efficiency compared to established breast cancer MCF-7 and SKBR3 cell lines. Furthermore, 10AT-Her2 cells are capable of initiating of tumor xenografts with extremely low numbers of implanted cells in athymic mice. 10AT-Her2 cells initiate tumor formation at greater efficiency and require fewer cells for tumor initiation than the empty vector transfected 10AT-Neo cells. The small molecule phytochemical indole-3-carbinol (I3C), a natural anticancer indolecarbinol from cruciferous vegetables of the *Brassica* genus such as bok choy and cabbage is effective in selectively preventing tumorsphere formation in 10AT-Her2 cells suggesting the natural anticancer molecule can target breast cancer stem cells. While, I3C does not alter CD44 or CD24 levels in 10AT-Her2 cells, it is effective in suppressing tumor formation *in vivo* thereby providing the first evidence that a natural anticancer molecule can target breast cancer stem cells.

INTRODUCTION

The heterogeneity of human breast cancers results from subpopulations of stem/progenitor cells that have the capacity for multi-lineage differentiation, ability to self renew, and initiate the formation of tumors (1-7). Cancer stem cells (CSCs) comprise of approximately 1% to 5% of the cells in primary breast tumors (1), and it has been proposed that the specific phenotypes of stem cell subpopulations direct the development of therapy-resistant tumors and relapse of the disease, which can significantly influence the effectiveness of a therapeutic strategy (8, 9). Therefore, a critical issue in breast cancer treatment is the identification of anticancer agents that can directly target cancer stem cells to prevent their self-renewal and/or tumor plasticity. An experimental constraint that has limited the characterization of CSC targeted molecules is the low number of cells that can be isolated from the CSC populations enriched *in vitro* in tumorspheres (6, 10), or enriched in side-populations of tumor-initiating cells isolated by flow cytometry from primary tumors (6, 11, 12). Furthermore, these cultured cancer stem cell populations can differentiate and lose the CSC phenotype and/or viability.

Signaling by the orphan epidermal growth factor (EGF) receptor gene family member HER2 is highly associated with aggressive metastatic forms of breast cancer (13, 14), and the gene is amplified in 20-30% of all human breast cancers (15). HER2 is also associated with an enhancement of cancer stem/progenitor cell population levels in populations of either normal mammary epithelial cells or certain breast cancer cell lines (11, 16). Expression of exogenous HER2 in normal mammary stem cell populations generated hyperplastic lesions when transplanted *in vivo* (16), and in breast cancer cells HER2 expression enhanced the occurrence of side-populations of tumor-initiating cells of the luminal subtype (11). HER2 can also be clinically correlated with stem/progenitor cell populations in that patients with HER2+ breast cancers treated with the HER2 inhibitor lapatinib show a significant reduction in the number of CD44⁺/CD24^{-/low} cells and a decreased tumorsphere forming efficiency (17).

By expressing exogenous HER2 in the MCF-10AT cell line, which is a well-established model of human mammary epithelial preneoplasia (18), we generated a novel breast cancer model cell line, denoted as 10AT-Her2, in which virtually all of the cells in the population have a stable stem cell-like character. The starting MCF-10AT cells were chosen for our studies because of the intrinsic low incidence of tumor formation (18) and the lack of any stem cell characteristics. Breast cancer stem cell levels can be identified by their CD44⁺/CD24⁻ phenotype (19) and expression of other cancer stem cell markers such as the nuclear GTPase nucleostemin, which is associated with the property of breast cancer stem cell self-renewal (19-21), and active aldehyde dehydrogenase-1 (ALDH-1) (22). Importantly, we show that 10AT-Her2 cells have a CD44⁺/CD24^{-/low} phenotype with high levels of nucleostemin and active ADLHDH-1. 10AT-Her2 cells are able to efficiently form tumors xenografts *in vivo* in athymic mice and form tumorspheres *in vitro* in cell suspensions at limiting cell dilutions. This system provided the experimental opportunity to directly test the hypothesis that cellular components defining the stem cell character can

confer selective responsiveness of anticancer compounds to target breast cancer cell stem populations.

Indole-3-carbinol (I3C), a natural indolecarbinol produced from the hydrolysis of glucobrassicin, is found in cruciferous vegetables of the *Brassica* genus such as broccoli and cabbage and is a promising anticancer compound (23-27). I3C treatment functionally inhibits tumorsphere formation and tumor xenograft growth in vivo in athymic mice.

MATERIALS AND METHODS

Generating the Mammary Epithelial Cancer Stem Cell Line

Preneoplastic MCF-10AT human mammary epithelial cells (obtained from the Barbara Ann Karmanos Cancer Institute, Detroit, MI) were stably transfected with either the human pCMV-HER2 expression vector, which also contains the neomycin resistance gene, or with the pCMV-Neo control vector forming 10AT-Her2 cells and 10AT-Neo cells, respectively. Cells were stably selected with G418 sulfate (Cellgro, Manassas, VA) for 2 months.

Cell Culture

The MCF-10AT parent cell line and the 10AT-Her2 and 10AT-Neo cell lines were cultured in DMEM/F-12, 10% fetal bovine serum, 50 U/mL penicillin, 50 U/mL streptomycin (all media components purchased from Lonza, Allendale, NJ), and cell culture plates purchased from NUNC-Fischer, Pittsburgh, PA), 0.02 µg/mL epidermal growth factor (purchased from Promega, Madison, Wisconsin, USA), 0.05 µg/mL hydrocortisone, 10 µg/mL insulin, and 0.1 µg/mL cholera toxin (obtained from Sigma-Aldrich). Cells were grown to subconfluency in a humidified chamber at 37°C containing 5% CO₂. For drug treatments, a 200 mmol/l stock solution of I3C, 10 mmol/l stock solution of 1-benzyl I3C, 50 mmol/l stock solution of Diindolymethane (DIM), 200 mmol/l stock solution of Tryptophol, and 300 mmol/l stock solution of Artemisinin (purchased from Sigma-Aldrich, St. Louis, MO) was dissolved in dimethyl sulfoxide (DMSO) and then diluted in the ratio 1:1000 in media before culture plate application. Before each drug treatment, cells are washed in ice cold phosphate-buffered saline (PBS) (obtained from Lonza).

Expression Plasmids and Transfections

Human cytomegalovirus (CMV)-HER2 expression plasmid was a kind gift from Dr. Leonard Bjeldanes, (Department of Nutritional Sciences and Toxicology, University of California at Berkeley). Transfection of expression vectors were performed using Superfect transfection reagent from QIAGEN per the manufacturers' recommended protocol.

Tumorspheres

Single-cell suspensions of 10AT-Her2 or 10AT-Neo cells were plated on ultra-low attachment plates (Corning, Costar) in MammoCult Human Medium (Stem Cell Technologies, Vancouver) and cultured at 37°C, 5% CO₂. Cells were incubated with or without 200 µM I3C for the indicated time durations and tumorsphere formation was assessed visually by phase microscopy and quantified by counting the number of spheres formed in culture.

Flow Cytometry and ALDEFLUOR ASSAY

To analyze cell surface expression, harvested cells were incubated for 1 hour at 4°C with CD44 or CD24 specific antibodies conjugated to Alexafluor488 secondary antibody. Cells were suspended in full media and kept on ice pending analysis. ALDEFLUOR assay was performed following manufacture's recommended guidelines and protocol (Stem Cell Technologies). Live single cells were gated for analysis using Epics XL-MCL flow cytometer (Beckman Coulter) with single 488 nm blue laser filtered at 525 BP/slot 1.

Western Blots

After the indicated treatments, cells were harvested in radioimmune precipitation assay buffer (150 mM NaCl, 0.5% deoxycholate, 0.1% NoNidet-p40 (Nonidet P-40, Fluta Biochemitra, Switzerland), 0.1% SDS, 50 mM Tris) containing protease and phosphatase inhibitors (50 g/ml phenylmethylsulfonyl fluoride, 10 g/mL aprotinin, 5 g/mL leupeptin, 0.1 g/mL NaF, 1 mM dithiothreitol, 0.1 mM sodium orthovanadate, and 0.1 mM glycerol phosphate). Equal amounts of total cellular protein were mixed with loading buffer (25% glycerol, 0.075% SDS, 1.25 ml of 14.4M β mercaptoethanol, 10% bromphenol blue, 3.13% 0.5M Tris-HCl, and 0.4% SDS (pH 6.8)) and fractionated on 10% polyacrylamide/0.1% SDS resolving gels by electrophoresis. Rainbow marker (Amersham Biosciences) was used as the molecular weight standard. Proteins were electrically transferred to nitrocellulose membranes (Micron Separations, Inc., Westboro, MA) and blocked for 1 hour with Western wash buffer (5% NFDM (10 mM Tris-HCl (pH 8.0), 150 mM NaCl, and 0.05% Tween 20, 5% nonfat dry milk). Protein blots were subsequently incubated for overnight at 4°C in primary antibodies. The antibodies used were as follows, Rabbit anti-Nucleostemin, (sc-67012), Mouse anti-CD44 (sc-65412), Mouse anti-CD-24 (sc-70598), Goat anti-ALDH-1 (sc-22588), were purchased from Santa Cruz Biotechnology and diluted in the ratio 1:1000 in TBST. Rabbit anti-actin (AAN01; Cytoskeleton, Denver CO) was diluted 1:1000 in TBST and used as a gel-loading control. Rabbit anti-HER2 (2165) was obtained from Cell Signaling. The working concentration for all antibodies was 1 μ g/mL in Western wash buffer. Immunoreactive proteins were detected after incubation with horseradish peroxidase conjugated secondary antibody diluted to 3×10^4 in Western wash buffer (goat anti-rabbit IgG, rabbit anti-goat IgG, and rabbit anti-mouse IgG (Bio-Rad)). Blots were treated with enhanced chemiluminescence reagents (PerkinElmer Life Sciences), and all proteins were detected by autoradiography. Equal protein loading was confirmed by Ponceau S staining of blotted membranes.

***In vivo* Tumor Xenografts in NIH III Nude Mice**

10AT-Her2 (3×10^5) or 10AT-Neo (3×10^6) cells were mixed with equal volume of matrigel (BD Biosciences, CA) and inoculated subcutaneously into right and left mammary fat pad region of athymic nude mice. In limiting dilutions to determine 10AT-Her2 xenograft efficiency 3×10^4 cells were used. Once the tumors reached a palpable size, the mice were given daily subcutaneous injections of I3C (300 mg/kg body mass). The stock solutions of I3C (300 mM) were dissolved initially in DMSO and then diluted in appropriate volume of PBS. I3C was injected subcutaneously in order to reduce the potential for formation of I3C condensation products, such as the natural dimer DIM, that normally occur in the acid conditions of the stomach. Mice were also palpated and tumor size was measured every other day with calipers. Tumor volume was calculated using the following equation $V = a \times b^2/2$, where a is the width and b is the length of the tumors. Xenografted tumors were excised at the termination of the experiment and photographed.

RESULTS

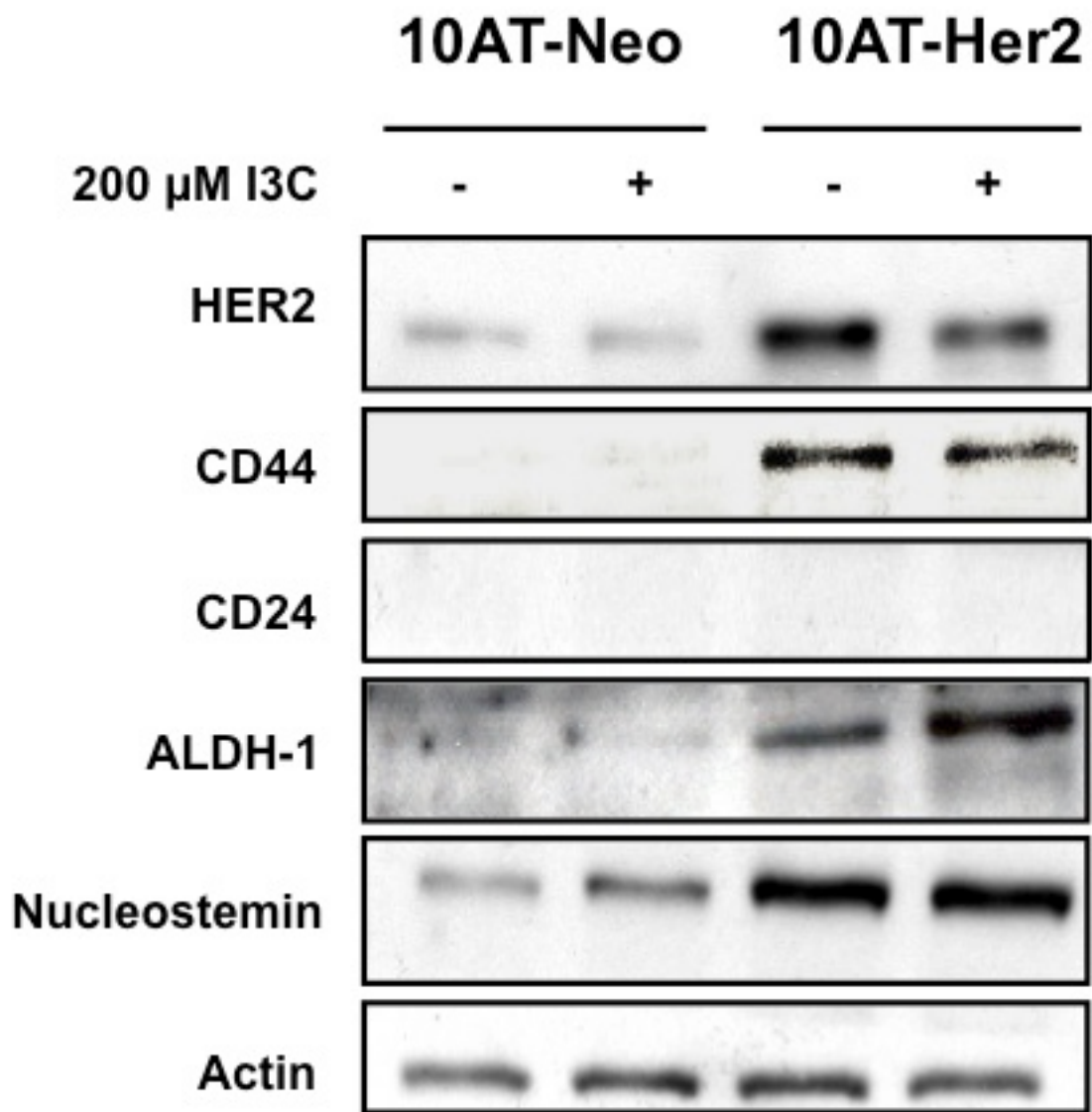
Expression of exogenous HER2 in preneoplastic mammary epithelial cells induces a cancer stem cell phenotype.

To generate a stable mammary epithelial cancer cell line with a stem cell-like character, preneoplastic MCF-10AT human mammary epithelial cells, which are essentially void of any cancer stem cell properties (18), were stably transfected with either the CMV-HER2 expression vector containing the neomycin resistance gene, or the control vector comprised of the CMV-Neomycin gene, forming 10AT-Her2 and 10AT-Neo cells, respectively. Western blot analysis demonstrated that 10AT-Her2 cells expressed significantly higher levels of HER2 compared to the control CMV-Neo cell line (Figure 7). The naturally occurring small molecule phytochemical, I3C had no effects on levels of HER2 protein expression. Western blots also demonstrated that 10AT-Her2 cells acquired a cancer stem cell phenotype based on expression of significantly higher levels of the CD44, ALDH-1 and nucleostemin. Nucleostemin is a generalized marker for stem cells and cancer stem cells. The levels of CD24 remained low in the population regardless of HER2 status. The control 10AT-Neo cells remained devoid of any CSC phenotype. The CD44⁺/CD24^{-/low} expression profile with high expression levels of nucleostemin and active ALDH-1 has been stably maintained in continuous cell culture over multiple generations of 10AT-Her2 cells.

Figure 7

Characterization of CSC markers by HER2 overexpression in MCF-10AT cells.

Cultured MCF-10AT cells transfected with either empty vector control CMV-Neo or CMV-HER2, now 10AT-Neo or 10AT-Her2, respectively, were treated with or without 200 μ M I3C for 48 hours. Production of HER2, CD44, CD24, ALDH-1, Nucleostemin, and Actin protein levels were determined by western blot analysis of electrophoretically fractionated total cell extracts.



Given the technical drawback of treating an entire population of cells as one sample in western blot analysis, levels of cell surface associated CD44 and CD24 were also quantified by flow cytometry using antibodies specific for either CD44 or CD24. As shown in Figure 8, greater than 98% of the 10AT-Her2 cell population express high levels of cell surface CD44 compared to the background levels observed with control transfected 10AT-Neo cells. Consistent with the western blot analysis, the level of cell surface CD24 remained low in both cell lines and expressed in less than 2% of the cell population. Based on the same principles of quantifying CD44 and CD24 cell surface marker expression by flow cytometry, and ALDEFLUOR assay was performed to evaluate ALDH-1 enzymatic activity. Greater than 88% of 10AT-Her2 cells express active ALDH-1 while less than 1% of 10AT-Neo cells show any ALDH-1 activity (Figure 9). ALDH-1 activity correlates strongly with maintaining cancer stem cell viability (28) and its activity remained elevated after multiple generations.

Figure 8

Quantification of cell surface marker CD44 and CD24.

Cell surface expression of CD44 and CD24 in 10AT-Her2 cells and 10AT-Neo cells was quantified by flow cytometry of 500,000 cells in triplicate independent cell cultures.

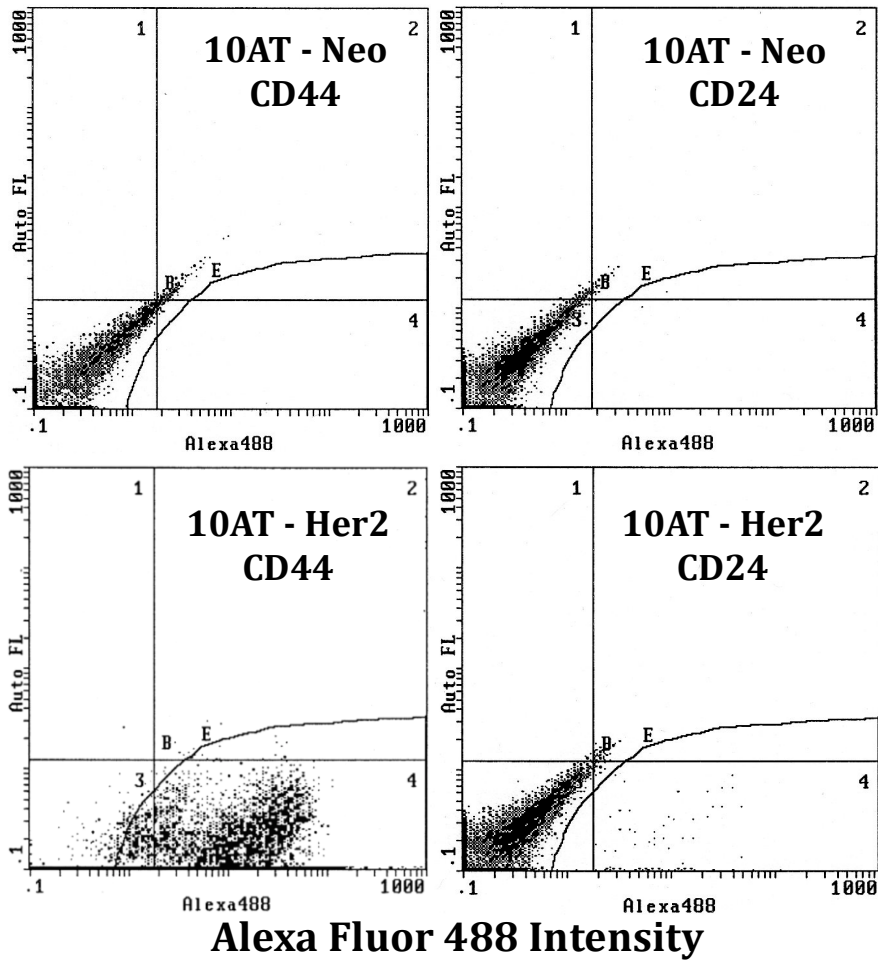
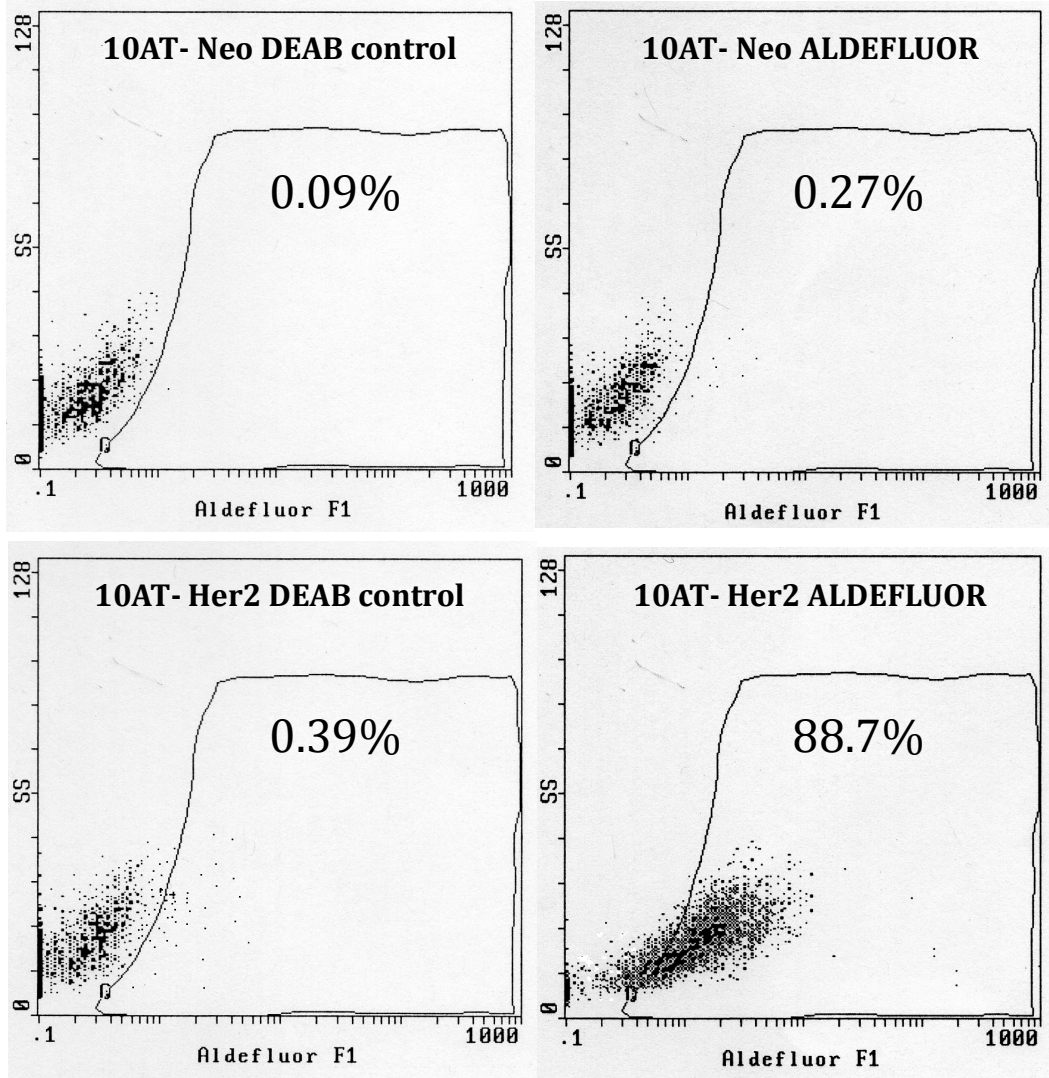


Figure 9

Quantification of ALDH-1 activity in 10AT-Her2 and 10AT-Neo cells.

ALDH-1 activity was analyzed by an ALDEFUOR assay converting uncharged ALDH-substrate BODIPY aminoacetaldehyde (BAAA) into a negatively charged reaction product, BAA- inducing fluorescence in cells expressing active ALDH-1. 10AT-Her2 cells and 10AT-Neo cells were quantified by flow cytometry of 500,000 cells in triplicate independent cell cultures.

Side Scatter



ALDEFUOR Forward Scatter

10AT-Her2 and 10AT-Neo cells were cultured at low density (~4,000 cells per ml) in cell suspensions, and *in vitro* tumorsphere formation, which is considered a property of cancer stem cells (6, 20), was monitored visually over a 6-day time course. As shown in Figure 10, 10AT-Her2 cells began to form tumorsphere-like structures within two days of culture and by six days the cells formed completed tumorspheres. In contrast, 10AT-Neo cells failed to form tumorspheres and remained dispersed in small cell aggregates. The tumorsphere forming efficiency of 10AT-Her2 cells was compared to that of two luminal subtype tumorigenic breast cancer cell lines, SKBR3 and MCF-7, which differ in their expression of HER2 (29). The western blot insert in Figure 11 showed that SKBR3 and 10AT-Her2 cells produce approximately the same levels of HER2 protein, whereas, MCF-7 cells produce significantly lower levels of HER2. By culturing increasing numbers of cells in suspension, the 10AT-Her2 cells were shown to be more than 10-fold more efficient in their tumorsphere forming capability compared to either SKBR3 or MCF-7 cells (Figure 11). For example, the number of tumorspheres formed from 2,000 10AT-Her2 cells was observed only when 25,000 SKBR3 cells or 50,000 MCF-7 cells are assayed. Also, because SKBR3 and 10AT-Her2 express similar levels of HER2 protein, the ability of 10AT-Her2 cells to form tumorspheres cannot be attributed to only the high level of exogenous HER2.

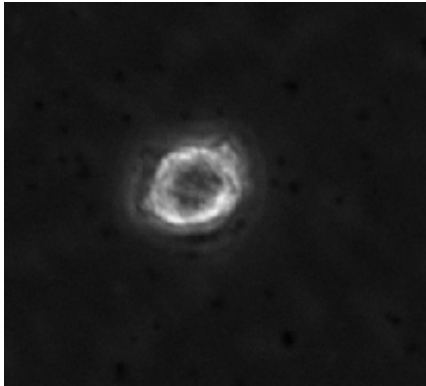
Figure 10

Formation of tumorspheres by 10AT-Her2 cells *in vitro*.

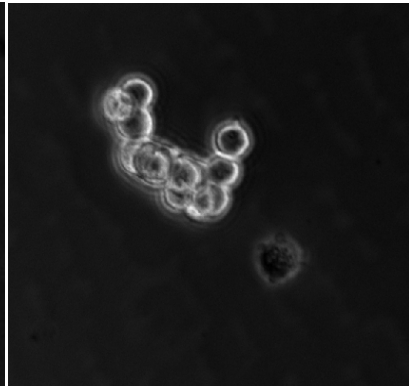
10AT-Her2 and 10AT-Neo cells were plated at a density of 4000 cells per well in serum free nonadherent culturing conditions. Single-cell suspensions were incubated for up to 6 days and monitored for tumorsphere formation. At the indicated days in culture, tumorsphere formation was assessed visually by phase microscopy.

10AT-Neo

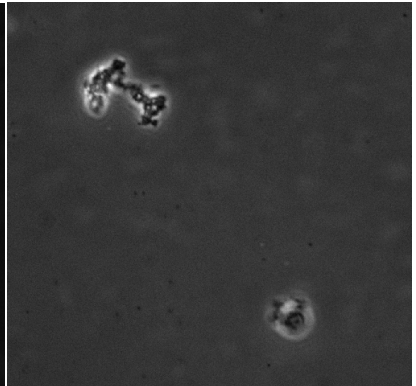
Day 2



Day 4

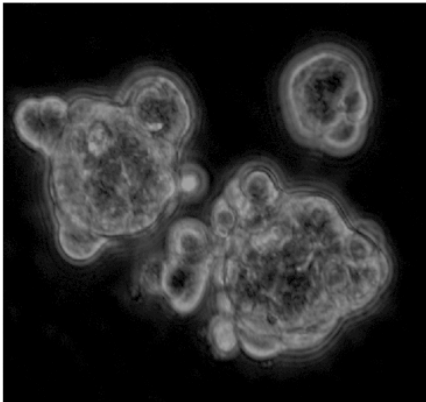


Day 6

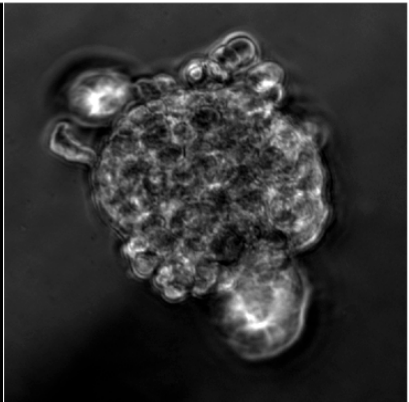


10AT-Her2

Day 2



Day 4



Day 6

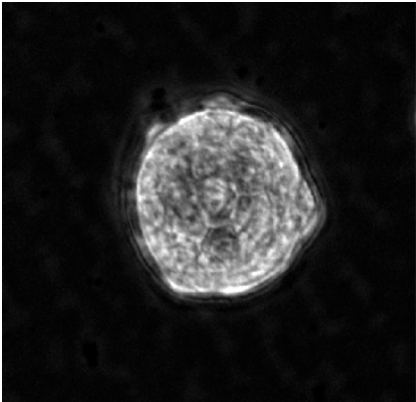
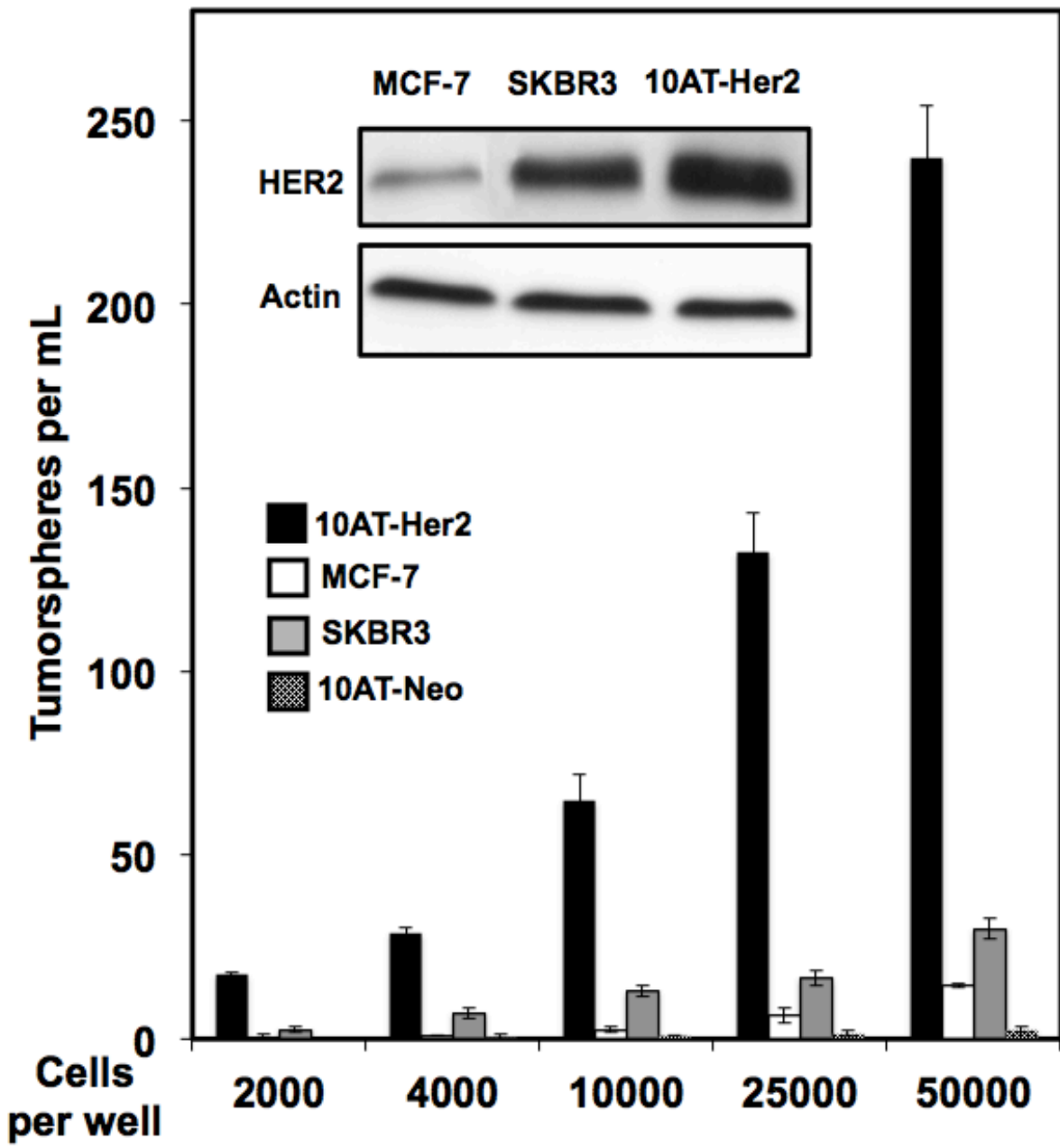


Figure 11

Comparing 10AT-Her2 tumorsphere forming efficiency.

10AT-Her2, 10AT-Neo, SKBR3 and MCF-7 breast cancer cells were incubated at the indicated cell densities and tumorsphere formation efficiency was quantified after 6 days in culture under nonadherent conditions. The presented values are an average of three independent experiments. The gel inserts are western blots showing relative levels of HER2 protein expression and actin controls from electrophoretically fractionated total cell extracts of MCF-7, SKBR3 and 10AT-Her2 cells.



I3C disrupts 10AT-Her2 cell tumorsphere formation and *in vivo* tumor xenograft growth.

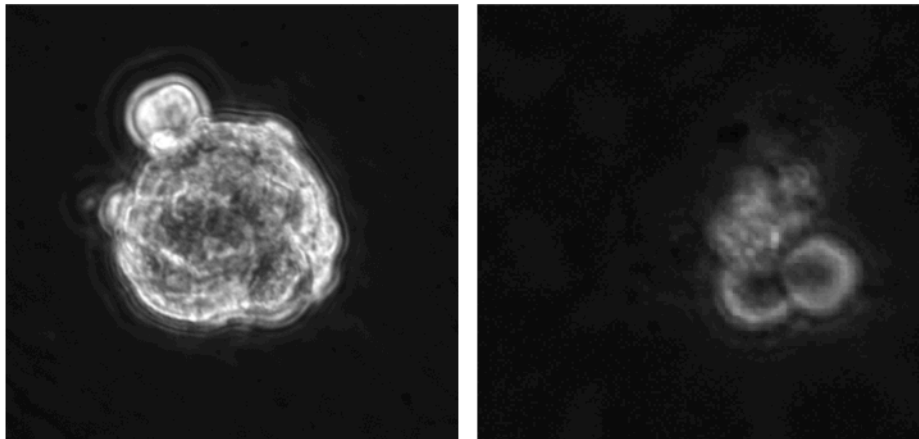
The 10AT-Her2 cells display a stable breast cancer stem cell-like phenotype, which provided the experimental opportunity to directly assess the ability of the small molecule phytochemical, I3C, to potentially target cancer stem cell populations. Treatment of 10AT-Her2 cell suspensions with or without 200 μ M I3C, the optimal concentration for its anticancer effects (30-34), for six days demonstrated that this indolecarbinol ablated the *in vitro* formation of tumorspheres (Figure 12), which is a critical cancer stem cell property that is predictive of tumor formation. Visual inspection by phase microscopy, demonstrates that pretreatment of I3C at the initial day of incubation prevents the ability of 10AT-Her2 cells to initiate tumorsphere formation. Further quantification in the efficiency of 10AT-Her2 cells to form tumorspheres demonstrated that I3C, and at lower concentrations its highly potent synthetic derivative 1-benzyl-I3C (35), had strong inhibitory effects on the CSC process compared to other phytochemicals that display antiproliferative responses in breast cancer cells such as the natural I3C dimer, 3,3'-diindolylmethane (DIM) (25), and artemisinin (36) that had no effect on tumorsphere formation (Figure 13).

Figure 12

I3C inhibition of tumorsphere formation in 10AT-Her2 cells.

10AT-Her2 cells were plated at a density of 4000 cells per well in tumorsphere culture conditions and incubated with or without I3C. Only one dose of I3C was administered in tumorsphere culture media at day 0 and after 6 days, tumorsphere formation was assessed visually by phase microscopy and quantified.

10AT-Her2 Tumorspheres



Vehicle Control

I3C Treated

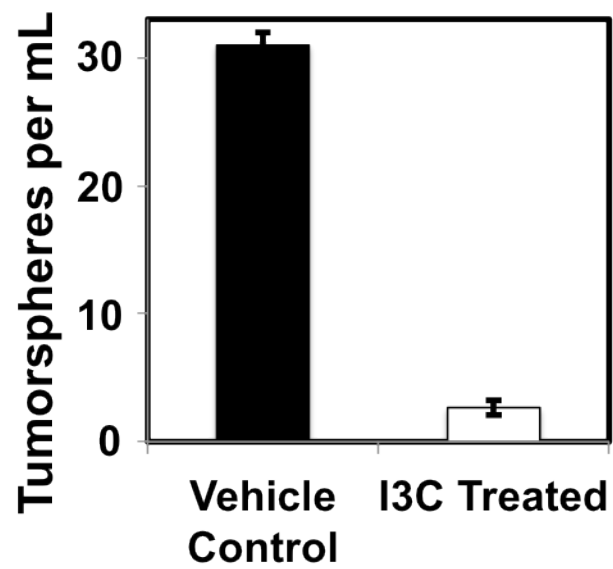
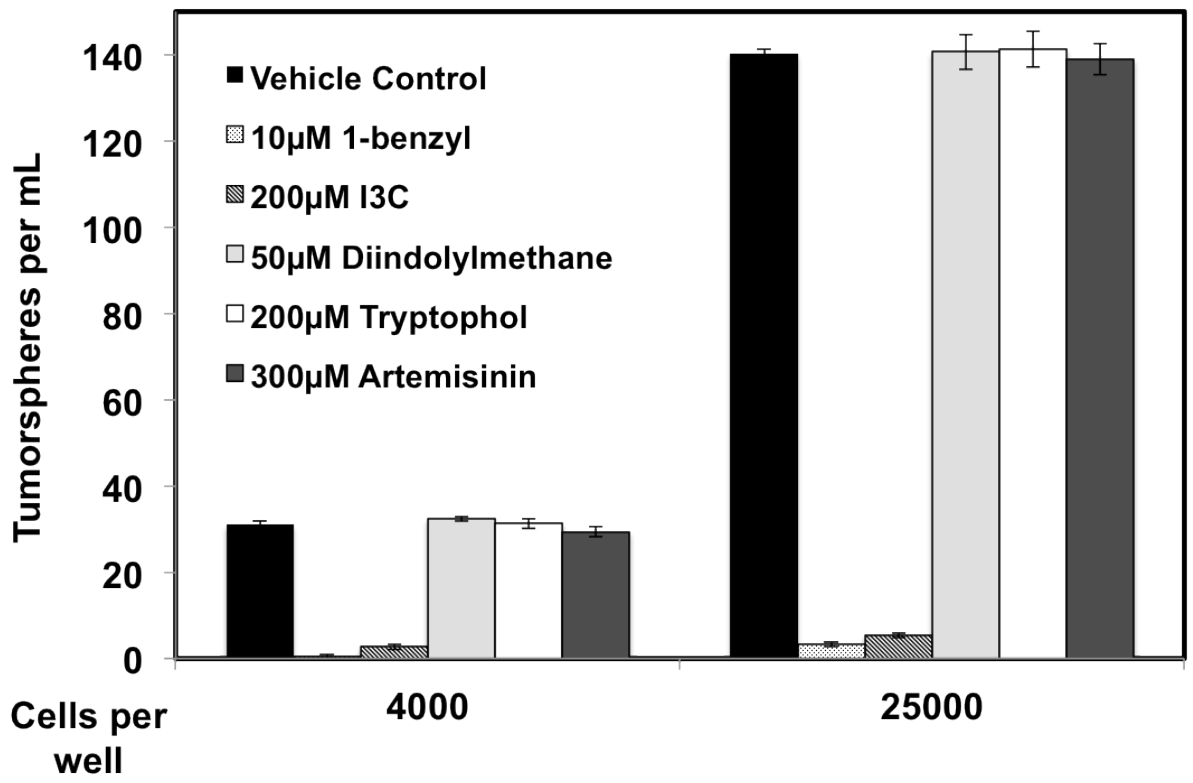


Figure 13

I3C and 1-benzyl-I3C selectively disrupts cancer stem cell tumorsphere formation.

Either 4,000 or 25,000 10AT-Her2 cells per well were plated in serum free nonadherent tumorsphere culture conditions and treated with the indicated phytochemicals or the vehicle control. Treatment was administered at day 0 and incubated for six days. Tumorsphere formation was quantified in three independent experiments by determining the total number of tumorspheres in each cell culture well.



Analysis of the *in vivo* formation of tumor xenografts in NIH III athymic nude mice demonstrated that 10AT-Her2 cells display CSC properties with regards to the efficiency of tumor initiating. 10AT-Her2 cells are capable of forming palpable, solid tumors at significantly lower cell numbers compared to tumorigenic human breast cancer cell lines such as MCF-7 and SKBR3. As low as 3×10^4 10AT-Her2 cells can be used to form tumors at 50% efficiency. As the number of 10AT-Her2 cells used per injection site approaches 3×10^5 , tumor-forming efficiency reaches 95% (Figure 14). The control 10AT-Neo cells display only a 20-25% tumor efficiency at high cell numbers, which is consistent with sporadic events associated with the preneoplastic nature of the parental MCF-10AT cell line (18, 37). To assess the *in vivo* effects of I3C on the growth of 10AT-Her2 cell-derived tumor xenografts, 300,000 10AT-Her2 cells were injected in NIH III athymic mice and the resulting tumors were first allowed to grow to an average volume of approximately 100 mm³. The mice were then injected subcutaneously with either I3C (300 mg/kg body mass) or with the DMSO vehicle control over a 19-day time course. Subcutaneous administration of I3C was preferred over intravenous or oral injections to minimize the potential for hydrolysis reactions converting I3C into its dimeric form, DIM. In vehicle control treated animals, the 10AT-Her2 cell tumor xenografts showed robust growth (Figure 15); the tumors also displayed highly concentrated gross tumor vascularization and were dense (Figure 15, micrograph insert), which is consistent with the rapid growth of cells within the tumor. In contrast, administration of I3C strongly suppressed the growth of 10AT-Her2 cells-derived tumor xenografts and the resulting tumors appeared less vascularized and much smaller in size. The texture of the residual tumors from I3C treated mice was pliable, consistent with reduced cell density in the xenografts.

Figure 14

Tumor-forming efficiency of 10AT-Her2 cells and control 10AT-Neo cells.

Three million 10AT-Neo cells or 300,000 10AT-Her2 cells were implanted into athymic NIH III nude mice to form tumor xenografts. After 5 weeks, the total number of palpable tumors was divided by the twenty total injection sites (two injections site per animal) to determine the percentage of tumor formation from three independent experiments.

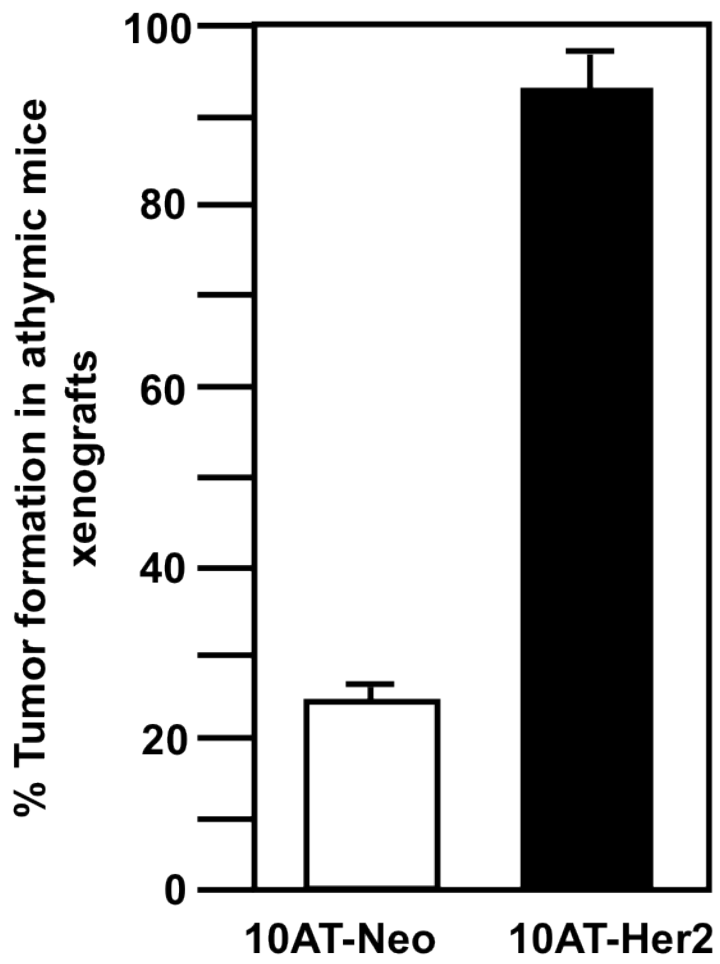
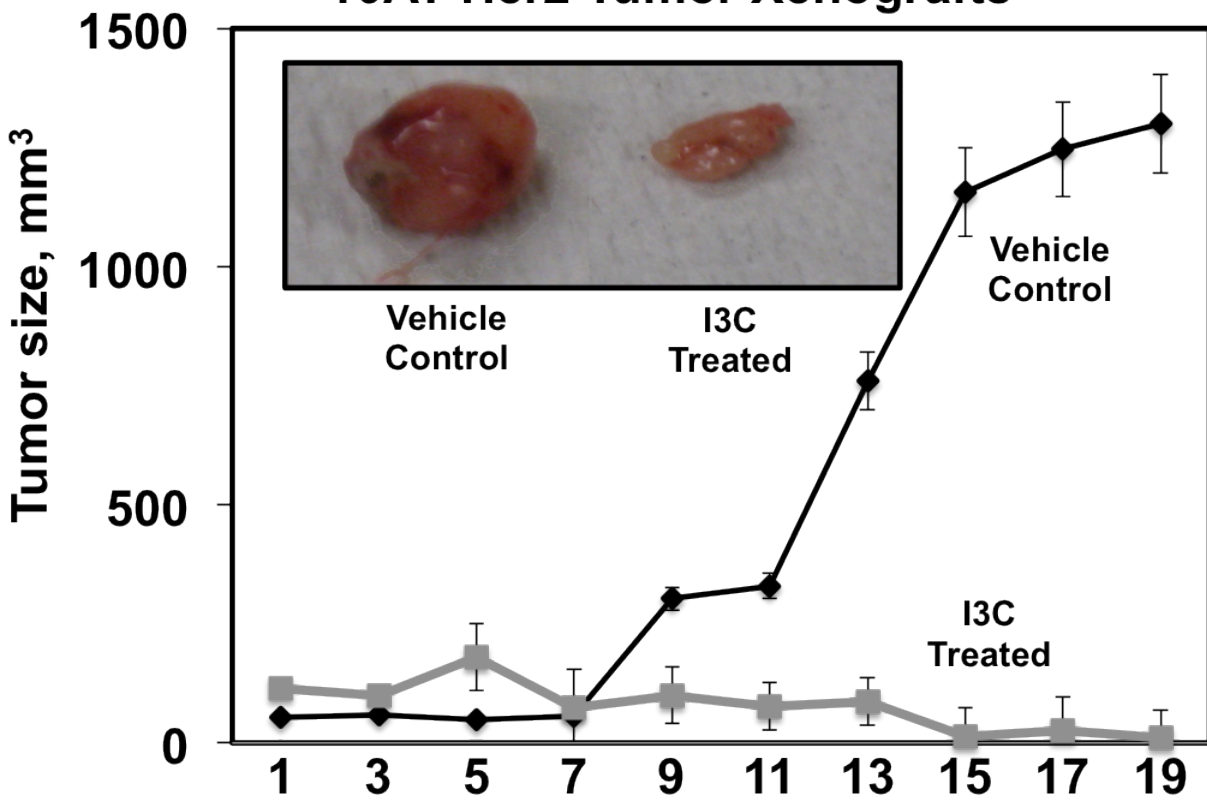


Figure 15

I3C inhibition of 10AT-Her2 Tumor Xenografts.

After the formation of detectable 10AT-Her2 cell-derived palpable tumor xenografts, athymic NIH III mice were treated subcutaneously with either 300 mg/kg of I3C or the DMSO vehicle control. Tumor volumes were quantified with a caliper from ten tumor xenografts per condition using two tumor sites per animal. The micrograph insert shows representative tumors excised from two week-post injection animals.

10AT-Her2 Tumor Xenografts



DISCUSSION

By expressing the HER2 member of the epidermal growth factor receptor superfamily in human mammary epithelial preneoplastic cells, we generated a unique human breast cancer stem cell model system, 10AT-Her2 cells, with a stable CD44⁺/CD24⁻/ALDH-1⁺/Nucleostemin⁺ phenotype. 10AT-Her2 cells display the stem cell properties of efficient *in vitro* tumorsphere formation in suspension cultures and *in vivo* tumor initiating capabilities at low cell number in tumor xenografts. The rationale for expressing exogenous HER2 is the functional connection between HER2 levels and enhanced stem cell populations that can be detected in primary breast tumors and breast cancer cell lines (16). 10AT-Her2 cells and the SKBR3 breast cancer cell line express generally similar levels of HER2 protein, however, only the 10AT-Her2 cells exhibit the ability to form tumorspheres at limiting cell dilutions. Thus, the level of HER2 does not necessarily trigger the cancer stem cell character of the newly developed model system. Conceivably a combination of HER2 signaling and the components constituting the preneoplastic phenotype inherent in the MCF-10AT cell line caused the emergence of the cancer stem cell properties in the 10AT-Her2 cells. Furthermore, the timing of ectopic HER2 elevation with regards to the transformative process of developing breast cancer may be critical for the genetic and epigenetic regulation of cancer stem cells. For example, introducing HER2 in preneoplastic MCF-10AT cells which are representative of early neoplasia and still undergoing cellular processes towards breast cancer may initialize the targets necessary for tumor initiating cells. This may further explain why SKBR3 cultured cells, which represents an advanced stage of metastatic breast cancer with high levels of HER2, fails to efficiently induce tumorspheres and compared to 10AT-Her2 cells, does not contain a high ratio of cancer stem cells to differentiated tumor cells.

An important feature of the 10AT-Her2 cell line is that virtually the entire cell population has a stable cancer stem cell phenotype that is reproducible and remains intact even after multiple passages. This property alleviates the experimental need to continually isolate limited numbers of enriched cancer stem cell populations from breast cancer tumors. Furthermore, utilizing an immortalized cell line allows for consistent experimental reproducibility and manipulation that would be lost each time a new population of cancer stem cells are harvested from a new tumor. We established that 10AT-Her2 cells were highly sensitive to the *in vivo* antiproliferative effects of the small molecule phytochemical I3C and it prevents tumorsphere formation *in vitro*. Meanwhile, control 10AT-Neo cells maintain their preneoplastic character regardless of I3C administration and in all conditions fail to initiate tumorspheres. Both I3C and its highly potent derivative 1-benzyl-I3C (35) disrupt 10AT-Her2 tumorsphere formation. In contrast, the natural I3C dimer 3,3'-diindolylmethane (DIM) and a structurally unrelated phytochemical artemisinin, which both strongly suppress the *in vitro* and *in vivo* proliferation of human breast cancer cells (36, 38), have no effect on tumorsphere formation. Therefore, an intriguing clinical significance of our study is the potential to develop I3C-based compounds as effective adjuvant therapies for breast cancer because of the ability to therapeutically target cancer stem cells.

With regards to breast cancer stem cells, determining what signaling factors and genetic changes results from HER2 overexpression becomes paramount for understanding how to selectively target and treat these cells. Furthermore, it will undoubtedly affect the clinical prognosis in breast cancer patients and may lead to new drug developments for personalize therapies. For example, HER2 correlates strongly with ALDH-1 (28) and in the 10AT-Her2 cancer stem cell model system HER2 also correlates with nucleostemin expression. Given the resistant nature of cancer stem cells, it is conceivable, a chemotherapeutic drug specifically capable of targeting active ALDH-1 or nucleostemin may be able to inhibit cancer stem cell proliferation or induce their differentiation making the treatment of breast cancer more manageable.

REFERENCES

1. Al-Hajj M (2007) Cancer stem cells and oncology therapeutics. *Curr Opin Oncol* 19(1):61-64.
2. Charafe-Jauffret E, Ginestier C, & Birnbaum D (2009) Breast cancer stem cells: tools and models to rely on. *BMC Cancer* 9:202.
3. Lawson JC, Blatch GL, & Edkins AL (2009) Cancer stem cells in breast cancer and metastasis. *Breast Cancer Res Treat* 118(2):241-254.
4. Marsden CG, Wright MJ, Pochampally R, & Rowan BG (2009) Breast tumor-initiating cells isolated from patient core biopsies for study of hormone action. *Methods Mol Biol* 590:363-375.
5. Reya T, Morrison SJ, Clarke MF, & Weissman IL (2001) Stem cells, cancer, and cancer stem cells. *Nature* 414(6859):105-111.
6. Stingl J & Caldas C (2007) Molecular heterogeneity of breast carcinomas and the cancer stem cell hypothesis. *Nat Rev Cancer* 7(10):791-799.
7. Zhou BB, *et al.* (2009) Tumour-initiating cells: challenges and opportunities for anticancer drug discovery. *Nat Rev Drug Discov* 8(10):806-823.
8. O'Brien CS, Howell SJ, Farnie G, & Clarke RB (2009) Resistance to endocrine therapy: are breast cancer stem cells the culprits? *J Mammary Gland Biol Neoplasia* 14(1):45-54.
9. Phillips TM, McBride WH, & Pajonk F (2006) The response of CD24(-/low)/CD44+ breast cancer-initiating cells to radiation. *J Natl Cancer Inst* 98(24):1777-1785.
10. Dontu G, *et al.* (2003) In vitro propagation and transcriptional profiling of human mammary stem/progenitor cells. *Genes Dev* 17(10):1253-1270.
11. Nakanishi T, *et al.* (2010) Side-population cells in luminal-type breast cancer have tumour-initiating cell properties, and are regulated by HER2 expression and signalling. *Br J Cancer* 102(5):815-826.
12. Ponti D, *et al.* (2005) Isolation and in vitro propagation of tumorigenic breast cancer cells with stem/progenitor cell properties. *Cancer Res* 65(13):5506-5511.
13. Freudenberg JA, *et al.* (2009) The role of HER2 in early breast cancer metastasis and the origins of resistance to HER2-targeted therapies. *Exp Mol Pathol* 87(1):1-11.
14. Zhang Y, *et al.* (2009) HER/ErbB receptor interactions and signaling patterns in human mammary epithelial cells. *BMC Cell Biol* 10:78.
15. Slamon DJ, *et al.* (1987) Human breast cancer: correlation of relapse and survival with amplification of the HER-2/neu oncogene. *Science* 235(4785):177-182.
16. Korkaya H, Paulson A, Iovino F, & Wicha MS (2008) HER2 regulates the mammary stem/progenitor cell population driving tumorigenesis and invasion. *Oncogene* 27(47):6120-6130.
17. Li X, *et al.* (2008) Intrinsic resistance of tumorigenic breast cancer cells to chemotherapy. *J Natl Cancer Inst* 100(9):672-679.
18. Heppner GH & Wolman SR (1999) MCF-10AT: A Model for Human Breast Cancer Development. *Breast J* 5(2):122-129.
19. Lin T, Meng L, Li Y, & Tsai RY (2010) Tumor-initiating function of nucleostemin-enriched mammary tumor cells. *Cancer Res* 70(22):9444-9452.

20. Kai K, Arima Y, Kamiya T, & Saya H (2010) Breast cancer stem cells. *Breast Cancer* 17(2):80-85.
21. Woodward WA & Sulman EP (2008) Cancer stem cells: markers or biomarkers? *Cancer Metastasis Rev* 27(3):459-470.
22. Ginestier C, et al. (2007) ALDH1 is a marker of normal and malignant human mammary stem cells and a predictor of poor clinical outcome. *Cell Stem Cell* 1(5):555-567.
23. Aggarwal BB & Ichikawa H (2005) Molecular targets and anticancer potential of indole-3-carbinol and its derivatives. *Cell Cycle* 4(9):1201-1215.
24. Ahmad A, Sakr WA, & Rahman KM (2010) Anticancer properties of indole compounds: mechanism of apoptosis induction and role in chemotherapy. *Curr Drug Targets* 11(6):652-666.
25. Safe S, Papineni S, & Chintharlapalli S (2008) Cancer chemotherapy with indole-3-carbinol, bis(3'-indolyl)methane and synthetic analogs. *Cancer Lett* 269(2):326-338.
26. Sarkar FH & Li Y (2009) Harnessing the fruits of nature for the development of multi-targeted cancer therapeutics. *Cancer Treat Rev* 35(7):597-607.
27. Weng JR, Tsai CH, Kulp SK, & Chen CS (2008) Indole-3-carbinol as a chemopreventive and anti-cancer agent. *Cancer Lett* 262(2):153-163.
28. Kang L, Guo Y, Zhang X, Meng J, & Wang ZY (2011) A positive cross-regulation of HER2 and ER-alpha36 controls ALDH1 positive breast cancer cells. *The Journal of steroid biochemistry and molecular biology* 127(3-5):262-268.
29. Neve RM, et al. (2006) A collection of breast cancer cell lines for the study of functionally distinct cancer subtypes. *Cancer Cell* 10(6):515-527.
30. Aronchik I, Bjeldanes LF, & Firestone GL (2010) Direct inhibition of elastase activity by indole-3-carbinol triggers a CD40-TRAF regulatory cascade that disrupts NF-kappaB transcriptional activity in human breast cancer cells. *Cancer Res* 70(12):4961-4971.
31. Brew CT, et al. (2006) Indole-3-carbinol activates the ATM signaling pathway independent of DNA damage to stabilize p53 and induce G1 arrest of human mammary epithelial cells. *Int J Cancer* 118(4):857-868.
32. Nguyen HH, et al. (2008) The dietary phytochemical indole-3-carbinol is a natural elastase enzymatic inhibitor that disrupts cyclin E protein processing. *Proc Natl Acad Sci USA* 105(50):19750-19755.
33. Brew CT, et al. (2009) Indole-3-carbinol inhibits MDA-MB-231 breast cancer cell motility and induces stress fibers and focal adhesion formation by activation of Rho kinase activity. *Int J Cancer* 124(10):2294-2302.
34. Marconett CN, et al. (2011) Indole-3-carbinol downregulation of telomerase gene expression requires the inhibition of estrogen receptor-alpha and Sp1 transcription factor interactions within the hTERT promoter and mediates the G1 cell cycle arrest of human breast cancer cells. *Carcinogenesis* 32(9):1315-1323.
35. Nguyen HH, et al. (2010) 1-Benzyl-indole-3-carbinol is a novel indole-3-carbinol derivative with significantly enhanced potency of anti-proliferative and anti-estrogenic properties in human breast cancer cells. *Chem Biol Interact* 186(3):255-266.

36. Tin AS, *et al.* (2012) Antiproliferative effects of artemisinin on human breast cancer cells requires the downregulated expression of the E2F1 transcription factor and loss of E2F1-target cell cycle genes. *Anticancer Drugs* 23(4):370-379.
37. Dawson PJ, Wolman SR, Tait L, Heppner GH, & Miller FR (1996) MCF10AT: a model for the evolution of cancer from proliferative breast disease. *The American journal of pathology* 148(1):313-319.
38. Firestone GL & Bjeldanes LF (2003) Indole-3-carbinol and 3-3'-diindolylmethane antiproliferative signaling pathways control cell-cycle gene transcription in human breast cancer cells by regulating promoter-Sp1 transcription factor interactions. *J Nutr* 133(7 Suppl):2448S-2455S.

Chapter II

Essential role of nucleostemin in indole-3-carbinol anti-proliferative targeting of breast cancer stem cells

ABSTRACT

Breast cancer serves as a classic example of cancer heterogeneity through cancer stem cells. For example, many estrogen sensitive breast cancer patients treated with conventional therapies like selective estrogen receptor modulators (SERMs) have been known to relapse and the cancer often returns as a more aggressive estrogen insensitive metastasis. This is attributed to the fact that the therapy only targets one subset of the overall population leaving behind another, more resistant subset. Given the specific stem cell features of self-renewal and differentiation, which can drive tumorigenesis and contribute to heterogeneity in tumor-initiating cells, a more rational approach in breast cancer prevention and treatment would be to target these specialized cells directly. Utilizing the 10AT-Her2 breast cancer stem cell model system we have identified indole-3-carbinol, a dietary small molecule phytochemical found in cruciferous vegetables of the *Brassica* genus, as a novel therapeutic capable of specifically targeting mammary cancer stem cells. Therapeutics able to specifically target the cancer stem cell phenotype would be strong candidates for breast cancer prevention. Co-immunoprecipitations and indirect immunofluorescence revealed that I3C treatment strongly stimulated protein interactions of nucleostemin, a nucleolar GTPase involved in the maintenance of cancer stem cells, with the p53 E3 ligase, MDM2. Upon I3C stimulation, nucleostemin sequestered MDM2 in the nucleoli, and disrupted MDM2 binding to p53. SiRNA knockdown of nucleostemin substantially disrupted the I3C apoptotic response by preventing the nucleolar localization of MDM2 and partially reversing the loss of MDM2 interactions with p53. I3C also results in the proteolytic degradation of Akt1 leading to the loss of MDM2 phosphorylation at serine-166. The cellular consequence of losing MDM2 phosphorylation, leads to the release of p53 to induce apoptosis. Furthermore, our results demonstrate that I3C requires the presence of nucleostemin to trigger its apoptotic response in the 10AT-Her2 cancer stem cell model system, thereby providing the first evidence that a natural anti-cancer molecule can target breast cancer stem cells by selectively altering the cellular interactions of an expressed stem cell marker protein. The implications of a naturally produced phytochemical capable of disrupting tumor-initiating cells is profound and has applications for a breast cancer preventative therapy. Elucidating the signaling pathway augmented by I3C will lead to a better understanding of breast cancer stem cell biology as well as establish a new preventative measure against breast cancer.

INTRODUCTION

Breast cancer is one of the most common malignancies in American women. Despite advances in early detection and adjuvant therapy, substantial proportions of patients are diagnosed with a heterogeneous, metastatic disease at initial presentation and often suffer a disease relapse (1-3). One of the difficulties in developing new therapeutic strategies for human breast cancer is the existence of several different classes of mammary tumors that differ in phenotype, proliferation, and responses to hormonal cues (4-6). Furthermore, many of the therapies lose effectiveness over time. The therapeutic limitations resulting from an intrinsic or acquired resistance to conventional therapies can be explained by the existence of cancer stem cells (CSC) or tumor-initiating cells (7).

Conventional therapies for breast cancer, like chemotherapy, radiotherapy, and hormone therapy, have had limited success with approximately half of women with early breast cancer suffering a relapse of the illness, often long after the primary treatment and remission (1, 2, 6). The mechanisms through which these cells reemerge have not yet been identified but underscore the need to investigate novel targeted therapies directed against CSC. The cancer stem cell hypothesis could not only explain tumor heterogeneity but also the recurrence, metastasis, and drug resistance.

A promising dietary anti-cancer molecule is indole-3-carbinol (I3C), which is derived by hydrolysis from glucobrassicin in Brassica vegetables. I3C has chemopreventative as well as potent anti-tumor properties in a wide range of reproductive cancer types (8-11). Exposing human cancer cells to I3C initiates a complex series of transcriptional, enzymatic, and metabolic set of signals that leads to cell cycle arrest and apoptosis. Although the precise mechanisms that account for the tumor-specific targeting by I3C is not well understood, we propose I3C may act directly to antagonize CSC formation and propagation. In addition to activating distinct sets of anti-proliferative signaling cascades in a wide range of human breast cancer cells (9-19), I3C inhibits the *in vivo* growth of human breast cancer cell-derived tumor xenografts in athymic mice (16), and reduces tumor metastasis and breast cancer cell migration (13, 15).

Utilizing the established 10AT-Her2 cancer stem cell model system, with a CD44⁺/CD24^{-/low} phenotype as well as active ALDH-1 and nucleostemin, we demonstrate that I3C induces an apoptotic effect mediated by preventing the protein-protein interactions between the MDM2 and p53. This process is dependent on the proteolytic degradation of Akt1 induced by I3C. We further functionally document that the stem cell marker nucleostemin is required for I3C to trigger its antiproliferative response in cancer stem cells. Furthermore, the interactions of nucleostemin, MDM2, and p53 play a critical role regulating mammary CSC and may serve as a key component for future therapies targeting mammary CSC. The levels of nucleostemin are critical for the maintenance of cellular homeostasis in stem cells and cancer stem cells, however, at present, the cellular function and regulation of nucleostemin remains unclear (20-23). Conflicting evidence has shown that either elevated or decreased levels of nucleostemin can lead to cellular outcomes such as differentiation, cell cycle arrest, and apoptosis (20, 22, 23). Thus, the targeting of

nucleostemin may be critical to developing anticancer therapies against cancer stem cells in the future.

Effective therapeutic treatments for cancer stem cells have been difficult and elusive because the molecular alterations identified thus far have been nonuniform. I3C is the first naturally occurring small molecule phytochemical capable of directly targeting cancer stem cells and understanding its molecular targets may lead to the development of additional targets and effective cancer therapies.

MATERIALS AND METHODS

Cell Culture

The MCF-10AT parent cell line and the 10AT-Her2 and 10AT-Neo cell lines were cultured in DMEM/F-12, 10% fetal bovine serum, 50 U/mL penicillin, 50 U/mL streptomycin (all media components purchased from Lonza, Allendale, NJ, and cell culture plates purchased from NUNC-Fischer, Pittsburgh, PA), 0.02 µg/mL epidermal growth factor (purchased from Promega, Madison, Wisconsin, USA), 0.05 µg/mL hydrocortisone, 10 µg/mL insulin, and 0.1 µg/mL cholera toxin (obtained from Sigma-Aldrich). Cells were grown to subconfluency in a humidified chamber at 37°C containing 5% CO₂. For drug treatments, a 200 mmol/l stock solution of I3C, 10 mmol/l stock solution of 1-benzyl I3C, 50 mmol/l stock solution of Diindolymethane (DIM), 200 mmol/l stock solution of Tryptophol, and 300 mmol/l stock solution of Artemisinin (purchased from Sigma-Aldrich, St. Louis, MO) was dissolved in dimethyl sulfoxide (DMSO) and then diluted in the ratio 1:1000 in media before culture plate application. Before each drug treatment, cells are washed in ice cold phosphate-buffered saline (PBS) (obtained from Lonza).

Expression Plasmids and Transfections

Human cytomegalovirus (CMV)-HER2 expression plasmid and the constitutively active Akt1 (CA-Akt1) expression plasmid was a kind gift from Dr. Leonard Bjeldanes, (Department of Nutritional Sciences and Toxicology, University of California at Berkeley). CMV-p53 dominant negative was a kind gift from Dr. Lin He (Department of Molecular and Cell Biology, University of California Berkeley). Transfection of expression vectors were performed using Superfect transfection reagent from QIAGEN per the manufacturers' recommended protocol.

Cell Proliferation assay

Sensitivity of cells to I3C was examined using the Cell-Counting Kit-8 (Dojindo, Japan) following manufacturer's protocol. Cells were plated at a density of 5000–7000 cells per well in 24-well plates containing 500 µl of culture medium. After indicated treatment and incubation times at 37°C, 50 µL CCK-8 reagent was then added into each well and incubated for 2 hours before reading at a wavelength of 450 nm.

Reverse Transcription and Polymerase Chain Reaction

10AT-Her2 cells treated with indicated doses of artemisinin and duration were harvested in Trizol (Invitrogen), and total RNA was extracted according to the manufacturer's protocol. This was quantified and 1 mg of total RNA was used for reverse transcription using Mu-MLV reverse transcriptase (Invitrogen) and random hexamers according to manufacturer's protocol. The cDNA pool was used (2 ml) in polymerase chain reaction and was amplified with primers of the following sequences:

Akt1 Forward: 5'-ACATCATCTCGTACATGACGA-3'

Akt1 Reverse: 5'-TGAGATTGTGTCAGCCCTGGA-3'

GAPDH Forward: 5'-TGAAGGTCGGAGTCAACGGATTTG-3'

GAPDH Reverse: 5'-CATGTGGGCCATGAGGTCCACCAC-3'

20 mL of this reaction PCR product was electrophoresed on a 1% agarose gel and visualized using a UV transilluminator.

Western Blots

After the indicated treatments, cells were harvested in radioimmune precipitation assay buffer (150 mM NaCl, 0.5% deoxycholate, 0.1% NoNidet-p40 (Nonidet P-40, Fluta Biochemitra, Switzerland), 0.1% SDS, 50 mM Tris) containing protease and phosphatase inhibitors (50 g/ml phenylmethylsulfonyl fluoride, 10 g/mL aprotinin, 5 g/mL leupeptin, 0.1 g/mL NaF, 1 mM dithiothreitol, 0.1 mM sodium orthovanadate, and 0.1 mM glycerol phosphate). Equal amounts of total cellular protein were mixed with loading buffer (25% glycerol, 0.075% SDS, 1.25 ml of 14.4M β mercaptoethanol, 10% bromphenol blue, 3.13% 0.5M Tris-HCl, and 0.4% SDS (pH 6.8)) and fractionated on 10% polyacrylamide/0.1% SDS resolving gels by electrophoresis. Rainbow marker (Amersham Biosciences) was used as the molecular weight standard. Proteins were electrically transferred to nitrocellulose membranes (Micron Separations, Inc., Westboro, MA) and blocked for 1 hour with Western wash buffer (5% NFDM (10 mM Tris-HCl (pH 8.0), 150 mM NaCl, and 0.05% Tween 20, 5% nonfat dry milk). Protein blots were subsequently incubated for overnight at 4°C in primary antibodies. The antibodies used were as follows, Rabbit anti-Nucleostemin, (sc-67012), Mouse anti-CD44 (sc-65412), Mouse anti-CD-24 (sc-70598), Goat anti-ALDH-1 (sc-22588), were purchased from Santa Cruz Biotechnology and diluted in the ratio 1:1000 in TBST. Rabbit anti-actin (AAN01; Cytoskeleton, Denver CO) was diluted 1:1000 in TBST and used as a gel-loading control. Rabbit anti-HER2 (2165) was obtained from Cell Signaling. The working concentration for all antibodies was 1 μ g/mL in Western wash buffer. Immunoreactive proteins were detected after incubation with horseradish peroxidase conjugated secondary antibody diluted to 3×10^4 in Western wash buffer (goat anti-rabbit IgG, rabbit anti-goat IgG, and rabbit anti-mouse IgG (Bio-Rad)). Blots were treated with enhanced chemiluminescence reagents (PerkinElmer Life Sciences), and all proteins were detected by autoradiography. Equal protein loading was confirmed by Ponceau S staining of blotted membranes.

Flow cytometry

To monitor the cell population DNA content, 4×10^4 of each cultured cell lines were plated onto Nunc six-well tissue culture dishes (NUNC-Fischer, Pittsburgh, PA). Triplicate samples were treated with indicated concentrations and durations of artemisinin. The medium was changed every 24 hours. Incubated cells were hypotonically lysed in 1 mL of DNA staining solution (0.5 mg/mL propidium iodide, 0.1% sodium citrate, and 0.05% Triton X-100) Lysates were filtered using 60 μ m Nitex flow mesh (Sefar America, Kansas City, MO) to remove cell membranes. Propidium iodide-stained nuclei were detected using a PL-2 detector with a 575 nm band pass filter on a Beckman-Coulter (Fullerton, CA) fluorescence-activated cell sorter analyzer with laser output adjusted to deliver 15 megawatts at 488 nm. Ten thousand nuclei were analyzed from each sample at a rate of \sim 600 nuclei per second. The percentages of cells within the G1, S, and G2/M phases of the cell cycle were determined by analyzing the histogram output with the multicycle computer program MPLUS, provided by Phoenix Flow Systems (San Diego, CA), in the Cancer Research Laboratory Microchemical Facility at the University of California at Berkeley.

Co-immunoprecipitation

After the indicated treatments, immunoprecipitations were performed as described previously (24). Precleared samples were then incubated with 50 µg of mouse anti-MDM2 or 50 µg of rabbit anti-nucleostemin overnight at 4°C. Immunoprecipitated protein was eluted from beads by addition of gel loading buffer (50 mM Tris-HCl, pH 6.8, 2% SDS, 10% glycerol, 1% β-mercaptoethanol, 12.5 mM EDTA, 0.02 mM bromophenol blue) and heating the sample at 100°C for 5 min. Samples were analyzed by Western blot.

Small Interfering RNA (siRNA)

Cells were grown and indicated treatments performed on 10-cm tissue culture plates from Nalgene Nunc International (Rochester, CA). Once cells reached 50% confluence, transfection with siRNA constructs was performed following transfection reagent manufacturer's protocol using HiPerfect with control siRNA or nucleostemin-specific siRNA (all purchased from QIAGEN, Valencia, CA).

Nuclear Extraction

10AT-Her2 cells were grown and indicated treatments were performed on 10 cm plates. Once harvested with ice cold PBS, nuclear extractions were performed using the manufacturer's protocol and guidelines (Thermo Scientific, Rockford, IL). Samples were analyzed by western blot.

Indirect Immunofluorescence

Cells were grown and indicated treatments performed on two-well chamber slides from Nalgene Nunc International. The cells were fixed with 3.75% formaldehyde in PBS for 15 min at room temperature. After three additional washes with PBS, the plasma membrane was permeabilized with 0.1% Triton-X-100, 10 mM Tris-HCl, pH 7.5, 120 mM sodium chloride, 25 mM potassium chloride, 2 mM EGTA, and 2 mM EDTA) for 10 min at room temperature. Slides were incubated with 3% bovine serum albumin (Sigma-Aldrich) before incubation with primary antibodies. Rabbit anti-nucleostemin antibody and mouse anti-MDM2 antibody was used at a 1:400 dilution. Secondary Alexa 488 anti-rabbit and Texas Red-conjugated phalloidin were used at 1:400 dilutions each. Stained cells mounted with Vectashield mounting medium containing 4,6-diamidino-2-phenylindole (DAPI) (Vector Laboratories, Burlingame, CA). Stained and mounted cells were then processed with an Axioplan epifluorescence microscope (Carl Zeiss, Thornwood, NY). The images were acquired and processed by M1/Hamamatsu Orca and QImaging MicroPublisher color cameras.

RESULTS

I3C induced p53-dependent apoptotic response in the stem cell-like 10AT-Her2 cell line.

To initially assess I3C anti-proliferative responsiveness, 10AT-Her2 cells and control 10AT-Neo cells cultured in adherent monolayers were treated with or without 200 μ M I3C over a 72 hour time course and total cell number determined by a CCK-8 assay (25). I3C rapidly inhibited the proliferation of 10AT-Her2 cells with a maximal response observed by 72 hours (Figure 16, left panel), although proliferation of the control 10AT-Neo cells remained relatively unaffected by I3C treatment (Fig 16, right panel). Under these conditions, I3C induced a significant increase in 10AT-Her2 cells with a sub-G1 DNA content, indicating the activation of apoptosis (Figure 17), and did not alter expression level of the stem markers CD44, CD24, ALDH1 and nucleostemin (Figure 7), showing that I3C treatment does not disrupt the cancer stem cell phenotype. As shown in Figure 18, western blot analysis verified the apoptotic response and revealed that I3C induced PARP cleavage in 10AT-Her2 cells, which is a substrate of activated caspase 3 in the apoptotic pathway (26). The control 10AT-Neo cells remain resistant to all anti-proliferative effects of I3C. Interestingly, p53 levels in 10AT-Her2 are significantly higher than 10AT-Neo cells and I3C has no effect on the level of p53 protein expression.

Figure 16

I3C inhibits 10AT-Her2 cell proliferation.

10AT-Her2 and 10AT-Neo cells were treated with or without 200 μ M I3C for the indicated durations and cell number was quantified by the CCK-8 proliferation assay.

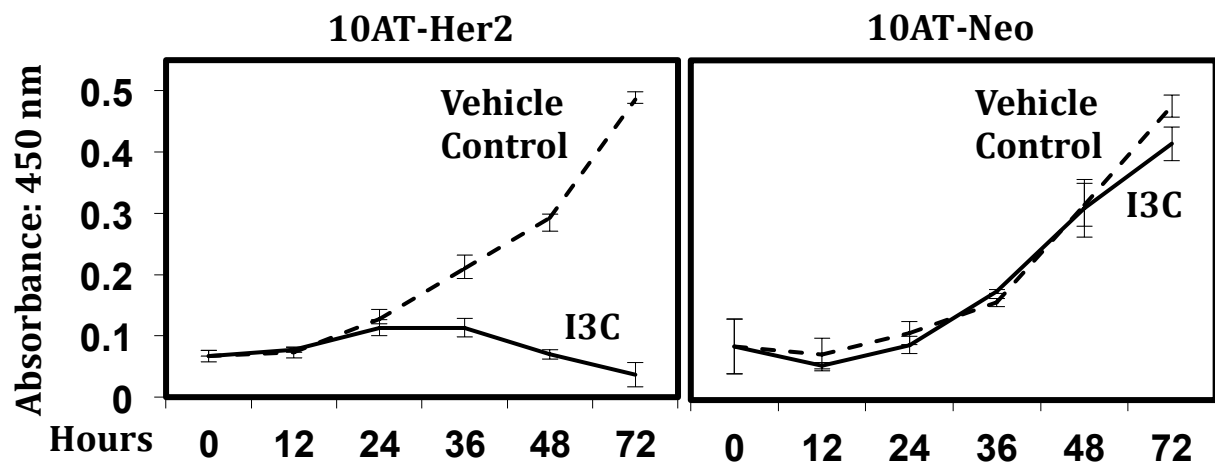


Figure 17

Flow cytometry analysis of the I3C induced apoptotic effects on 10AT-Her2 cells. 10AT-Her2 and 10AT-Neo cells were treated with or without 200 μ M I3C for 48 hours, cells lysed in hypotonic propidium iodide, and DNA content determined by flow cytometry.

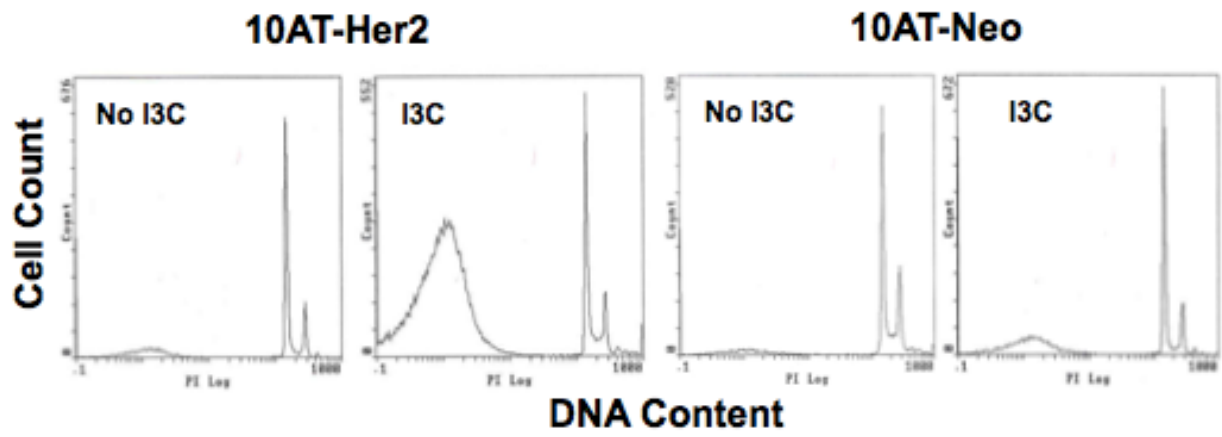
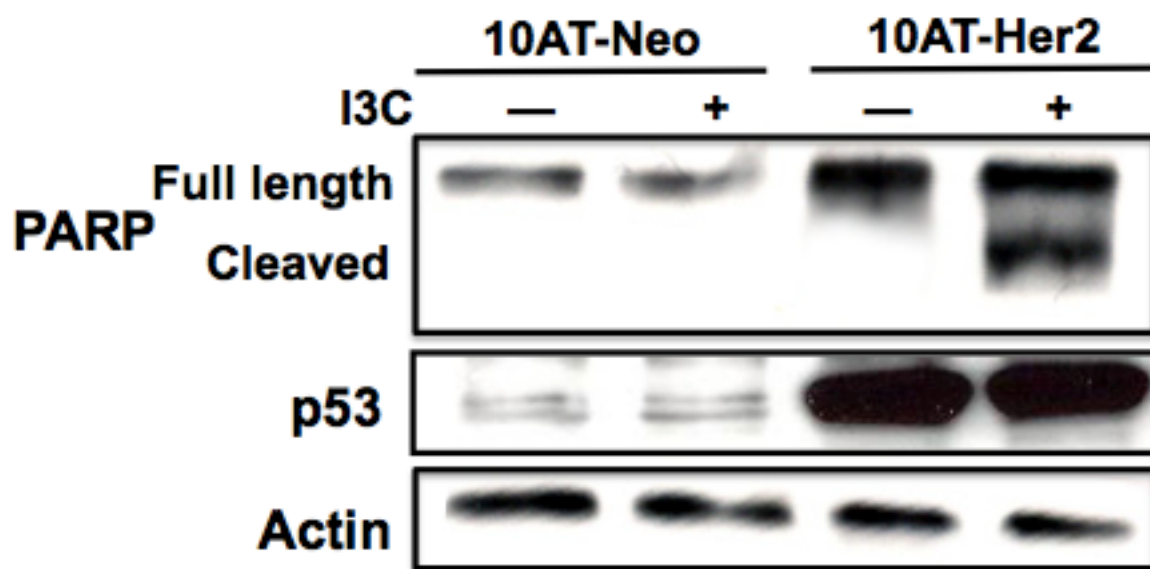


Figure 18

I3C induces PARP cleavage in 10AT-Her2 breast cancer stem cells.

10AT-Neo and 10AT-Her2 cells were treated with or without 200 μ M I3C for 48 hours, and total cell extracts were electrophoretically fractionated and western blots probed for PARP, p53 and the actin gel loading control.



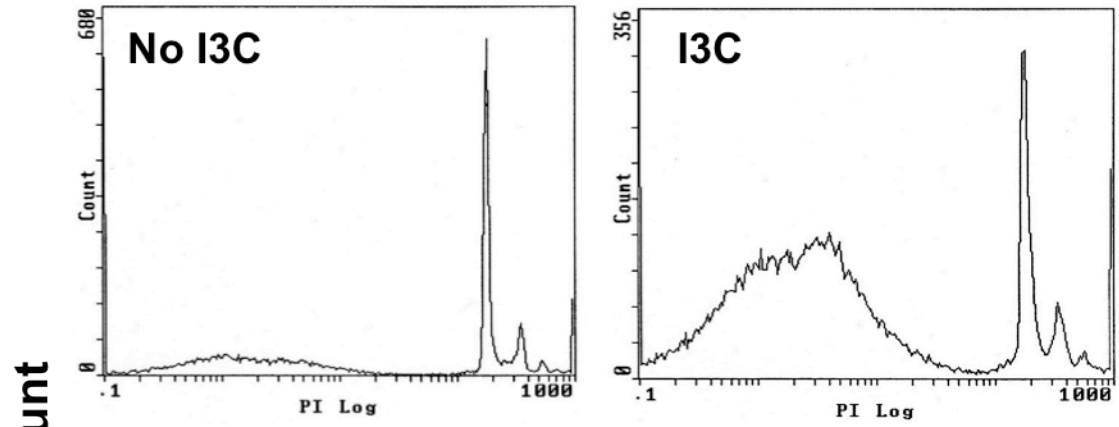
The p53 tumor suppressor gene, also known as the guardian of the genome, plays a critical role in the control of cellular apoptosis and regulates genes involved in the cell cycle and proliferation (27). While, I3C treatment did not alter the level of p53 expressed in 10AT-Her2 cells, its activation or subcellular localization may be altered which is not detectable by western blot analysis. To functionally assess the role of p53 in the I3C apoptotic response, 10AT-Her2 cells were transfected with a dominant negative form of p53 (DNp53) that is known to disrupt p53 function (28) or with an empty expression vector. As shown in Figure 19, flow cytometry of I3C treated and untreated cells demonstrated that expression of dominant negative p53 prevented the I3C apoptotic response, whereas I3C efficiently induced apoptosis of 10AT-Her2 cells transfected with the empty vector. These results show that I3C triggers its anti-proliferative signaling in 10AT-Her2 cells through a p53-dependent response that we propose requires an upstream component of p53 pathway that is associated with the cancer stem cell phenotype.

Figure 19

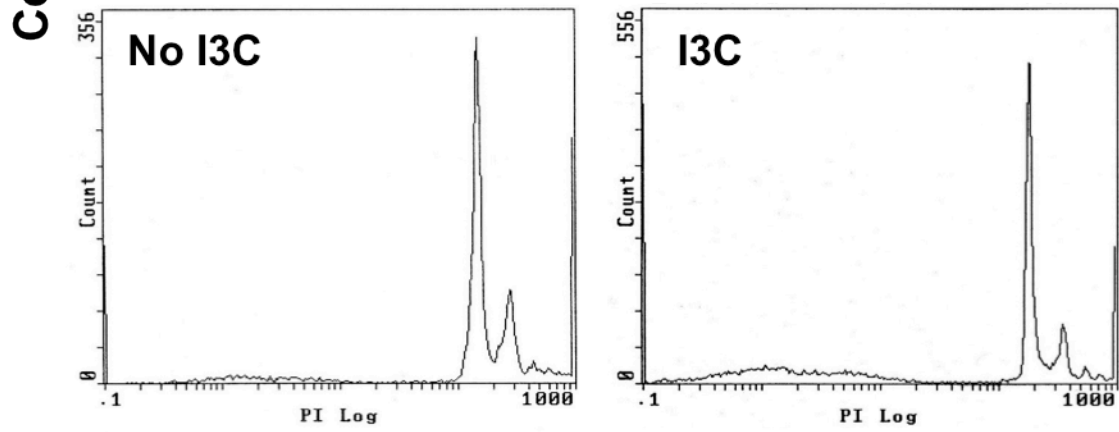
I3C induced apoptotic response is mediated by p53.

10AT-Her2 cells were transfected with either a dominant negative p53 (DNp53) expression vector or with the empty vector control (empty), and then treated with or without 200 μ M I3C for 48 hours. DNA content was assessed by flow cytometry.

Empty Vector



DN p53



DNA Content

I3C promotes the interaction of the stem cell marker protein nucleostemin with the MDM2 inhibitor of p53 and disrupts the MDM2-p53 interaction.

One molecular marker highly expressed in self-renewing cancer stem cells that is generally associated with the p53 pathway is nucleostemin (21), which is a nucleolar GTPase that can bind to MDM2, an inhibitor of p53 (20). MDM2 is an E3 ligase and the phosphorylated form of MDM2 prevents the apoptotic activity of p53 by binding to and sequestering p53 away from its pro-apoptotic targets (29). I3C has no effect on the relatively high levels of nucleostemin expressed in 10AT-Her2 cells (Figure 7). To examine whether I3C regulates nucleostemin protein-protein interactions, nucleostemin was immunoprecipitated from I3C treated or untreated 10AT-Her2 cells and MDM2 binding was detected by western blot analysis of electrophoretically fractionated nucleostemin. As shown in Figure 20, I3C treatment strongly enhanced nucleostemin interactions with both the Ser166 phosphorylated MDM2 protein and of total MDM2 protein, even though I3C treatment down-regulated the phosphorylated form of MDM2. Co-immunoprecipitation analysis, in which immunoprecipitated MDM2 was examined for its interactions with p53 by western blots, showed that I3C treatment of 10AT-Her2 cells ablated MDM2 interactions with p53 (Figure 21), and thereby likely freeing p53 to trigger an apoptotic response.

Figure 20

I3C induces nucleostemin-mdm2 interactions in cancer stem cells.

10AT-Her2 cells were treated with or without 200 μ M I3C for 48 hours. Total cell extracts were immunoprecipitated with nucleostemin antibodies. As a control, non-immune antibodies (IgG) and samples not immunoprecipitated (No IP) were used. All extracts were electrophoretically fractionated and probed by western blot analysis. Antibodies specific to either serine-166 phosphorylated MDM2 or total MDM2 were used.

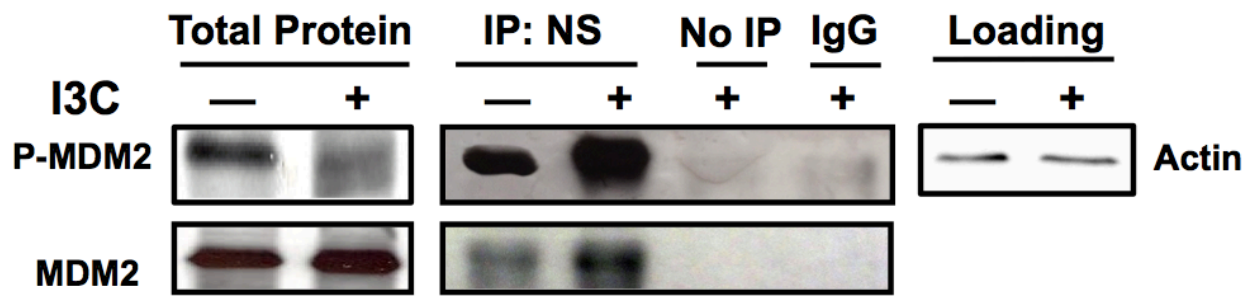
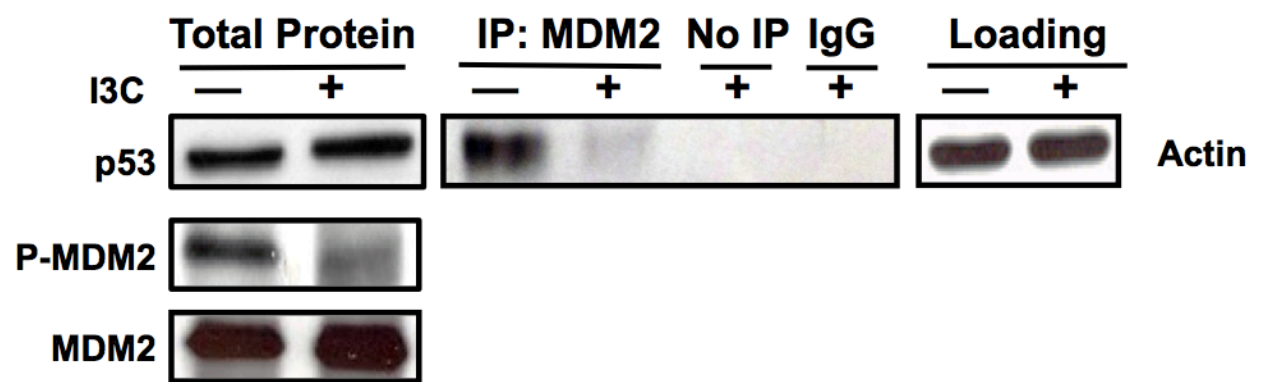


Figure 21

I3C releases p53 from its E3 ligase, MDM2 in cancer stem cells.

10AT-Her2 cells were treated with or without 200 μ M I3C for 48 hours. Total cell extracts were immunoprecipitated with MDM2 antibodies. As a control, non-immune antibodies (IgG) and samples not immunoprecipitated (No IP) were used. All extracts were electrophoretically fractionated and probed by western blot analysis. Antibodies specific to p53, Serine-166 phosphorylated MDM2 or total MDM2 were used.



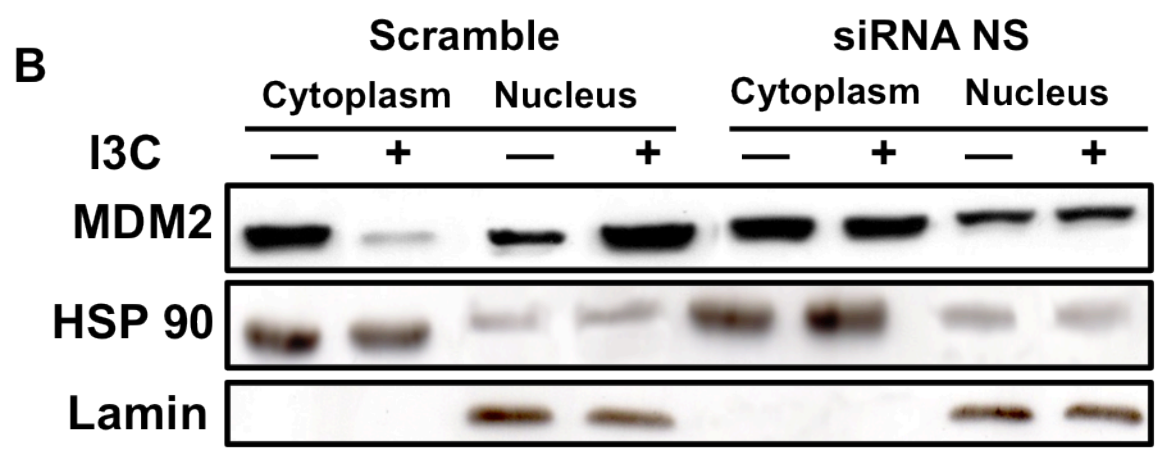
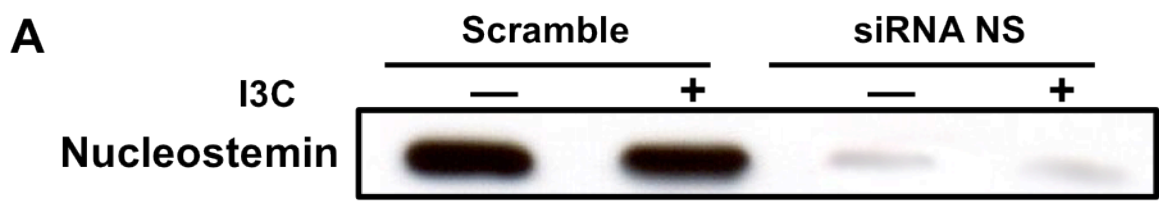
Interfering RNA knockdown of nucleostemin disrupts the I3C stimulated nucleolar localization of MDM2.

Given that nucleostemin resides in the nucleolus (21) and MDM2 translocates between the cytoplasm and nucleus (29), an intriguing issue is whether the I3C induced nucleostemin-MDM2 interaction drives the localization of MDM2 to the nucleus in I3C treated cells. This possibility was functionally examined after siRNA knockdown of nucleostemin production. Western blots showed that transfection of nucleostemin siRNA efficiently reduced the levels of nucleostemin compared to cells receiving scrambled siRNA (Figure 22A). The localization of MDM2 was initially examined in cells treated with or without I3C and then biochemically fractionated into nuclear and cytoplasmic extracts. Western blots showed that in cells transfected with scrambled siRNA, I3C treatment causes the re-localization of MDM2 from both the cytoplasmic and nuclear fractions into predominantly the nuclear fraction (Figure 22B). In contrast, knockdown of nucleostemin prevented the I3C induced re-localization of MDM2. Under each of these conditions, the cytoplasmic fraction remained enriched in the cytoplasmic marker HSP90, whereas, the nuclear compartment was enriched in nuclear marker lamin.

Figure 22

I3C induced MDM2 translocation into the nucleus requires nucleostemin expression.

10AT-Her2 cells were transfected with control scramble siRNA or nucleostemin siRNA, and then treated with or without 200 μ M I3C for 48 hours. (A) The level of nucleostemin protein was determined by western blot analysis. (B) Cell extracts were biochemically separated into nuclear enriched and cytoplasmic fractions, electrophoretically fractionated, and western blots probed with antibodies specific for MDM2, the cytoplasmic marker HSP90 and the nuclear marker lamin.

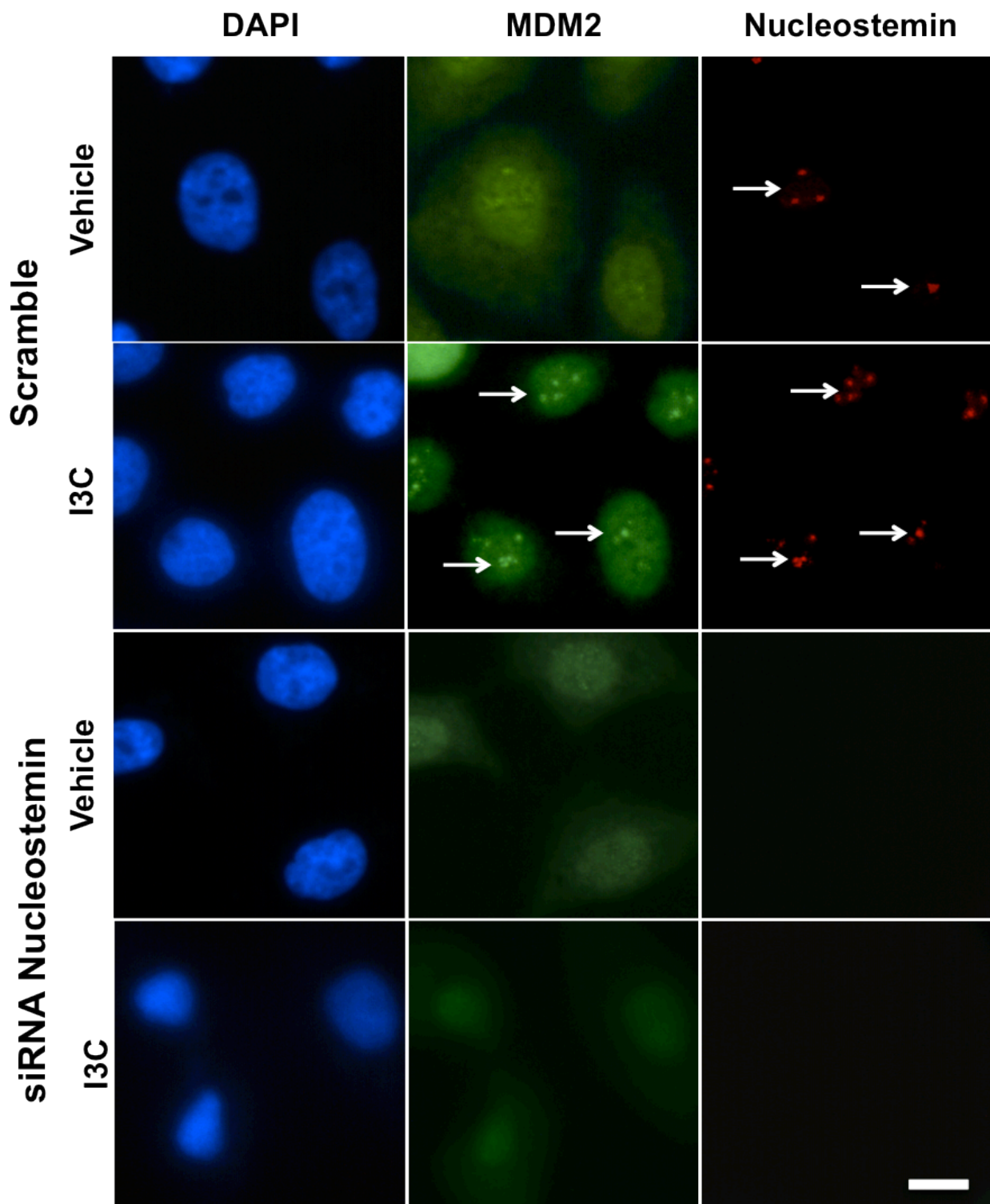


In 10AT-Her2 cells transfected with scrambled siRNA, indirect immunofluorescence revealed that nucleostemin is localized to punctate foci in the nucleus in the presence or absence of I3C, which is indicative of the nucleolus compartment (Figure 23, top panels). Strikingly, I3C treatment triggered the redistribution of MDM2 from being generally distributed to the nucleus and cytoplasm, to an enriched punctate staining pattern as foci in the nucleus. Nucleostemin and MDM2 co-localize into essentially identical foci staining patterns (see arrows in top panel set). Importantly, siRNA knockdown of nucleostemin completely disrupted the nuclear foci staining of MDM2 in I3C treated cells, and the overall localization of MDM2 resembled that observed in cells not treated with I3C (Figure 23, bottom panels).

Figure 23

MDM2 translocates into the nucleus and colocalizes with nucleostemin foci upon I3C treatment.

The subcellular localization of MDM2 and nucleostemin was determined by indirect immunofluorescence microscopy. DAPI staining was used to visualize DNA stained nuclei. The bar represents 4 microns.



Interfering RNA knockdown of nucleostemin strongly attenuates the I3C induced apoptotic response and partially reverses the disruption of MDM2-p53 interactions in 10AT-Her2 cells.

To determine whether the I3C apoptotic response in 10AT-Her2 cells requires nucleostemin, cells transfected with either nucleostemin or scrambled siRNA were treated with or without I3C and the effects on cellular DNA content monitored by flow cytometry over a 48-hour time course. The relative apoptotic response was quantified as the ratio of sub-G1 content DNA in untreated to I3C treated cells. As shown in Figure 24, siRNA knockdown of nucleostemin significantly attenuated the apoptotic response observed in cells transfected with scrambled siRNA. Beyond 48 hours, the efficiency of the siRNA knockdown becomes diminished and therefore the experiment did not go beyond this time point. Co-immunoprecipitations of 48 hour I3C treated and untreated cells demonstrated that knockdown of nucleostemin production partially reversed the I3C disruption of MDM2-p53 protein interactions (Figure 25). The level of MDM2 binding to p53 observed in vehicle control treated cells with scrambled siRNA was approximately the same as the level of interactions detected in I3C treated cells transfected with nucleostemin siRNA (Figure 25). Taken together, these results demonstrate that I3C requires nucleostemin to mediate its anti-proliferative signaling through the p53 apoptotic pathway in stem cell-like 10AT-Her2 cells.

Figure 24

Nucleostemin knockdown diminishes I3C induced release of p53 from MDM2.

10AT-Her2 cells were transfected with either scrambled siRNA or nucleostemin specific siRNA, and then treated with or without 200 μ M I3C for 48 hours. Total cell extracts were immunoprecipitated with MDM2 antibodies, electrophoretically fractionated and western blots probed with p53 specific antibodies. Negative controls were immunoprecipitations carried out with non-immune antibodies (IgG) or samples that were not immunoprecipitated (No IP). Western blots of total cell extracts (Total Protein) were analyzed for p53, serine-166 phosphorylated MDM2 and total MDM2.

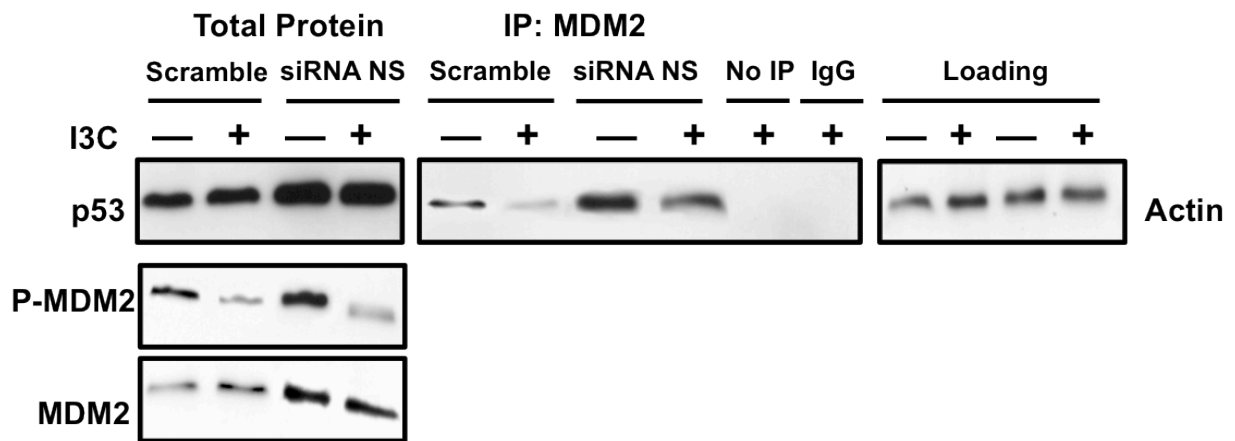
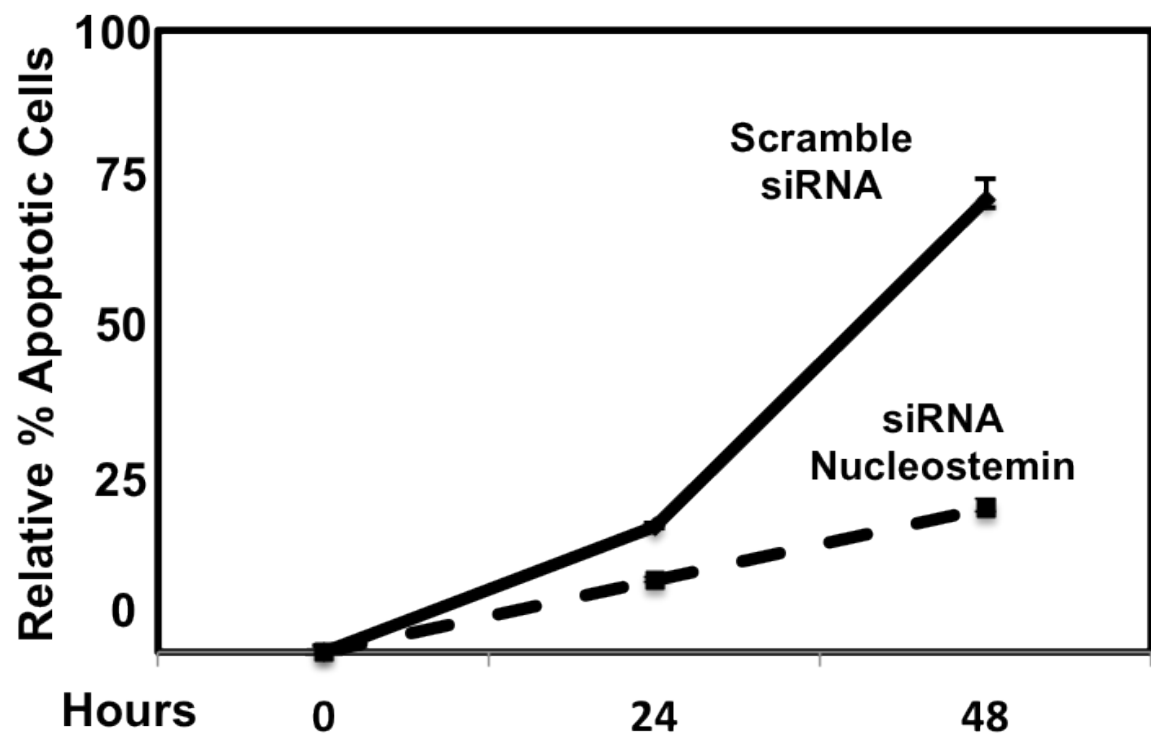


Figure 25

Nucleostemin siRNA overrides the I3C induced apoptosis in cancer stem cells. 10AT-Her2 cells transfected with nucleostemin siRNA or with scrambled siRNA control were treated with or without 200 μ M I3C for the indicated durations and cell number was quantified by CCK-8 proliferation assay. The amount of apoptotic cells treated with I3C were normalized to DMSO vehicle control treated cells.



I3C downregulates Akt1 protein level by altering protein stability.

While nucleostemin is clearly required for I3C to induce apoptosis via p53 activation, regardless of the status of nucleostemin, I3C inhibits MDM2 phosphorylation. Given that MDM2 phosphorylation at serine 166 is required for its activation and ability to inhibit p53, we examined Akt1, the kinase responsible for phosphorylating and activating MDM2. In 10AT-Her2 breast cancer stem cells, treatment with I3C results in a dramatic downregulation of Akt1 protein levels but no effect on mRNA transcript levels (Figure 26), suggesting the decrease in protein levels observed may have to deal with protein stability of Akt1. Akt1 levels in the control 10AT-Neo cells remain unaltered by I3C. To investigate whether I3C alters the turnover of Akt1, we co-treated 10AT-Her2 cells with 5 μ M MG 132, a proteasome inhibitor in the presence or absence of I3C. Immunoprecipitation of Akt1 showed a recovery in Akt1 levels in the presence of MG 132 even with treatment of I3C as well as an increase in the ubiquitination of Akt1 (Figure 27). Given that MG 132 does not affect the proteasomal tag targeting Akt1 for degradation, we can conclude that ultimately I3C targets Akt1 for proteasomal degradation. Ultimately, this suggests that I3C induction of apoptosis is predicated on the ability of Akt1 to phosphorylate and activate MDM2 and thus inhibit the effects of p53.

Figure 26

I3C downregulates Akt1 expression at the protein level.

10AT-Her2 and 10AT-Neo cells were treated with or without 200 μ M I3C for 48 hours. To assess I3C regulation at the protein level, total cell extracts were electrophoretically fractionated and western blots probed for Akt1 and the actin gel loading control. To assess I3C regulation at the transcript level, total RNA was isolated. The transcript levels of Akt1 and GAPDH were determined by reverse transcription-polymerase chain reaction using specific primers and the products fractionated by electrophoresis on a 1.5% agarose gel and visualized on an ultraviolet transilluminator. GAPDH served as a gel loading control.

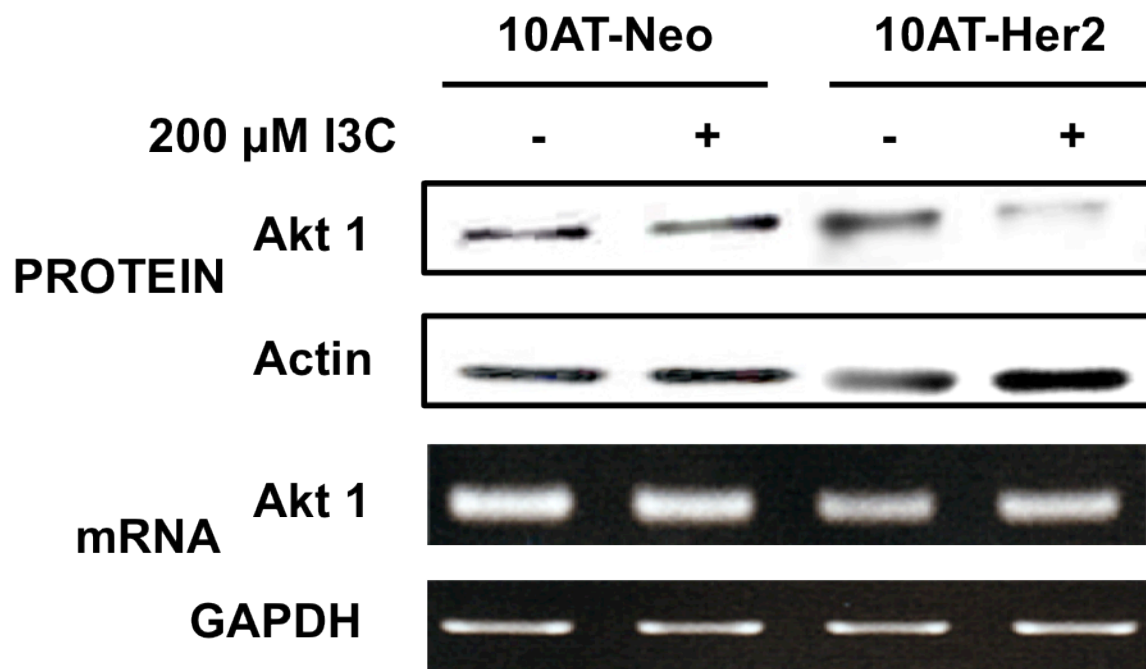
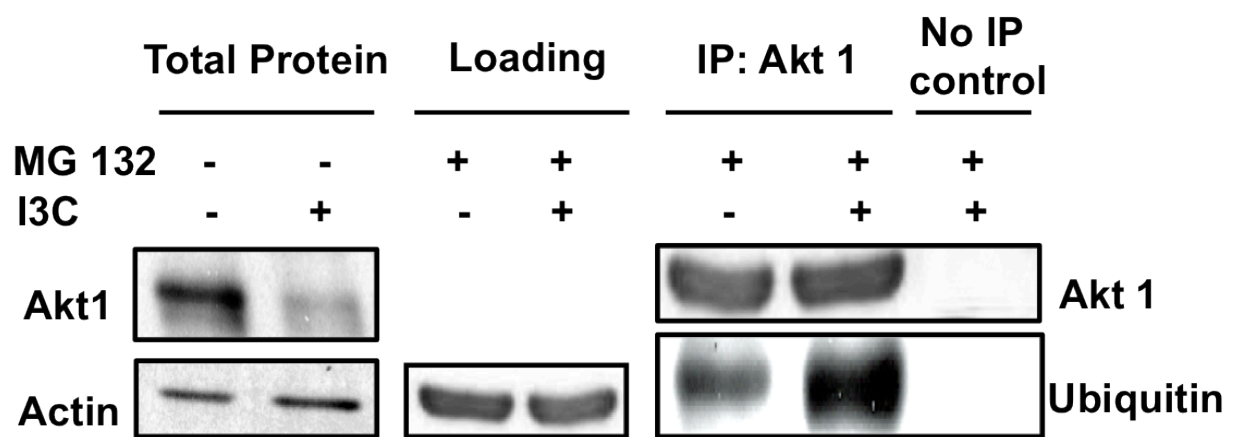


Figure 27

I3C induces the ubiquitination and 26S proteasome degradation of Akt1.

10AT-Her2 cells were treated with the indicated combinations of 200 μ M I3C and 5 mM MG132. Total cell extracts were immunoprecipitated with mouse- anti Akt1 antibodies and electrophoretically fractionated samples blotted with either rabbit-anti-Akt1, rabbit-anti-ubiquitin antibodies, or rabbit-anti-actin. Results were repeated three times, representative blot shown. Actin served as a gel loading control.



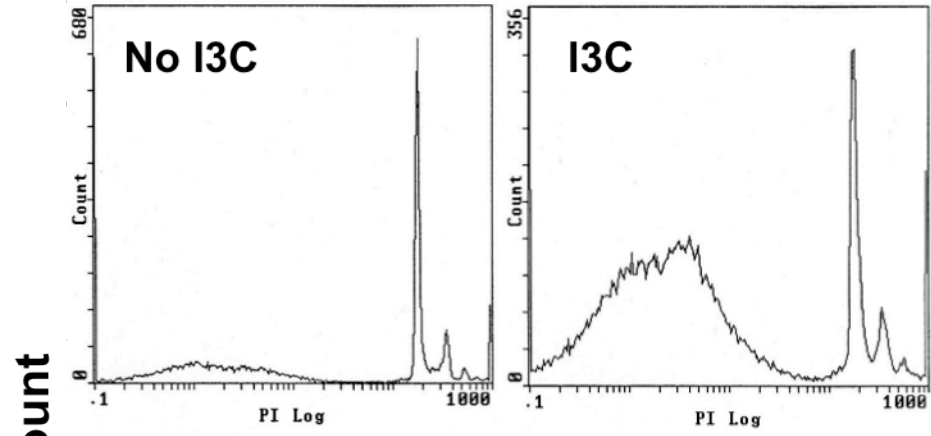
In order to verify that the apoptotic I3C effect is a direct response to the Akt1 degradation and subsequent loss of MDM2 phosphorylation to release the apoptotic effect by p53, we transiently transfected either constitutively active Akt1 or the empty vector control into 10AT-Her2 cells and measured their apoptotic response to I3C stimulus by flow cytometry. Constitutively active Akt1 was able to partially override the I3C induced apoptotic response (Figure 28). 10AT-Her2 cells transfected with the empty vector control resulted in apoptosis with I3C treatment. One possible explanation for why constitutively active Akt1 is not able to fully recover the apoptotic response may have to do with MDM2 sequestration by nucleostemin. Altogether, this result suggests that I3C downregulation of Akt1 protein levels prevents phosphorylation and activation of MDM2 and thus allows p53 to induce apoptosis. To functionally test the robustness of the protein-protein interactions, 10AT-Her2 cells were transfected with either constitutively active Akt1 or an empty vector control and Akt1 was subsequently immunoprecipitated from MDM2 (Figure 29A). As expected, co-immunoprecipitation of MDM2 shows a decrease in the interactions with Akt1 upon treatment with I3C. To test the molecular consequence of Akt1 on nucleostemin, a necessary component in regulating cancer stem cells, MDM2, and the I3C response, the same experiment was repeated except nucleostemin was immunoprecipitated from 10AT-Her2 cells (Figure 29B). In spite of transfecting constitutively active Akt1, I3C still increased the interactions between MDM2 and nucleostemin, which can also account for why constitutively active Akt1 can only partially reverse the I3C apoptotic response.

Figure 28

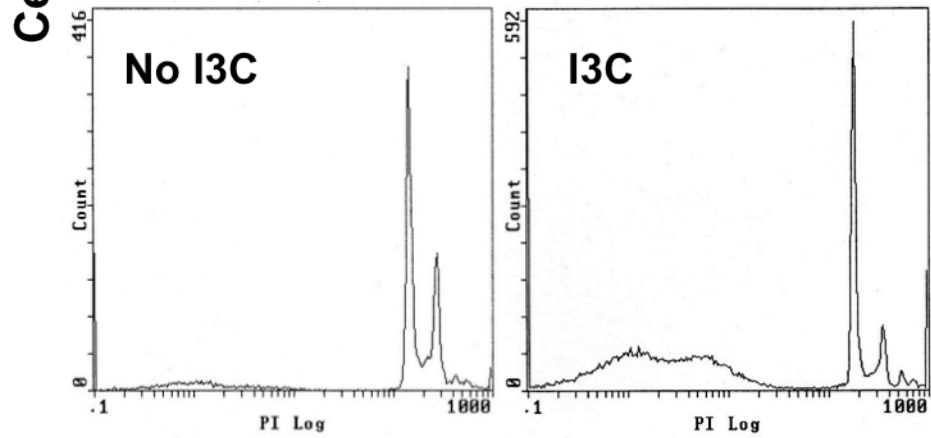
Constitutively active Akt1 can partially override the I3C induced apoptotic response.

10AT-Her2 cells were transfected with either a constitutively active Akt1 expression vector or with the empty vector control, and then treated with or without 200 μ M I3C for 48 hours. DNA content was assessed by flow cytometry.

Empty Vector



Constitutively Active Akt1

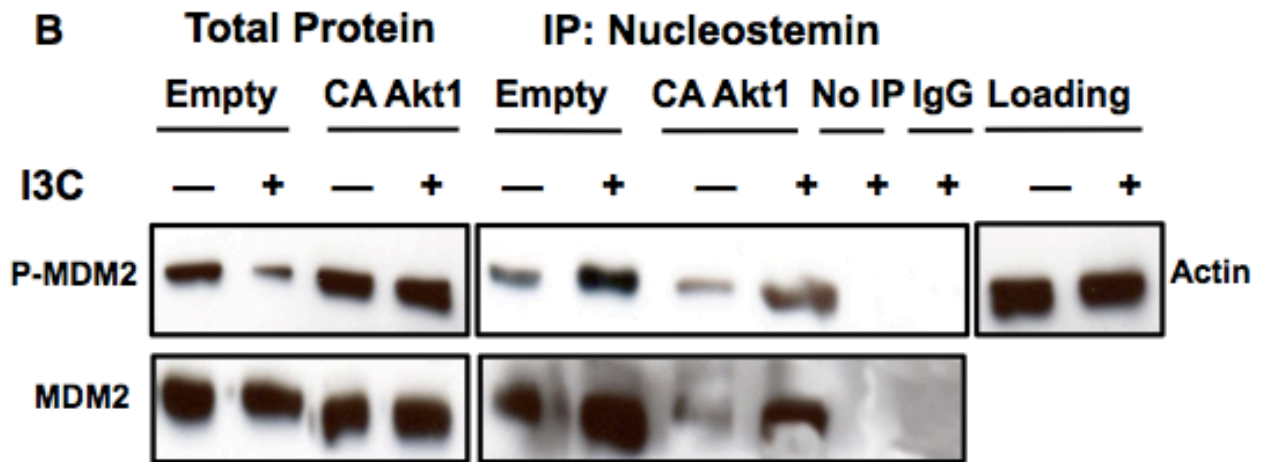
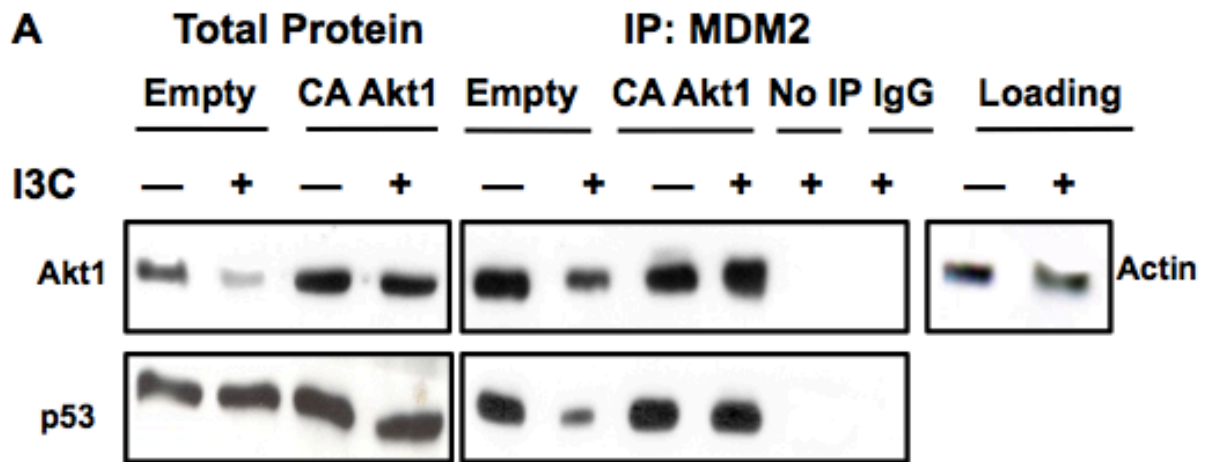


DNA Content

Figure 29

Constitutively active Akt1 alters I3C regulation on the molecular interactions between nucleostemin, MDM2, and p53.

10AT-Her2 cells were transfected with either constitutively active Akt1 or an empty vector control and then treated with or without 200 μ M I3C for 48 hours. Total cell extracts were immunoprecipitated with MDM2 (A) or nucleostemin (B) antibodies, electrophoretically fractionated and western blots probed with Akt1, p53 serine-166 phosphorylated MDM2, total MDM2, or actin specific antibodies as indicated. Negative controls were immunoprecipitations carried out with non-immune antibodies (IgG) or samples that were not immunoprecipitated (No IP).



DISCUSSION

Our model describes a breast cancer stem cell model that is responsive to I3C and inhibited by two mechanisms of action. Characterization of the 10AT-Her2 cell system provided the first direct evidence that I3C signaling promotes interactions of nucleostemin with the MDM2 inhibitor of the p53 tumor suppressor protein as well as the downregulation of Akt1. Combined, these I3C specific signaling processes may explain the inhibitory capacity of I3C to prevent proliferation of mammary cancer stem cells. Only limited information has been uncovered concerning the functional significance of nucleostemin-MDM2 interactions (20, 21). A key consequence of the I3C stimulated binding of nucleostemin to MDM2 is the sequestering of MDM2 in the nucleolus away from p53, thereby likely freeing active p53 to trigger its cellular apoptotic response. Consistent with these processes, expression of dominant negative p53 prevented the I3C apoptotic response in 10AT-Her2 cells, whereas, knockdown of nucleostemin disrupted the I3C induced localization of MDM2 into nuclear foci. It is interesting to note that the presence of nuclear-localized nucleostemin *per se* is not sufficient to sequester MDM2 into nuclear foci because the nuclear sequestering of MDM2 is only observed after I3C treatment, even though nucleostemin is still detected in the presence or absence of I3C treatment. Furthermore, how nucleostemin becomes activated in response to I3C remains unclear. We cannot ignore the possibility though that another factor induces MDM2 translocation into the nucleus and as a result of increased nuclear MDM2 concentration, nucleostemin sequestration of MDM2 into foci can be visualized. Although nucleostemin has been implicated to play a role in stem cell development and the limitless replicative potential of cancer cells, its role in cancer stem cells with MDM2 and p53 has not been fully elucidated. The MDM2 interaction with p53 was partially reversed in I3C treated cells after knockdown of nucleostemin, suggesting that in the absence of nucleostemin, MDM2 can still interact with p53, although at lower efficiency.

Nucleostemin is required for the I3C antiproliferative response in the 10AT-Her2 cancer stem cell line, and conceivably I3C signaling pathways may target either nucleostemin or MDM2 as a priming mechanism that enhances the nucleostemin-MDM2 protein binding interaction. Consistent with this possibility, I3C treatment significantly reduced the level of phosphorylated MDM2, which in other systems can influence MDM2-p53 interactions (29). Akt1 degradation prevents MDM2 phosphorylation and activation. Understanding the molecular mechanisms of Akt1 degradation and nucleostemin activation makes targeted cancer therapies a real possibility for future drug developments. Several recent studies have shown that the p14^{ARF} tumor suppressor protein can bind to either MDM2 or to nucleostemin, although the regulation of interactions involving each binding partner is not well understood (23). We are currently examining whether I3C regulates either of these nucleostemin bimolecular interactions in a way that could influence p53 function in the 10AT-Her2 cancer stem cells. We have previously demonstrated in human breast cancer cells that I3C and 1-benzyl-I3C acts as noncompetitive direct inhibitors of neutrophil elastase (16), which causes the loss of proteolytic processing of the CD44 member of the tumor necrosis receptor family and subsequent alterations in down stream signaling that leads to the indolecarbinol anti-

proliferative responses (16, 30). Based on the precise down stream effectors of I3C signaling that target nucleostemin and MDM2 function, important future directions will be to identify the upstream I3C target protein and characterize the down stream I3C triggered signaling pathway that requires nucleostemin for apoptotic responsiveness of breast cancer stem cells.

This study presents I3C as an effective anticancer phytochemical that exerts growth inhibition against cancer stem cells by modulating the Akt1/ MDM2 pathway as well as activating nucleostemin to sequester MDM2. These cancer stem cells are shown to undergo apoptosis in response to I3C, implicating this small molecule phytochemical as an effective adjuvant therapy for breast cancer patients to prevent further relapse. The potential for I3C and its related derivatives represent a promising therapeutic avenue in the future for personalized and targeted cancer therapies.

REFERENCE

1. Voduc KD, *et al.* (2010) Breast cancer subtypes and the risk of local and regional relapse. *Journal of clinical oncology : official journal of the American Society of Clinical Oncology* 28(10):1684-1691.
2. Stockler M, Wilcken NR, Ghersi D, & Simes RJ (2000) Systematic reviews of chemotherapy and endocrine therapy in metastatic breast cancer. *Cancer treatment reviews* 26(3):151-168.
3. Schultz LB & Weber BL (1999) Recent advances in breast cancer biology. *Current opinion in oncology* 11(6):429-434.
4. Cianfrocca M & Gradishar W (2009) New molecular classifications of breast cancer. *CA: a cancer journal for clinicians* 59(5):303-313.
5. Perou CM, *et al.* (2000) Molecular portraits of human breast tumours. *Nature* 406(6797):747-752.
6. Slamon DJ, *et al.* (1987) Human breast cancer: correlation of relapse and survival with amplification of the HER-2/neu oncogene. *Science* 235(4785):177-182.
7. Al-Hajj M, Wicha MS, Benito-Hernandez A, Morrison SJ, & Clarke MF (2003) Prospective identification of tumorigenic breast cancer cells. *Proceedings of the National Academy of Sciences of the United States of America* 100(7):3983-3988.
8. Marconett CN, *et al.* (2011) Indole-3-carbinol downregulation of telomerase gene expression requires the inhibition of estrogen receptor-alpha and Sp1 transcription factor interactions within the hTERT promoter and mediates the G1 cell cycle arrest of human breast cancer cells. *Carcinogenesis* 32(9):1315-1323.
9. Aggarwal BB & Ichikawa H (2005) Molecular targets and anticancer potential of indole-3-carbinol and its derivatives. *Cell Cycle* 4(9):1201-1215.
10. Ahmad A, Sakr WA, & Rahman KM (2010) Anticancer properties of indole compounds: mechanism of apoptosis induction and role in chemotherapy. *Current drug targets* 11(6):652-666.
11. Firestone GL & Sundar SN (2009) Minireview: modulation of hormone receptor signaling by dietary anticancer indoles. *Mol Endocrinol* 23(12):1940-1947.
12. Firestone GL & Bjeldanes LF (2003) Indole-3-carbinol and 3-3'-diindolylmethane antiproliferative signaling pathways control cell-cycle gene transcription in human breast cancer cells by regulating promoter-Sp1 transcription factor interactions. *The Journal of nutrition* 133(7 Suppl):2448S-2455S.
13. Brew CT, *et al.* (2006) Indole-3-carbinol activates the ATM signaling pathway independent of DNA damage to stabilize p53 and induce G1 arrest of human mammary epithelial cells. *International journal of cancer. Journal international du cancer* 118(4):857-868.
14. Nguyen HH, *et al.* (2008) The dietary phytochemical indole-3-carbinol is a natural elastase enzymatic inhibitor that disrupts cyclin E protein processing. *Proceedings of the National Academy of Sciences of the United States of America* 105(50):19750-19755.
15. Meng Q, Goldberg ID, Rosen EM, & Fan S (2000) Inhibitory effects of Indole-3-carbinol on invasion and migration in human breast cancer cells. *Breast cancer research and treatment* 63(2):147-152.

16. Aronchik I, Bjeldanes LF, & Firestone GL (2010) Direct inhibition of elastase activity by indole-3-carbinol triggers a CD40-TRAF regulatory cascade that disrupts NF-kappaB transcriptional activity in human breast cancer cells. *Cancer research* 70(12):4961-4971.
17. Rahman KM, Aranha O, Glazyrin A, Chinni SR, & Sarkar FH (2000) Translocation of Bax to mitochondria induces apoptotic cell death in indole-3-carbinol (I3C) treated breast cancer cells. *Oncogene* 19(50):5764-5771.
18. Moiseeva EP, Heukers R, & Manson MM (2007) EGFR and Src are involved in indole-3-carbinol-induced death and cell cycle arrest of human breast cancer cells. *Carcinogenesis* 28(2):435-445.
19. Marconett CN, *et al.* (2010) Indole-3-carbinol triggers aryl hydrocarbon receptor-dependent estrogen receptor (ER)alpha protein degradation in breast cancer cells disrupting an ERalpha-GATA3 transcriptional cross-regulatory loop. *Molecular biology of the cell* 21(7):1166-1177.
20. Meng L, Hsu JK, & Tsai RY (2011) GNL3L depletion destabilizes MDM2 and induces p53-dependent G2/M arrest. *Oncogene* 30(14):1716-1726.
21. Lo D & Lu H (2010) Nucleostemin: Another nucleolar "Twister" of the p53-MDM2 loop. *Cell Cycle* 9(16):3227-3232.
22. Dai MS, Sun XX, & Lu H (2008) Aberrant expression of nucleostemin activates p53 and induces cell cycle arrest via inhibition of MDM2. *Molecular and cellular biology* 28(13):4365-4376.
23. Ma H & Pederson T (2007) Depletion of the nucleolar protein nucleostemin causes G1 cell cycle arrest via the p53 pathway. *Molecular biology of the cell* 18(7):2630-2635.
24. Failor KL, Desyatnikov Y, Finger LA, & Firestone GL (2007) Glucocorticoid-induced degradation of glycogen synthase kinase-3 protein is triggered by serum- and glucocorticoid-induced protein kinase and Akt signaling and controls beta-catenin dynamics and tight junction formation in mammary epithelial tumor cells. *Mol Endocrinol* 21(10):2403-2415.
25. Ishiyama M, *et al.* (1996) A combined assay of cell viability and in vitro cytotoxicity with a highly water-soluble tetrazolium salt, neutral red and crystal violet. *Biological & pharmaceutical bulletin* 19(11):1518-1520.
26. Walsh JG, *et al.* (2008) Executioner caspase-3 and caspase-7 are functionally distinct proteases. *Proceedings of the National Academy of Sciences of the United States of America* 105(35):12815-12819.
27. Zilfou JT & Lowe SW (2009) Tumor suppressive functions of p53. *Cold Spring Harbor perspectives in biology* 1(5):a001883.
28. Vogelstein B & Kinzler KW (1992) p53 function and dysfunction. *Cell* 70(4):523-526.
29. Moll UM & Petrenko O (2003) The MDM2-p53 interaction. *Molecular cancer research : MCR* 1(14):1001-1008.
30. Aronchik I, *et al.* (2012) Target protein interactions of indole-3-carbinol and the highly potent derivative 1-benzyl-I3C with the C-terminal domain of human elastase uncouples cell cycle arrest from apoptotic signaling. *Molecular carcinogenesis* 51(11):881-894.

Chapter III

Artemisinin antiproliferative response in human breast cancer cells requires the down-regulated expression of the E2F1 transcription factor and loss of E2F1-target cell cycle genes

ABSTRACT

Artemisinin, a sesquiterpene phytolactone derived from *Artemisia annua*, is a potent antimalarial compound with promising anticancer properties, although the mechanism of its anticancer signaling is not well understood. Artemisinin inhibited the proliferation and induced a strong G1 cell cycle arrest of cultured MCF-7 cells, an estrogen responsive human breast cancer cell line that represents a luminal A, early stage cancer phenotype, and effectively inhibited the *in vivo* growth of MCF-7 cell-derived tumors from xenografts in athymic nude mice. Artemisinin also induced a growth arrest of tumorigenic human breast cancer cell lines with preneoplastic and late stage cancer phenotypes, but failed to arrest the growth of a nontumorigenic human mammary cell line. Concurrent with the cell cycle arrest of MCF-7 cells, artemisinin selectively down-regulated the transcript and protein levels of the CDK2 and CDK4 cyclin dependent kinases, cyclin E, cyclin D₁ and the E2F1 transcription factor. Analysis of CDK2 promoter-luciferase reporter constructs showed that the artemisinin ablation of CDK2 gene expression was accounted for by the loss of CDK2 promoter activity. Chromatin immunoprecipitation revealed that artemisinin inhibited E2F1 interactions with the endogenous MCF-7 cell CDK2 and cyclin E promoters. Moreover, constitutive expression of exogenous E2F1 prevented the artemisinin induced cell cycle arrest and down regulation of CDK2 and cyclin E gene expression. Taken together, our results demonstrate that the artemisinin disruption of E2F1 transcription factor expression mediates the cell cycle arrest of human breast cancer cells and represents a critical transcriptional pathway by which artemisinin controls human reproductive cancer cell growth.

INTRODUCTION

Breast cancer is the most common malignancy in nonsmoking women within the western hemisphere. Clinical management of breast cancer has been arduous owing to the complex heterogeneity in phenotypes as well as emergence of resistant states with current therapy options (1, 2). Breast cancer can manifest itself as a hormone responsive disease marked by presence of functional estrogen receptors or as a steroid unresponsive phenotype that can involve the loss of estrogen receptor expression (3-5). Determination of this trait is critical to prescribing appropriate therapy to the patient. Hormone responsive breast cancer can be managed by employment of selective estrogen receptor modulators (SERM) such as tamoxifen, and aromatase inhibitors such as letrozole (6). However, patients receiving such therapy have a high recurrence rate within five years, and present resistant states or increased risk for other gynecological malignancy (7). Hormone unresponsive breast cancer patients undergo more drastic therapy that includes a possible combination of surgery, radiation and immunotherapy, which exert deleterious side effects (8, 9). Currently, there is a strong demand for therapy that is effective against a wide variety of breast cancer phenotypes with minimum side effects.

Naturally occurring phytochemicals represent a largely untapped source of potential therapeutic molecules to control different types of cancers with very minimal side effects (10-12). One such promising compound is artemisinin, a sesquiterpene lactone that was isolated from the aerial portions of *Artemisia annua* plants (more commonly known as qinghaosu or sweet wormwood). Artemisinin and a number of its derivatives have been used to effectively treat different forms of malaria the past three decades (13). More recently, artemisinin and its related compounds have been shown to exhibit potent anticancer effects in a variety of human cancer cell model systems including leukemic, colon, melanoma, breast, ovarian, prostate, central nervous system, and renal cancer cells (14-16). Molecular, cellular and physiological studies have demonstrated that, depending on the tissue type and experimental system, the responses to artemisinin and its derivatives in a variety of cancer cell lines and tumor xenografts can involve a cell cycle arrest, apoptosis, inhibition of angiogenesis and cell migration, as well as modulation of nuclear receptor responsiveness and signal transduction pathways (17-19).

One proposed mechanism by which artemisinin targets cancer cells is the presence of relatively high concentrations of iron that induces cleavage of the endoperoxide bridge, thereby allowing the formation of free radical molecules such as reactive oxygen species and resulting oxidative damage to the cells, as well as iron depletion in the cells (20, 21). This mechanism resembles the action of artemisinin in malarial parasites. However, expression profiling of several classes of tumor cells revealed that artemisinin treatment causes selective changes in expression of many more oncogenes and tumor suppressor genes than can be accounted for by changes restricted only to genes responsible for iron metabolism (22, 23). This result suggests that the anticancer properties of artemisinin cannot be explained only by the global toxic effects of oxidative damage. Mechanistic information on the effects of artemisinin and its derivatives on the expression and activity of specific transcription factors have been limited. We previously demonstrated that artemisinin did not alter general Sp1 transcription factor responsiveness or expression, but

selectively disrupted the endogenous interactions of the Sp1 transcription factor with the CDK4 promoter to inhibit CDK4 gene expression (24). This result suggests that cell cycle gene-specific transcriptional responses to artemisinin may control cell cycle progression in different types of human cancer cells. In this current study, we report that the artemisinin cell cycle arrest of MCF-7 human breast cancer cells is mediated by the down regulated expression of the E2F1 transcription factor that leads to the disruption of CDK2 promoter activity and loss of gene transcription. We further show that exogenous expression of constitutively expressed E2F1 confers resistance of these breast cancer cells to the antiproliferative effects of artemisinin, demonstrating the critical importance of E2F1 expression in mediated this artemisinin response.

MATERIALS AND METHODS

Cell Culture

The MCF-7 and MDA-MB-231 cell lines were obtained from ATCC (Manassas, VA) and MCF-10AT and MCF-10A cells were kind gifts from Dr. Fred Miller at the Barbara Ann Karmanos Cancer Center (Wayne State University). MCF-7 cells were cultured in Dulbecco's Modified Eagles Medium (DMEM), supplemented with 10 % fetal bovine serum 10 µg/mL insulin, 50 U/mL penicillin, 50 U/mL streptomycin, and 2 mM L-glutamine (all media components purchased from Lonza, Allendale, NJ). MDA-MB-231 cells were cultured similarly to MCF-7 cells except with the use of Iscove's Modified Dulbecco's Medium (obtained from Lonza) and without supplementation of insulin. MCF-10AT and MCF-10A cells were cultured in Dulbecco's Modified Eagles Medium/F-12 (DMEM/F-12), 10 % fetal bovine serum, 50 U/mL penicillin, 50 U/mL streptomycin, 10 µg/mL insulin (all obtained from Lonza, Allendale, NJ), 0.02 µg/mL epidermal growth factor (purchased from Promega, Madison, WI), 0.5 µg/mL hydrocortisone, and 0.1 µg/mL cholera toxin (purchased from Sigma-Aldrich, St. Louis, MO). Cells were grown to subconfluency in a humidified chamber at 37°C containing 5% CO₂. A 300 mmol/l stock solution of Artemisinin (purchased from Sigma-Aldrich, St. Louis, MO) was dissolved in dimethyl sulfoxide (DMSO) and then diluted in the ratio 1:1000 in media before culture plate application. Before each drug treatment, cells are washed in ice cold phosphate-buffered saline (PBS) (obtained from Lonza).

Plasmids and Transfections

Indicated plasmids (1 mg) were transfected into MCF-7 cells using Superfect reagent (Qiagen) using manufacturer's instructions. Cells were treated with 300 nM artemisinin 24 hours post transfection and harvested in ice cold PBS. The cells were subjected to immunoblotting as described, or to luciferase assays with the luciferase assay kit (Promega). The CDK2 luciferase plasmids were kind gifts from Dr. Leonard Bjeldanes, UC Berkeley. The CMV-E2F1 expression vector was a kind gift from Dr. Kahryn Calame's, Columbia University.

Reverse Transcription and Polymerase Chain Reaction

MCF-7 cells treated with indicated doses of artemisinin and duration were harvested in Trizol (Invitrogen), and total RNA was extracted according to the manufacturer's protocol. This was quantified and 1 mg of total RNA was used for reverse transcription using Mu-MLV reverse transcriptase (Invitrogen) and random hexamers according to manufacturer's protocol. The cDNA pool was used (2 ml) in polymerase chain reaction and was amplified with primers of the following sequences:

E2F1 Forward: 5'-CAGATCTCCCTTAAGAGC-3'

E2F1 Reverse: 5'-CAGTCGAAGAGGTCTCTG-3'

Cyclin D1 Forward: 5'-CTACTACCGCCTCACACGCTT-3'

Cyclin D2 Reverse: 5'-GGCTTGACTCCAGGGCT-3'

Cyclin E Forward: 5'-CCGGCTTCGTCGTTTCATATGG-3'

Cyclin E Reverse: 5'-CTCGCCATTCTTCGTCTCG-3'

CDK2 Forward: 5'-ATGGACGGAGCTTGTTATCG-3'

CDK2 Reverse: 5'-GGAGAGGGTGAGATTAGGGC -3'
CDK4 Forward: 5'-CTGAGAATGGCTACCTCTCGATATG-3'
CDK4 Reverse: 5'-AGAGTGTAACAACCACGGGTGTAAG-3'
GAPDH Forward: 5'-TGAAGGTCGGAGTCAACGGATTTG-3'
GAPDH Reverse: 5'-CATGTGGGCCATGAGGTCCACCAC-3'

20 mL of this reaction was electrophoresed on a 1% agarose gel and visualized using a UV transilluminator.

Western Blots

After the indicated treatments, cells were harvested in radioimmune precipitation assay buffer (150 mM NaCl, 0.5% deoxycholate, 0.1% NoNidet-p40 (Nonidet P-40, Fluta Biochemitra, Switzerland), 0.1% SDS, 50 mM Tris) containing protease and phosphatase inhibitors (50 g/mL phenylmethylsulfonyl fluoride, 10 g/mL aprotinin, 5 g/mL leupeptin, 0.1 g/mL NaF, 1 mM dithiothreitol, 0.1 mM sodium orthovanadate, and 0.1 mM glycerol phosphate). Equal amounts of total cellular protein were mixed with loading buffer (25% glycerol, 0.075% SDS, 1.25 mL of 14.4M β mercaptoethanol, 10% bromphenol blue, 3.13% 0.5M Tris-HCl, and 0.4% SDS (pH 6.8)) and fractionated on 10% polyacrylamide/0.1% SDS resolving gels by electrophoresis. Rainbow marker (Amersham Biosciences) was used as the molecular weight standard. Proteins were electrically transferred to nitrocellulose membranes (Micron Separations, Inc., Westboro, MA) and blocked for 1 hour with Western wash buffer (5% NFDM (10 mM Tris-HCl (pH 8.0), 150 mM NaCl, and 0.05% Tween 20, 5% nonfat dry milk). Protein blots were subsequently incubated for overnight at 4°C in primary antibodies. The antibodies used were as follows, Rabbit anti-E2F1 (sc-193), Mouse anti-Sp1 (sc-420), Mouse anti-CDK2 (sc-6248), Rabbit anti-CDK4 (sc-749), Mouse anti-Cyclin E (sc-248), Mouse anti-Cyclin D1 (sc-6281), Mouse anti-c-Fos (sc 447), Rabbit anti-c-Jun (sc44), and Goat anti-p21 (sc397) were purchased from Santa Cruz Biotechnology (Santa Cruz, CA) and diluted 1:1000 in TBST. Rabbit anti-actin (#AANO1 Cytoskeleton, Inc. Denver, CO) was diluted 1:1000 in TBST and used as a gel-loading control. Rabbit anti-HER2 (2165) was obtained from Cell Signaling. The working concentration for all antibodies was 1 μ g/mL in Western wash buffer. Immunoreactive proteins were detected after incubation with horseradish peroxidase conjugated secondary antibody diluted to 3×10^4 in Western wash buffer (goat anti-rabbit IgG, rabbit anti-goat IgG, and rabbit anti-mouse IgG (Bio-Rad)). Blots were treated with enhanced chemiluminescence reagents (PerkinElmer Life Sciences), and all proteins were detected by autoradiography. Equal protein loading was confirmed by Ponceau S staining of blotted membranes.

Flow Cytometry

To monitor the cell population DNA content, 4×10^4 of each cultured cell lines were plated onto Nunc six-well tissue culture dishes (NUNC-Fischer, Pittsburgh, PA). Triplicate samples were treated with indicated concentrations and durations of artemisinin. The medium was changed every 24 hours. Incubated cells were hypotonically lysed in 1 mL of DNA staining solution (0.5 mg/mL propidium iodide, 0.1% sodium citrate, and 0.05% Triton X-100) Lysates were filtered using 60 μ m Nitex flow mesh (Sefar America, Kansas City, MO) to remove cell membranes. Propidium iodide-stained nuclei were detected using a PL-2 detector with a 575 nm band pass filter on a Beckman-Coulter (Fullerton, CA) fluorescence-

activated cell sorter analyzer with laser output adjusted to deliver 15 megawatts at 488 nm. Ten thousand nuclei were analyzed from each sample at a rate of ~600 nuclei per second. The percentages of cells within the G1, S, and G2/M phases of the cell cycle were determined by analyzing the histographic output with the multicycle computer program MPLUS, provided by Phoenix Flow Systems (San Diego, CA), in the Cancer Research Laboratory Microchemical Facility at the University of California at Berkeley.

Chromatin Immunoprecipitation

MCF-7 cells were grown to a subconfluency and treated for 48 hours with 300 μ M artemisinin or DMSO vehicle control. Crosslinking of proteins to DNA was obtained by the addition of formaldehyde at 1% of the final concentration for 5 min at room temperature to cultured cells. Fixation was quenched with glycine for a final concentration of 125 mM for 5 min. Harvested cells were lysed with chromatin immunoprecipitation (ChIP) lysis buffer (50 mM NaCl, 1% Triton X-100 and 0.1% sodium deoxycholate) and protease inhibitors (50 g/ml phenylmethylsulfonyl fluoride, 10 g/mL aprotinin, 5 g/mL leupeptin, 0.1 g/mL NaF, 1 mM dithiothreitol, 0.1 mM sodium orthovanadate, and 0.1 mM glycerol phosphate). Cells were sonicated and the supernatants were standardized based on protein content using Bio-Rad Protein Assay (Bio-Rad, Hercules, CA). One milligram of protein was used for each immunoprecipitation. Protein-DNA complexes were immunoprecipitated overnight with 15 μ l antibodies recognizing E2F1 (Santa Cruz Biotechnology). Complexes were precipitated using Sepharose-G beads (GE Healthcare, Piscataway, NJ), followed by 2x ChIP lysis buffer, 2x ChIP wash buffer (10mM Tris, pH 8.0, 250 mM LiCl, 0.5% NP-40, 0.5% sodium deoxycholate and 1 mM ethylenediaminetetraacetic acid) and 2x Tris-ethanolamin. Immunoprecipitation and input samples were eluted 65°C/18 h in elution buffer (50 mM Tris, pH 8.0, 1% sodium dodecyl sulfate and 10 mM ethylenediaminetetraacetic acid). PCR amplification was carried out in a total volume of 50 μ l using specific primers and PCR mix (1 U *Taq* polymerase (NEB), 1.5mM MgCl₂, 0.2 μ M deoxynucleoside triphosphates) as follows: Cyclin E (Forward : 5'-CCAATGCACTGACGGATGAAT-3'; Reverse: 5'-AAATCCCTGCGCGGAACCG -3') was cycled 36 times (95°C, 30s/ 55°C 50s/72°C, 30s) with a 72°C, 10 min extension and a 95°C 5 min hot start. The same settings were used for CDK2 (Forward : 5'-CATCCCAAGAGGAGA GGATT-3' Reverse: 5'-TGGCACTGATTCTGAGGCTT-3') and E2F1 (Forward : 5'-CCAAGCCATGACGCTCAC-3' Reverse: 5'-GCGGGTTAAAGCCAATAGGAA -3') except annealing time was 30s. These primers frame a 178 bp promoter fragment spanning from -1064 to -1142 upstream of the CDK2 gene transcription start site, frame a 682 bp promoter fragment spanning from -1289 to -1971 upstream of the cyclin E gene transcription start site, and frame a 255 bp promoter fragment spanning from +10 to -245 upstream of the E2F1 gene transcription start site. The PCR products were electrophoresed on a 1.5% agarose gel and visualized using a transilluminator.

***In vivo* tumor xenografts**

Immunocompromised 40 day old female NIH III athymic nude mice were subcutaneously implanted with a mixture of 5x10⁶ MCF-7 cells and matrigel (Becton Dickinson, San Jose, CA) in the ratio of 1:1 by volume at each injection site. The mice received 17 β -estradiol as daily subcutaneous injections (1 mg), and were palpated for three weeks until tumors developed. The mice were randomized (5 per group) and treated with an effective dose

of 100 mg/kg body mass of artemisinin suspended in sterile DMSO/PBS or with sterile DMSO/PBS vehicle control in drinking water with replacement of drug containing water every two days. Calculated dose of administered artemisinin in drinking water, is based on average water intake of 7.7 ± 0.3 mL/30 g body weight. Tumor volumes were calculated based on the formula ($\pi /6 * L * W * H$).

RESULTS

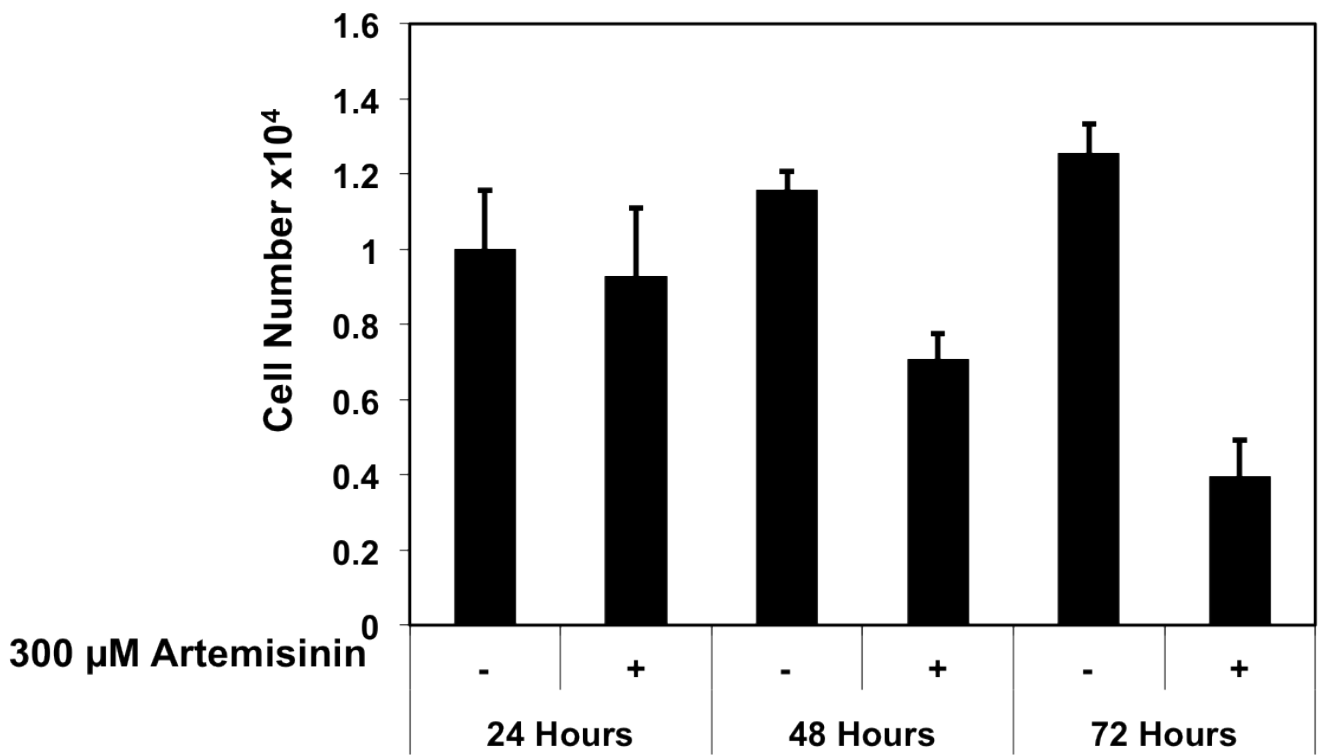
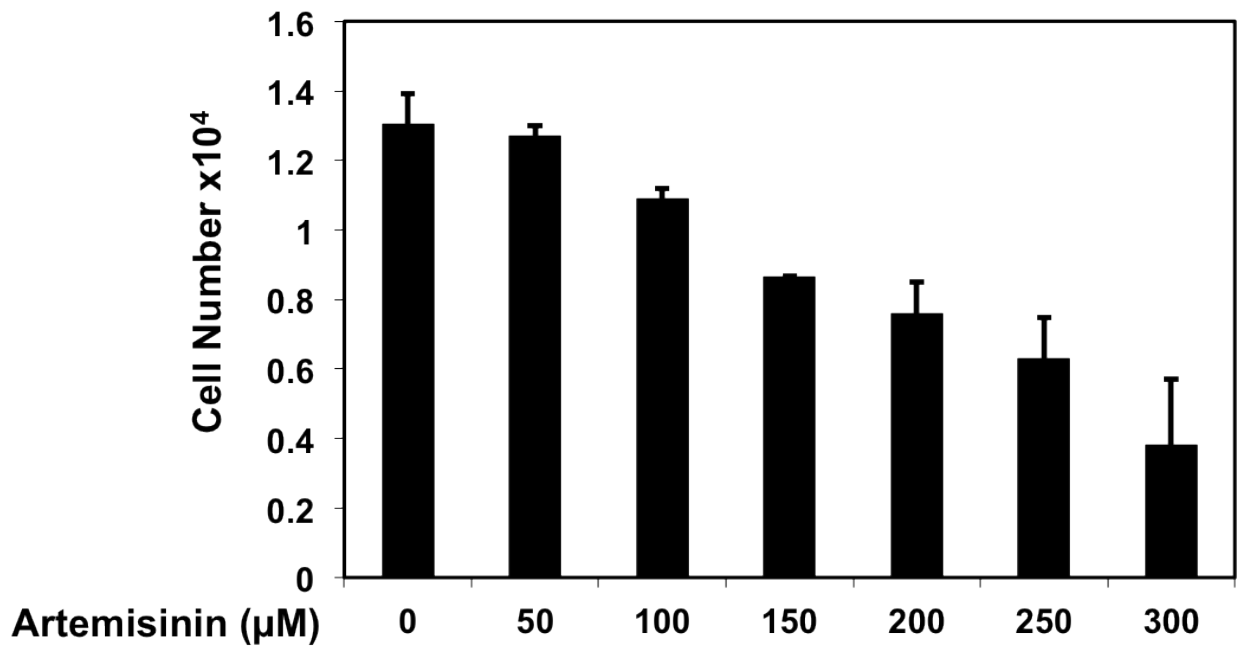
Artemisinin inhibits the proliferation and *in vivo* tumor growth of MCF-7 human breast cancer cells.

The cellular and *in vivo* antiproliferative effects of artemisinin were initially examined in the MCF-7 human breast cancer cell line that has an estrogen responsive and tumorigenic, but poorly invasive, phenotype representative of an early stage breast cancer (25, 26). Cells were treated with increasing concentrations of artemisinin for 48 hours, and an analysis of cell number revealed that 300 μ M artemisinin was the most effective dose that inhibits cellular proliferation in the absence of any apoptosis (Figure 30, top panel). Upon establishing the ideal concentration of artemisinin, a similar time course study revealed the inhibition of cellular proliferation by artemisinin begins as early as 24 hours and can persist up to 72 hours before (Figure 30, bottom panel). This effective concentration of artemisinin is generally consistent with what has been reported in other cell systems to induce a growth arrest without any apoptotic response (27), and likely reflects a combination of cellular transport, stability and target protein interactions.

Figure 30

Artemisinin reduces MCF-7 cell number in culture.

Artemisinin inhibits the proliferation of cultured MCF-7 human breast cancer cells and growth of MCF-7 tumor xenografts in vivo. Equal numbers (~300 000) of MCF-7 cells were treated with the indicated concentrations of artemisinin and time points (48 hours for top panel) and the final cell number determined by counting the trypsin-releasable cells in a hemocytometer. Cell numbers were analyzed in triplicate-independent cultures of each tested concentration of artemisinin.

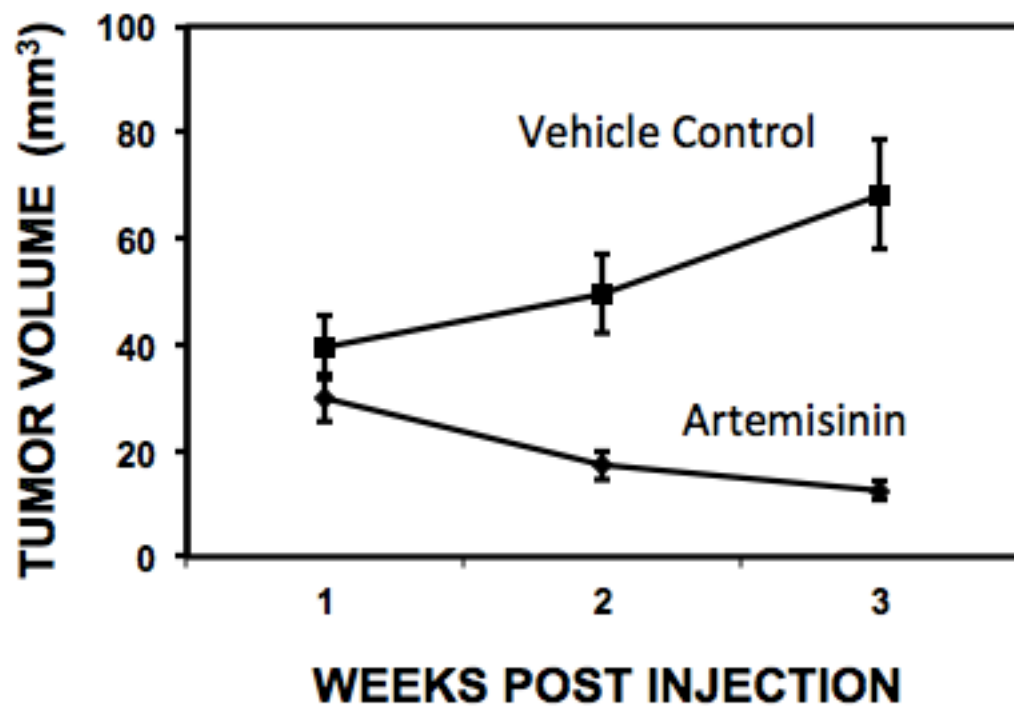


The efficacy of artemisinin towards inhibition of MCF-7 cell growth *in vivo* was investigated in tumor xenografts in nude athymic NIH III mice. The tumor xenografts were allowed to grow to an average size of approximately 35 mm³ and then the mice were given either artemisinin dissolved in DMSO/PBS or vehicle control in the drinking water. Effective administered amount of artemisinin was calculated to be 100 mg/kg/day based on water intake consumption of 7.7 ± 0.3 mL/ 30g body weight. As shown in Figure 31, administration of artemisinin effectively inhibited the growth of MCF-7 cell-derived tumor xenografts. Also, in artemisinin-treated animals, the tumors appeared to show a robust inhibition of angiogenesis as indicated by the significantly reduced coloring of the tumors at the 3-week post injection time point (Fig 28, micrograph insert). The antiangiogenic effect of artemisinin has been attributed in other xenograft models to the inhibition of VEGF and VEGFR expression (28, 29).

Figure 31

Artemisinin inhibition of MCF-7 tumor xenografts.

Palpable MCF-7 cell derived tumor xenografts were formed in athymic NIH III nude mice. Animals were treated orally with either 100 mg/kg bw of artemisinin or with a DMSO/PBS vehicle control and tumor volumes monitored with a caliper and volume calculated as $V = \pi/6 \times L \times W \times H$. Three weeks post injection representative tumors were excised and shown in the bottom panel.



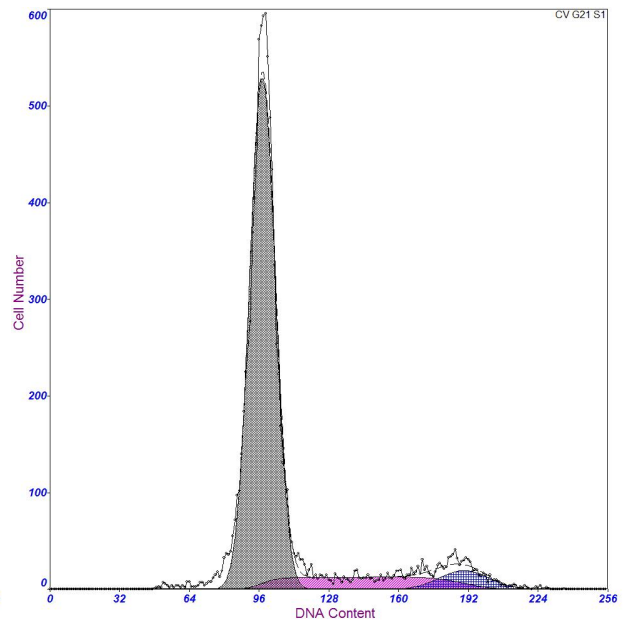
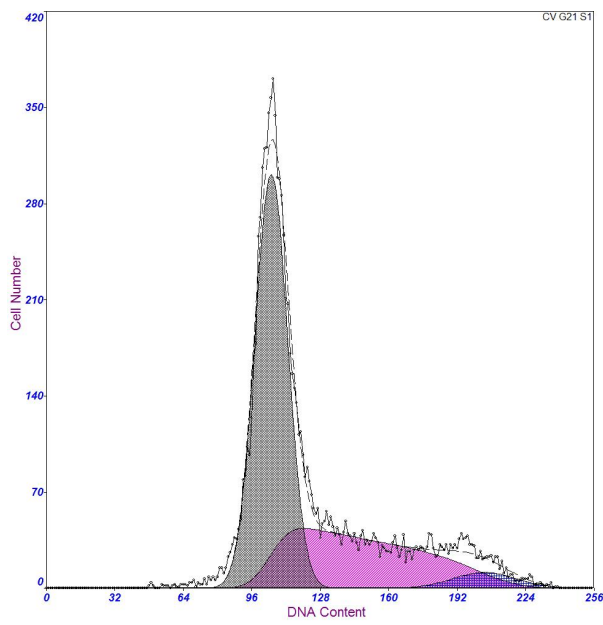
Artemisinin induced G1-cell cycle arrest of MCF-7 human breast cancer cells.

The artemisinin-mediated inhibition of cellular and *in vivo* MCF-7 cell proliferation suggested that this small molecule phytochemical has selective effects on the human breast cancer cell cycle. To determine the dose and time dependent of effects of artemisinin on the cell cycle distribution, initially, MCF-7 cells were treated at the optimal dose of 300 μM of artemisinin for 48 hours as determined by the cell proliferation assay (Figure 32). Once treated, MCF-7 cells were harvested, stained with propidium iodide and then subjected to flow cytometry to determine DNA content of each cell population. The flow cytometry profiles of MCF-7 cells treated with or without 300 μM artemisinin showed that in growing untreated conditions, the DNA content of the cells was dispersed throughout the cell cycle, whereas, after artemisinin treatment, the majority of the cell population was arrested with a G1 DNA content. This process was repeated at the indicated concentrations and time points to establish that the observed G1 cell cycle arrest on MCF-7 cells is both dose and time dependent. As shown in Figure 33, artemisinin caused a robust accumulation of cells with a G1 DNA content with a proportional decline in the number of cells in S phase. Consistent with the cellular proliferation analysis in Figure 30, 300 μM artemisinin induced a G1-cell cycle arrest without any observed accumulation of sub G1-DNA, which is typically indicative of apoptosis. Therefore, this concentration of artemisinin was employed in all experiments unless otherwise specified. We also observed that artemisinin arrested the proliferation of several types of tumorigenic human breast cancer cells representing various clinical stages of disease manifestation (Figure 34). In addition to MCF-7 cells, artemisinin induced a G1 cell cycle arrest of MDA-MB-231 breast cancer cells, which represent a late stage, triple negative cancer phenotype. Interestingly, nontumorigenic MCF-10A human mammary epithelial cells were resistant to artemisinin induced cell cycle arrest, whereas artemisinin triggered a G1 cell cycle arrest in the MCF-10AT preneoplastic cell line variant of MCF-10A cells.

Figure 32

Artemisinin induces a G1 cell cycle arrest in MCF-7 breast cancer cells.

MCF-7 cells were treated with 300 μ M artemisinin for 48 hours and the cell population DNA content was quantified by flow cytometry. The graphs are representative flow cytometry histograms of cells treated with or without 300 μ M artemisinin.



	I3C	-	+	-
+	+	+	-	+

Loading

Figure 33

Dose response and time course of artemisinin induced G1 cell cycle arrest.

MCF-7 cells were treated with artemisinin at the indicated concentrations and time points and the cell population DNA contents quantified by flow cytometry. The bar graphs show the average DNA content corresponding to the cell cycle phases in three independent experiments.

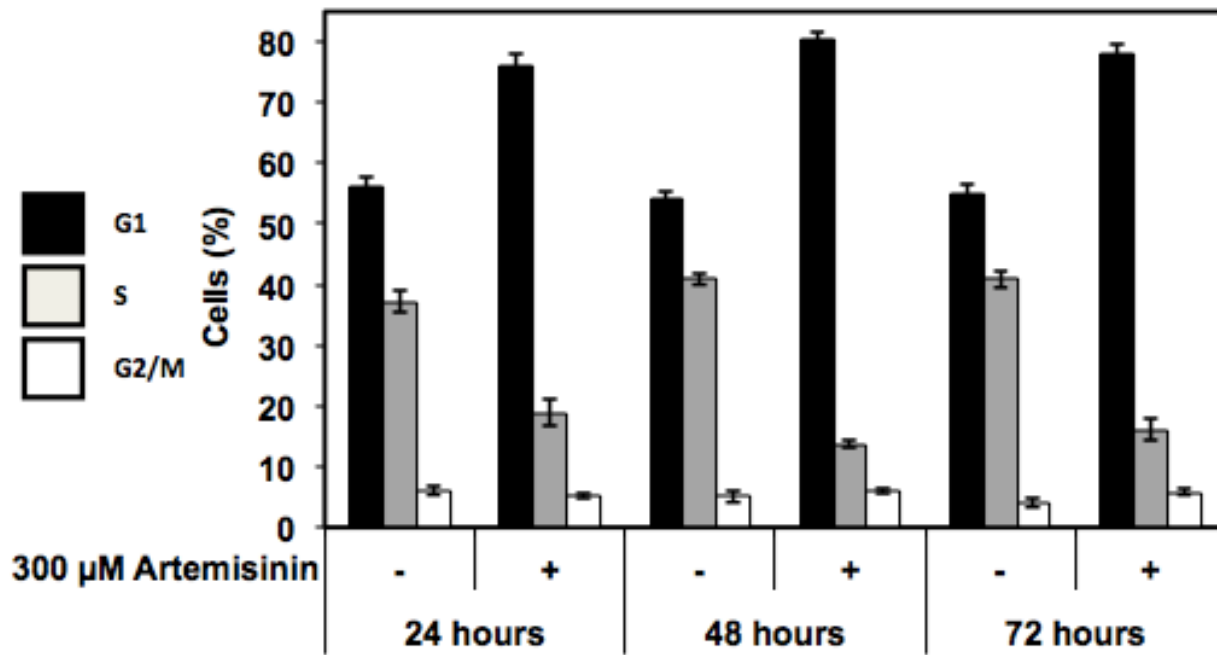
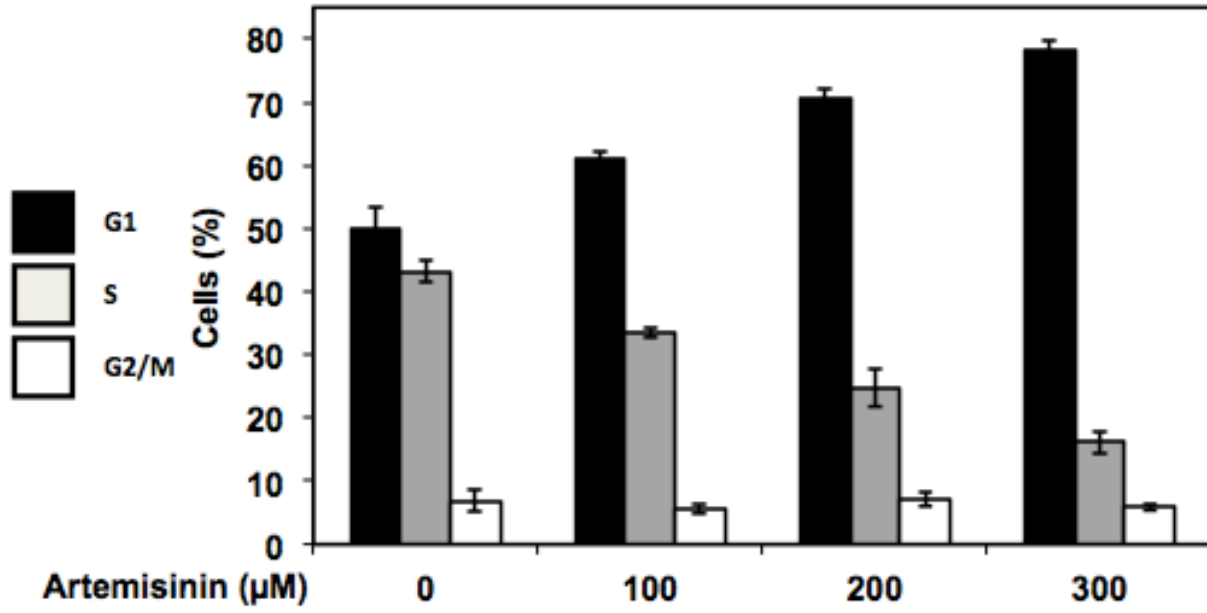


Figure 34

Flow cytometry analysis of artemisinin cell cycle effects in human breast cancer cell lines with distinct phenotypes.

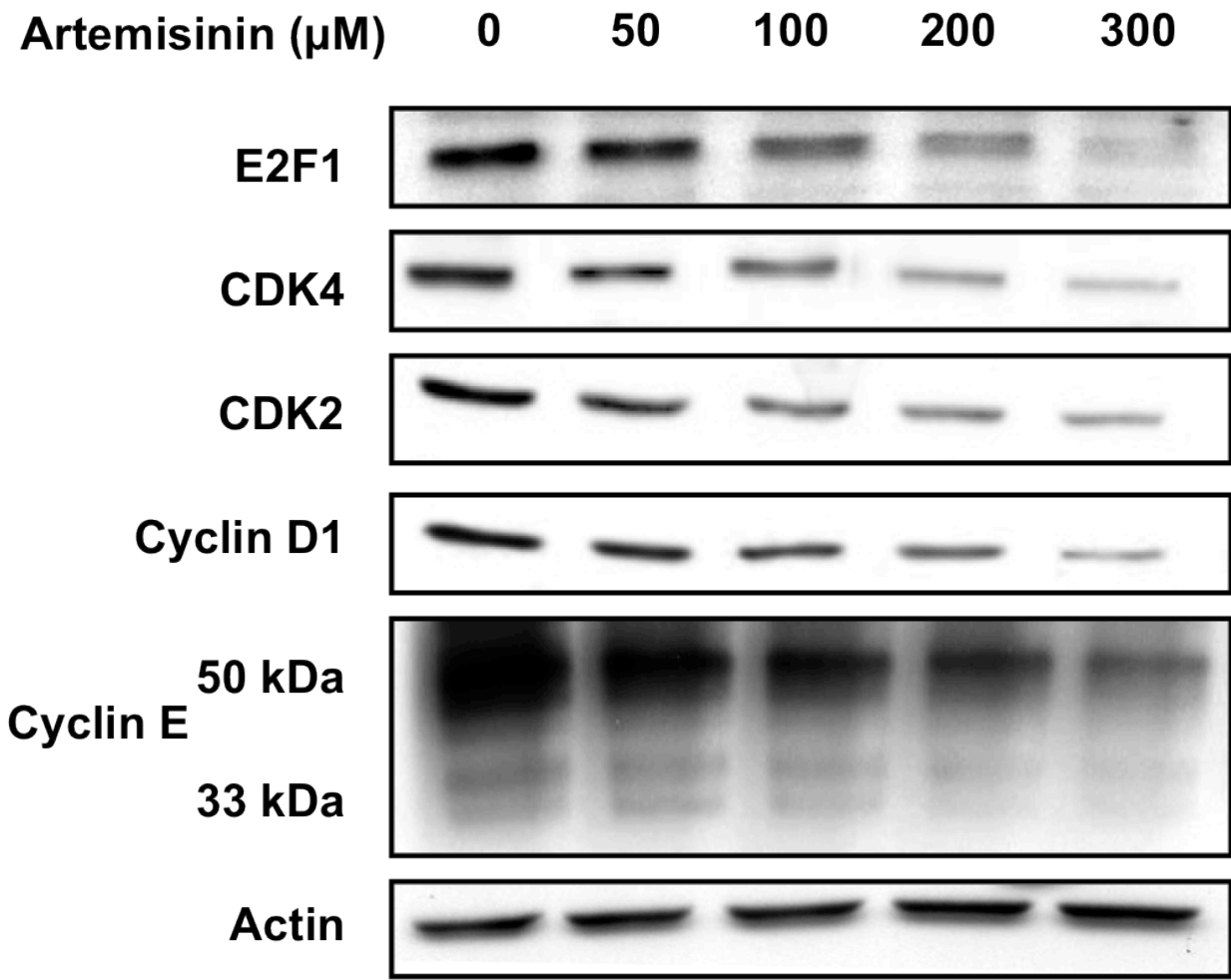
Breast cancer cells were treated with or without 300 μ M artemisinin for 48 hours, and the cell population DNA contents quantified by flow cytometry after staining with propidium iodide. The results are an average of independent triplicate results. The average error was approximately between -/+ 1% to -/+ 2% for each of the results.

Cell Line	Phenotype	Vehicle Control			Artemisinin		
		G1	S	G2/M	G1	S	G2/M
MCF-7	Luminal A Estrogen Responsive Growth Tumorigenic Poorly invasive Wild Type p53	50%	42%	8%	77%	12%	11%
MDA-MB-231	Triple Negative Estrogen Independent Growth Tumorigenic Highly Invasive Mutant p53	57%	31%	12%	75%	18%	7%
MCF-10AT	Estrogen Dependent Growth Preneoplastic Poorly Tumorigenic Wild Type p53	52%	41%	7%	74%	11%	15%
MCF-10A	Estrogen Independent Growth Non Tumorigenic Wild Type p53	71%	20%	9%	73%	17%	10%

To further characterize the artemisinin induced a G1 cell cycle arrest, MCF-7 cells were treated with varying concentrations of artemisinin for 48 hours and total cell lysates electrophoretically fractionated and western blots probed with specific antibodies for several key G1-acting cell cycle gene products. As shown in Figure 35, artemisinin strongly down regulated the protein levels of the G1-acting cyclin dependent kinases (CDK) CDK2 and CDK4, both the 50 kDa and 33 kDa forms of cyclin E protein, cyclin D1, and the E2F1 transcription factor, which is a CDK2 and CDK4 substrate. This suggests that the induction of G1 cell cycle arrest by artemisinin is triggered by the dose dependent loss of one or more of these specific G1-acting cell cycle genes. Also, co-treatment of MCF-7 with effective concentrations of dithiothreitol or ascorbic acid, two potent antioxidants, failed to reverse the artemisinin mediated cell cycle arrest and down regulation of cell cycle genes, indicating that the antiproliferative effects are not due to oxidative effects of artemisinin leading to apoptosis.

Figure 35

Artemisinin ablates key G1 cell cycle regulators in a dose dependent manner. Cultured MCF-7 cells were treated with increasing doses of artemisinin for 48 hours. Total cell extracts were electrophoretically fractionated and western blots probed for the indicated G1-acting cell cycle genes. Analysis of actin protein levels was used as a gel loading control.



To begin to assess potential functional relationships between the artemisinin down-regulation of the E2F1 transcription factor and altered expression of the cell cycle genes, the kinetics of expression was investigated in cells exposed to 300 μ M artemisinin. At the indicated treatment times, the levels of E2F1, Sp1, c-Fos, c-Jun, CDK4, CDK2, cyclin D1, cyclin E, p21, and Actin protein were determined by western blot analysis of total cell extracts (Figure 36). Interestingly, each protein showed varying degrees of downregulation at different time points. For example, protein levels of E2F1 and CDK2 decreased as early as 24 hours but protein levels of CDK4 only began changing at 48 hours. To establish an order of protein downregulation, shorter time points chosen and as shown in Figure 37, by 12 hours the artemisinin down-regulation of E2F1 levels was mostly complete, which was the most rapid response to this phytochemical. The down regulation of CDK2 protein was not detectable at 12 hours, however in the following 12 hours the level of CDK2 protein was reduced by nearly 90%. Closely following CDK2 was the loss of cyclin D1 protein and at a later time point the down-regulation of CDK4 and cyclin E were clearly observed. No changes were observed in levels of the Sp1, C-Fos or C-Jun transcription factors or in the levels of the CDK inhibitor gene p21^{Waf/Cip1} underscoring the selectivity of artemisinin mediated effects. These kinetic results implicate the rapid down regulation of the E2F1 transcription factor as potentially important regulatory event in the artemisinin cell cycle arrest of MCF-7 human breast cancer cells.

Figure 36

Time dependent regulation of artemisinin on key G1 cell cycle regulators.

Cultured MCF-7 cells were treated with 300 μ M artemisinin for 24, 28, and 72 hours. Total cell extracts were electrophoretically fractionated and western blots probed for the indicated G1-acting cell cycle genes. Analysis of actin protein levels was used as a gel loading control.

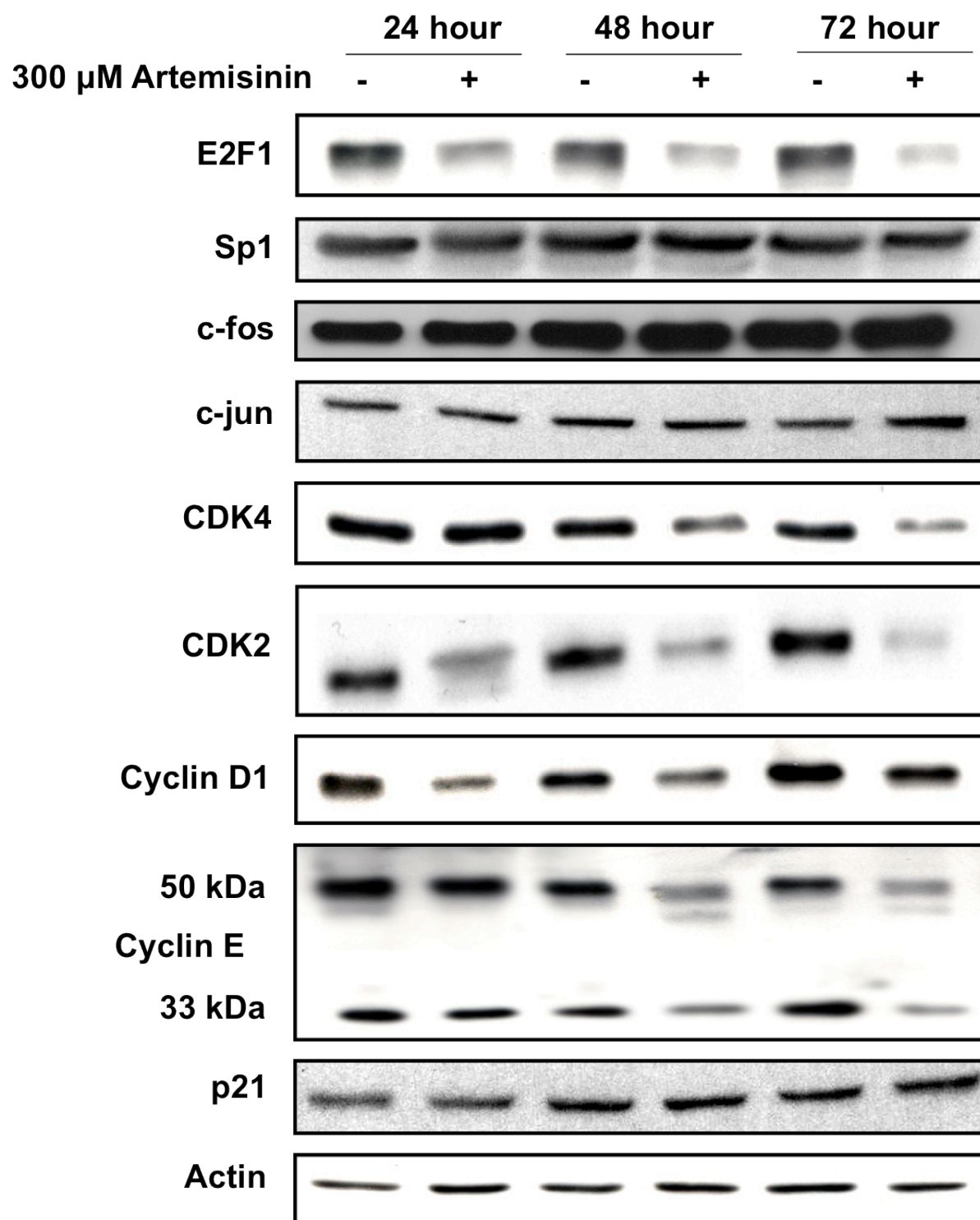
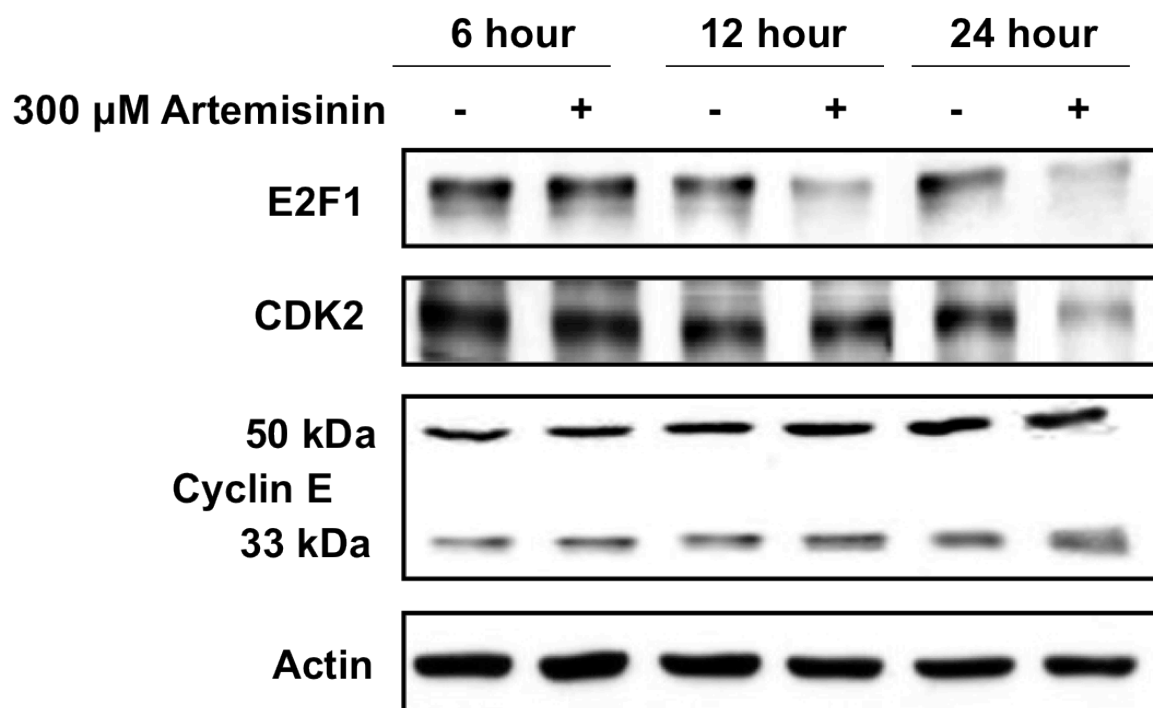


Figure 37

E2F1 protein downregulation by artemisinin occurs as early as 12 hours.

Cultured MCF-7 cells were treated with 300 μ M artemisinin for 6, 12, and 24 hours. Total cell extracts were electrophoretically fractionated and western blots probed for the indicated G1-acting cell cycle genes. Analysis of actin protein levels was used as a gel loading control.



Artemisinin disruption of E2F1 promoter interactions and downregulation of CDK2 gene expression and promoter activity.

RT-PCR analysis of total RNA isolated from artemisinin treated and untreated cells revealed that artemisinin induced a significant decline in the levels of CDK2, CDK4, Cyclin D1, Cyclin E and E2F1 transcripts (Figure 38), which quantitatively accounts for the loss of the corresponding proteins. The most rapid response was the loss of transcripts encoding the E2F1 transcription factor, which was noticeably reduced by 12 hours of artemisinin treatment. Because of the importance of CDK2 in controlling progression through the G1 phase of the cell cycle and the nearly complete ablation of CDK2 transcript levels by artemisinin, we further evaluated whether the artemisinin had an effect on CDK2 promoter activity. To test this possibility, MCF-7 cells were transfected with pGL2 plasmids containing either of two CDK2 gene promoter regions (-2400 or -800 bp) fused to the luciferase reporter, and transfected cells were treated with or without 300 μ M artemisinin for 24 hours prior to assaying luciferase activity in the isolated cell extracts. As shown in Figure 39, artemisinin strongly inhibited luciferase activity in cells transfected with the reporter plasmid driven by the -2400 CDK2 promoter, but not in cells transfected with the -800 bp CDK2-luciferase reporter plasmid.

Figure 38

Artemisinin ablates transcript levels of G1 cell cycle regulators.

MCF-7 cells were treated with or without 300 μ M artemisinin for the indicated times and total RNA isolated. The transcript levels of E2F1, cyclin D, cyclin E, CDK2, CDK4, and GAPDH were determined by reverse transcription-polymerase chain reaction using specific primers, and the products fractionated by electrophoresis on a 1.5% agarose gel and visualized on an ultraviolet transilluminator. GAPDH served as a gel loading control.

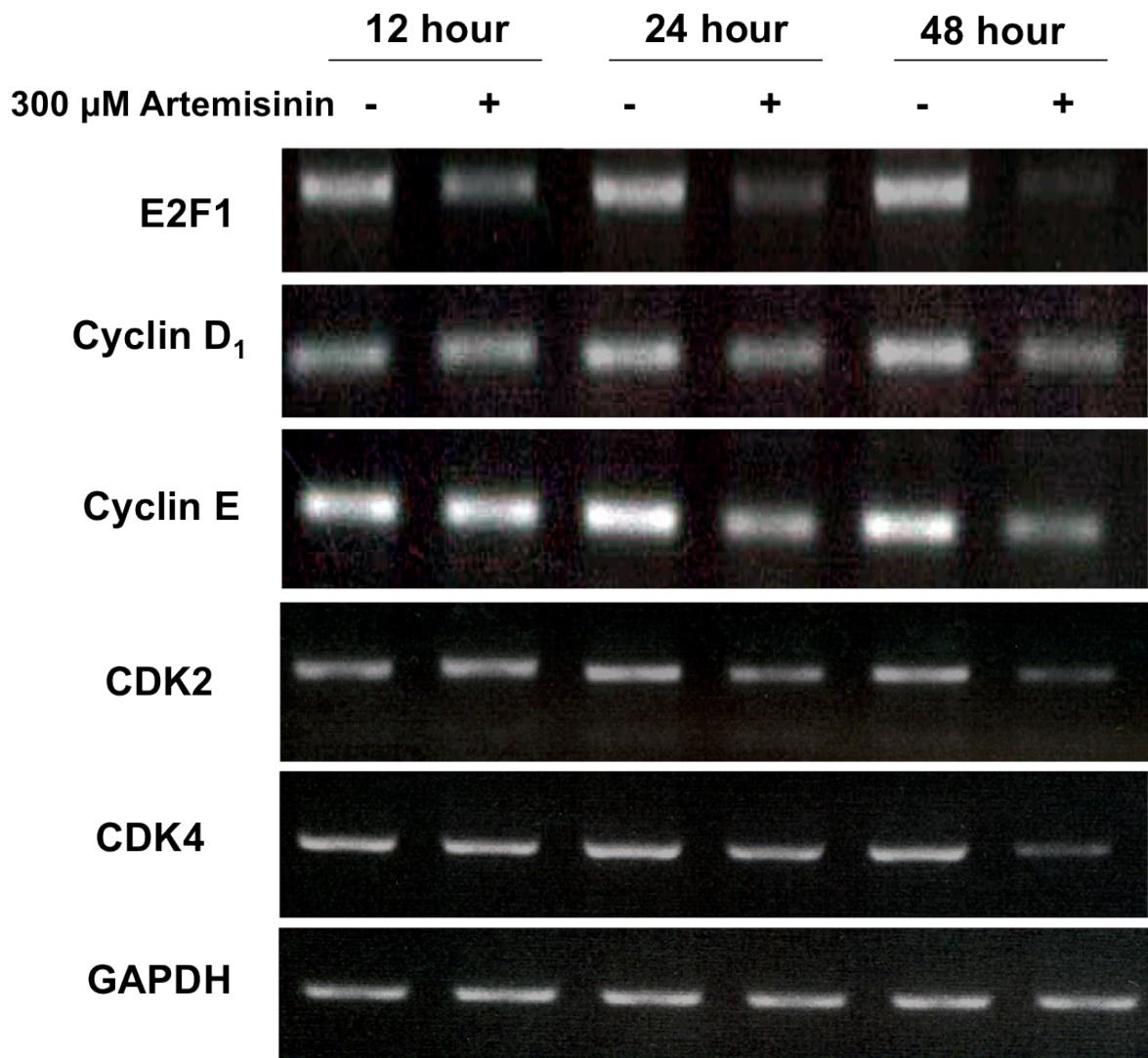
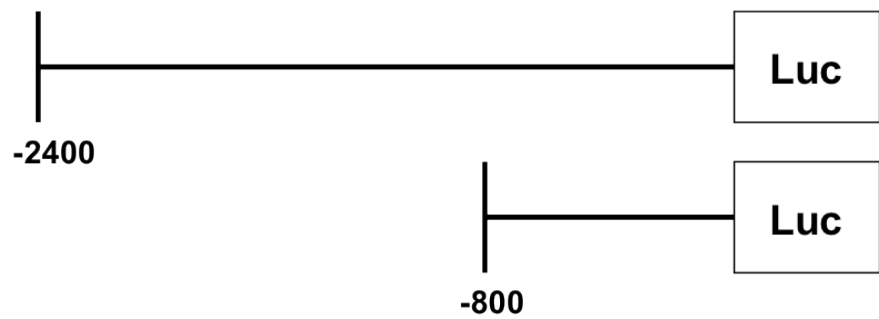
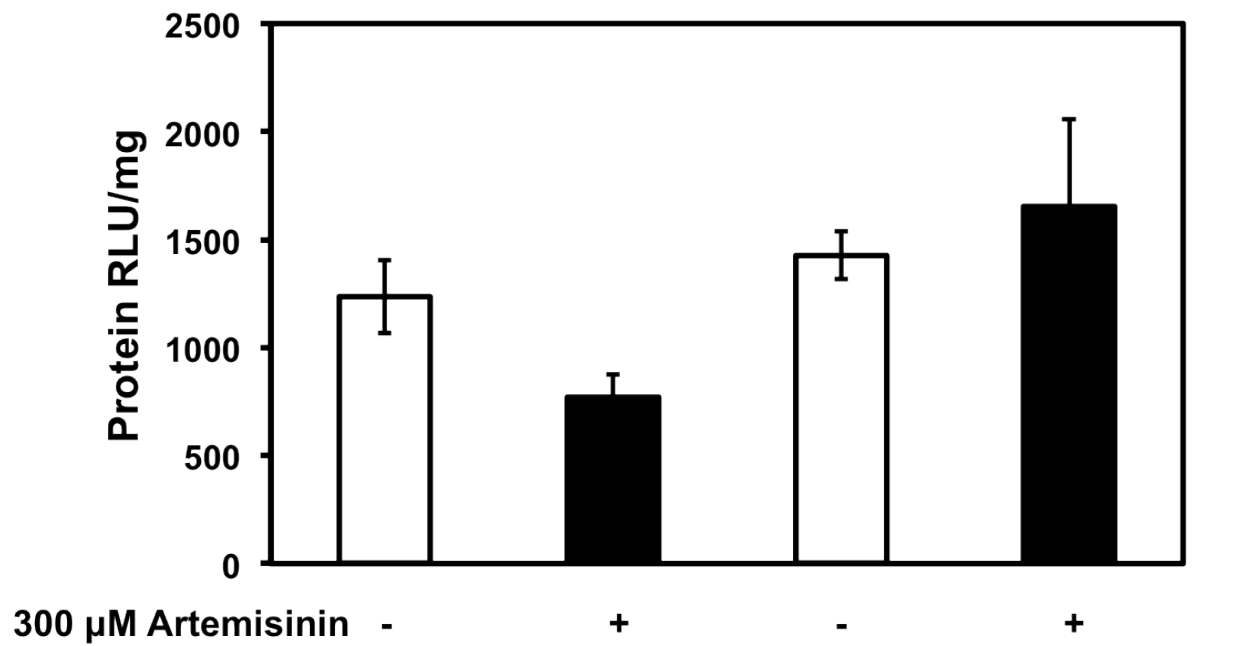


Figure 39

Artemisinin regulates CDK2 promoter activity.

MCF-7 cells were transfected with either of the two indicated CDK2 promoter luciferase reporter plasmids (5' ends of either -2400 bp or -800 bp), treated with or without 300 μ M artemisinin for 24 h, and assayed for luciferase activity. The luciferase assay baseline was determined by the level of activity observed in the presence of 1 mg/mL of the general polymerase II transcription inhibitor actinomycin D (1 mg/ml)

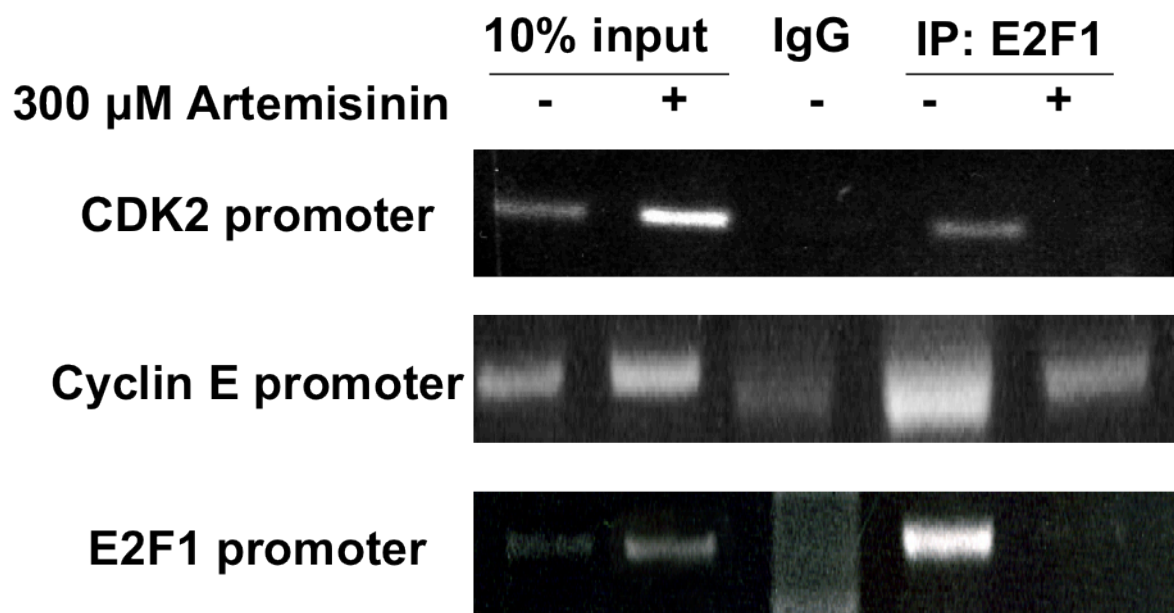


Analysis of consensus transcription factor binding sites within the relatively large artemisinin-regulated region of the CDK2 promoter (-2400 to -800) using the Transfac program revealed the presence of several transcription factor consensus binding sites within the artemisinin regulated region of the CDK2 promoter including a single E2F binding site at -1117 bp from the transcriptional start. The relatively rapid artemisinin down-regulation of E2F1 gene expression suggested that the control of E2F1 levels could potentially play an important role in the artemisinin inhibition of CDK2 promoter activity. In addition, both the Cyclin E promoter and the E2F1 promoter itself contain consensus sites for the E2F1 transcription factor. Chromatin immunoprecipitation was used to directly determine whether artemisinin disrupts the endogenous interactions of E2F1 with the CDK2, Cyclin E and E2F1 promoters (Figure 40). MCF-7 cells were treated with or without 300 μ M artemisinin for 48 hours, and the genomic fragments cross-linked to protein were immunoprecipitated with anti-E2F1 antibodies, or with an IgG control antibody. Primers specific to each of the tested promoters revealed that artemisinin nearly ablated the endogenous binding of E2F1 to its binding sites on the CDK2 promoter (-1117 bp from start site), cyclin E promoter (-1614 bp and -1659 from start site) and the E2F1 promoter (-15 bp from start site). 10% input was used as a loading control.

Figure 40

Loss of the E2F1 signaling inhibits CDK2, Cyclin E, and E2F1 promoter activity.

Chromatin immunoprecipitation (ChIP): MCF-7 cells were treated with or without 300 μ M artemisinin for 24 hour, fixed and subjected to chromatin immunoprecipitation (ChIP) with E2F1 antibody followed by PCR of the E2F1 consensus binding sites in the CDK2, cyclin E, and E2F1 gene promoters. Ten percent input served as the loading control. IgG, immunoglobulin G. IP, immunoprecipitated.



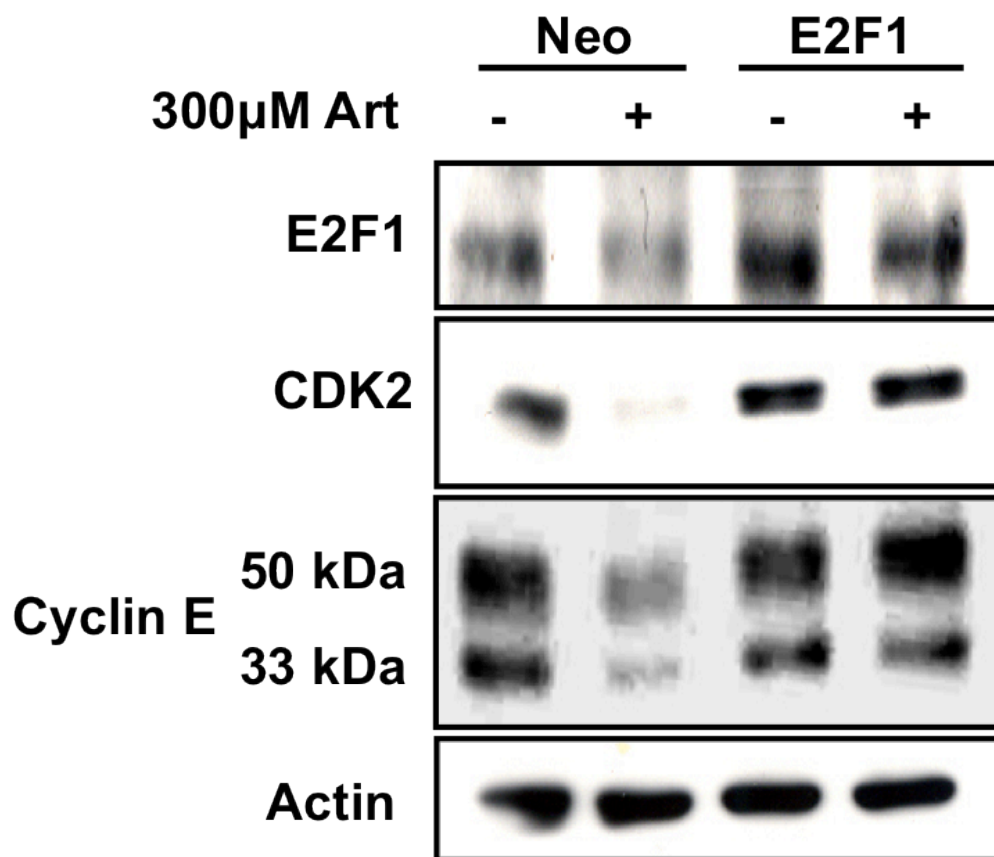
Expression of exogenous E2F1 reverses the artemisinin down regulation of CDK2 and Cyclin E expression and the G1-cell cycle arrest.

The ChIP analysis implicates that the disruption of E2F1 interactions with the CDK2 and cyclin E promoters directly leads to the loss of CDK2 and cyclin E gene expression, resulting in a G1 cell cycle arrest. To functionally test the significance of artemisinin down regulation of E2F1 gene expression, MCF-7 cells were transfected with either a constitutive E2F1 expression plasmid (pCMV-E2F1) or with an empty expression vector (pCMV-neo) as a transfection control, and the cells were then treated with or without 300 μ M artemisinin for 48 hours. Western blot analysis revealed that in MCF-7 cells transfected with the constitutive E2F1 expression vector, the total levels of E2F1 protein remained unchanged in the presence or absence of artemisinin. Importantly, artemisinin failed to down-regulate CDK2, cyclin E in cells expressing the exogenous E2F1, whereas, in the empty vector transfected cells, artemisinin strongly inhibited production of CDK2, cyclin E and E2F1 (Figure 41). These results demonstrate that the artemisinin down-regulation of E2F1 levels is required for the artemisinin down-regulation of CDK2 and cyclin E levels.

Figure 41

Constitutive expression of E2F1 overrides artemisinin-mediated downregulation of cyclin E and CDK2.

MCF-7 cells were transfected with the empty expression vector (Neo) or constitutive expression vector for E2F1 (E2F1), and treated with or without 300 μ M artemisinin for 48 hours. The total cell extracts were electrophoretically fractionated and the levels of E2F1, CDK2, and cyclin E analyzed by western blots. The level of actin protein was used as a gel loading control.

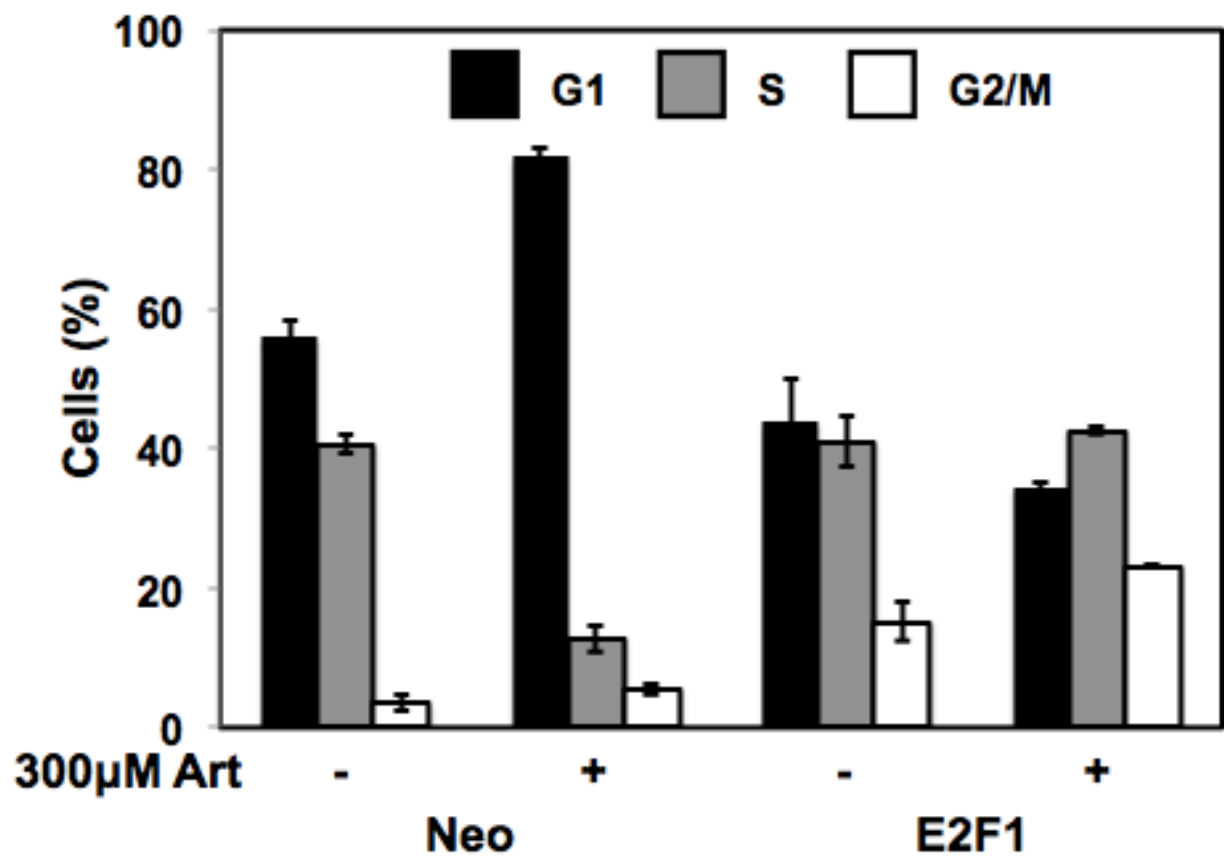


To examine effects on cell cycle progression, the cell population DNA contents of transfected cells treated with or without artemisinin were analyzed by flow cytometry. As shown in Figure 42, control transfected cells (Neo) showed a robust artemisinin mediated cell cycle arrest that displayed a significant increase in the number of cells in the G₁ phase. In contrast, in cells constitutively expressing exogenous E2F1, artemisinin treatment failed to induce a G₁ cell cycle arrest. In transfected cells ectopically expressing elevated levels of E2F1, both artemisinin treated and untreated cells, the number of cells with a G₁ DNA content remained at approximately 40%, while in both conditions a significant fraction of cell population displayed an S phase DNA content (Figure 42) that is indicative of rapidly proliferating cells. These results show that the down-regulation of E2F1 transcription factor levels is required for the artemisinin induced G₁ cell cycle arrest of MCF-7 human breast cancer cells, which as uncovered a new transcriptional pathway that is targeted by this phytochemical.

Figure 42

Constitutive expression of E2F1 prevents artemisinin induced G1 cell cycle arrest.

The cell population DNA content and cell cycle phase of MCF-7 cells transfected with the empty expression vector (Neo) or constitutive expression vector for E2F1 (E2F1) were analyzed after treatment with 300 μ M artemisinin for 48 hours. Breast cancer cells were treated with or without 300 μ M artemisinin for 48 hours and the cell population DNA contents quantified by flow cytometry after staining with propidium iodide. The results are an average of independent triplicate results. The average error was approximately between $\pm 1\%$ and $\pm 2\%$ for each of the results.



DISCUSSION

Artemisinin, an antimalarial phyto sesquiterpene lactone, has been shown to have antiproliferative effects in a variety of cellular and animal models of cancer (19, 30), and in several of the tested systems, artemisinin or its derivatives were shown to modulate transcriptional and/or cell signaling pathways (31). We have observed that artemisinin exerts a potent G1 cell cycle arrest of cultured MCF-7 human breast cancer cells as well as strongly inhibit the growth of MCF-7 cell-derived tumor xenografts *in vivo*. One of the earliest responses to artemisinin treatment was the decline in levels of the E2F1 transcription factor, which was followed by the loss in expression of several key G1 acting cell cycle genes. Artemisinin was shown to disrupt the binding of E2F1 to the CDK2 and cyclin E promoters, resulting in the loss of expression of both cell cycle genes and triggering a G1 block in cell cycle progression. The constitutive expression of exogenous E2F1 prevented the artemisinin down regulation of both CDK2 and cyclin E expression as well as precluded the G1 cell cycle arrest which functionally demonstrates the critical role of E2F1 as a downstream target of artemisinin antiproliferative signaling in human breast cancer cells. The CDK2-cyclin E complex is known to hyperphosphorylate Rb leading to release of E2F1, which then increases transcription of CDK2 and cyclin E (32). In addition, the hyperphosphorylated Rb leads to an increase in E2F1 gene expression because the E2F1 promoter binds preferentially to the E2F1/E2F3 members of this transcription factor family, which drives transcription of the gene (33). Because artemisinin rapidly down-regulates E2F1 expression and its CDK2 and cyclin E target genes, we propose that artemisinin mediates its antiproliferative response by disrupting an E2F1 auto-regulatory loop that reduces E2F1 levels and triggers a G1 block in cell cycle progression.

In MCF-7 breast cancer cells, the most significant effects of artemisinin on expression of cell cycle genes was the strong down regulation of CDK2, CDK4, cyclin E, cyclin D1, whereas, expression of the other main G1 acting cell cycle genes remained relatively unchanged. The disrupted expression of this set of cell cycle genes is likely critical for the anticancer effects of artemisinin and related compounds. Expression of CDK2, CDK4, cyclin D1 and cyclin E have been strongly associated with increased breast cancer recurrence, and overexpression of CDK2 correlated positively with lymph node metastasis (34). Other studies have implicated CDK2 enzymatic activity in mediating Sp1 phosphorylation and consequently matrix metalloproteinase 2 (MMP-2) expression (35). Similar effects have been reported with another potent anticancer phytochemical indole-3-carbinol, which attenuates CDK2 activity and MMP-2 expression (36, 37). Elevated expression of cyclin E has also been shown to correlate with poorer prognosis, increased genomic instability, as well as higher grade of tumors (38). Also, the percentage of E2F1 positive cells increased positively with increasing stages of breast cancer (39), which likely controls the expression levels of CDK2 and cyclin E in the late stage cancers.

We uncovered direct evidence that the loss of CDK2 and cyclin E expression was due to the disruption of E2F1 binding to both promoters, and we are currently attempting to identify the artemisinin regulated transcription factor(s) that account for the loss of cyclin D1 and CDK4 expression. In this regard, cyclin D1 expression is maintained in an estrogen

receptor alpha (ER α) dependent manner in estrogen responsive breast cancer cells, and artemisinin down regulated ER α promoter activity (40) suggesting that the loss of cyclin D1 expression is likely linked to the down regulation of ER α expression. We also previously reported that the artemisinin induced G1 cell cycle arrest of LNCaP prostate cancer cells was controlled by the ablation of CDK2 and CDK4 expression and that down regulated of CDK4 promoter activity was due to the artemisinin mediated inhibition of cellular Sp1 activity (24). Consistent with our results, artemisinin has been shown to induce a G1 cell cycle arrest of cultured liver cancer cells by down-regulating CDK2, CDK4, cyclin D1 and cyclin E (23); however, the mechanism of down-regulation of these cell cycle gene was not investigated. In pancreatic cancer cells (41), human colon cancer cells (42), and in leukemia (43) the artemisinin mediated growth arrest is associated with the down regulation of the NF κ B transcription factor, although the critical target genes were not functionally characterized. Taken together, an emerging concept is that artemisinin based compounds mediate key features of their anticancer responses through the transcriptional down regulation of genes directly involved in cellular proliferation and/or cell survival.

Artemisinin was more effective in triggering a proliferative arrest of tumorigenic breast cancer cell lines (MCF-7, MDA-MB-231, and MCF-10AT) compared to a nontumorigenic cell line (MCF-10A) that was resistant to artemisinin. The MCF-7 breast cancer cells represent a relatively early stage estrogen responsive breast cancer phenotype, whereas, MDA-MB-231 cells represent a steroid independent late stage cancer phenotype (44). This observation showed that artemisinin's efficacy did not depend on the cellular expression of ER α because MDA-MB-231 cells have a silenced ER α expression due to promoter hypermethylation (45). The artemisinin sensitive MCF-10AT cells, which have a preneoplastic phenotype that can form tumors at a low rate in vivo (46), were derived from the artemisinin resistant MCF-10A cells, which are a nontumorigenic pseudo-diploid breast cell line (47). The selectivity of artemisinin to cancerous cells has been observed in other tissue types. For example, the leukemic cell line Molt4 is sensitive to artemisinin, but normal primary lymphocytes are resistant to this phytochemical (48). Similar differences in artemisinin sensitivity were observed with ovarian cancer cells compared to normal ovarian epithelial cells (49). The selectivity that artemisinin exhibits in exerting a growth arrest is a major asset to its potential as a cancer management strategy. This study also presents artemisinin as an effective mitostatic phytochemical in early breast cancer preneoplastic cell line, providing a promising candidate for breast cancer prevention. Thus, artemisinin and its related derivatives represent promising anticancer therapeutic molecules for a variety of human cancer cell types because of their selective modulation of expression and activity of key transcription factors that affect expression of specific cell cycle regulators.

REFERENCES

1. Cianfrocca M & Gradishar W (2009) New molecular classifications of breast cancer. *CA: a cancer journal for clinicians* 59(5):303-313.
2. Perou CM, *et al.* (2000) Molecular portraits of human breast tumours. *Nature* 406(6797):747-752.
3. Fuqua SA, *et al.* (1991) Variant human breast tumor estrogen receptor with constitutive transcriptional activity. *Cancer research* 51(1):105-109.
4. Darbre PD & Daly RJ (1990) Transition of human breast cancer cells from an oestrogen responsive to unresponsive state. *The Journal of steroid biochemistry and molecular biology* 37(6):753-763.
5. Stingl J & Caldas C (2007) Molecular heterogeneity of breast carcinomas and the cancer stem cell hypothesis. *Nature reviews. Cancer* 7(10):791-799.
6. Wang T, You Q, Huang FS, & Xiang H (2009) Recent advances in selective estrogen receptor modulators for breast cancer. *Mini reviews in medicinal chemistry* 9(10):1191-1201.
7. Abdulhaq H & Geyer C (2008) Safety of adjuvant endocrine therapy in postmenopausal women with breast cancer. *American journal of clinical oncology* 31(6):595-605.
8. Arslan C, Dizdar O, & Altundag K (2009) Pharmacotherapy of triple-negative breast cancer. *Expert opinion on pharmacotherapy* 10(13):2081-2093.
9. Aapro M, Monfardini S, Jirillo A, & Basso U (2009) Management of primary and advanced breast cancer in older unfit patients (medical treatment). *Cancer treatment reviews* 35(6):503-508.
10. Scott EN, Gescher AJ, Steward WP, & Brown K (2009) Development of dietary phytochemical chemopreventive agents: biomarkers and choice of dose for early clinical trials. *Cancer Prev Res (Phila)* 2(6):525-530.
11. Brasseur P, *et al.* (2011) Changing patterns of malaria during 1996-2010 in an area of moderate transmission in southern Senegal. *Malaria journal* 10:203.
12. Kappagoda S, Singh U, & Blackburn BG (2011) Antiparasitic therapy. *Mayo Clinic proceedings. Mayo Clinic* 86(6):561-583.
13. Meshnick SR (2002) Artemisinin: mechanisms of action, resistance and toxicity. *International journal for parasitology* 32(13):1655-1660.
14. Efferth T, Dunstan H, Sauerbrey A, Miyachi H, & Chitambar CR (2001) The anti-malarial artesunate is also active against cancer. *International journal of oncology* 18(4):767-773.
15. Tan W, *et al.* (2011) Anti-cancer natural products isolated from chinese medicinal herbs. *Chinese medicine* 6(1):27.
16. Stockwin LH, *et al.* (2009) Artemisinin dimer anticancer activity correlates with heme-catalyzed reactive oxygen species generation and endoplasmic reticulum stress induction. *International journal of cancer. Journal international du cancer* 125(6):1266-1275.
17. Efferth T (2006) Molecular pharmacology and pharmacogenomics of artemisinin and its derivatives in cancer cells. *Current drug targets* 7(4):407-421.

18. Efferth T (2007) Willmar Schwabe Award 2006: antiplasmodial and antitumor activity of artemisinin--from bench to bedside. *Planta medica* 73(4):299-309.
19. Firestone GL & Sundar SN (2009) Anticancer activities of artemisinin and its bioactive derivatives. *Expert reviews in molecular medicine* 11:e32.
20. Meshnick SR, Thomas A, Ranz A, Xu CM, & Pan HZ (1991) Artemisinin (qinghaosu): the role of intracellular hemozoin in its mechanism of antimalarial action. *Molecular and biochemical parasitology* 49(2):181-189.
21. Bustos MD, Gay F, & Diquet B (1994) In-vitro tests on Philippine isolates of Plasmodium falciparum against four standard antimalarials and four qinghaosu derivatives. *Bulletin of the World Health Organization* 72(5):729-735.
22. Efferth T, Olbrich A, & Bauer R (2002) mRNA expression profiles for the response of human tumor cell lines to the antimalarial drugs artesunate, artemether, and artemether. *Biochemical pharmacology* 64(4):617-623.
23. Hou J, Wang D, Zhang R, & Wang H (2008) Experimental therapy of hepatoma with artemisinin and its derivatives: in vitro and in vivo activity, chemosensitization, and mechanisms of action. *Clinical cancer research : an official journal of the American Association for Cancer Research* 14(17):5519-5530.
24. Willoughby JA, Sr., et al. (2009) Artemisinin blocks prostate cancer growth and cell cycle progression by disrupting Sp1 interactions with the cyclin-dependent kinase-4 (CDK4) promoter and inhibiting CDK4 gene expression. *The Journal of biological chemistry* 284(4):2203-2213.
25. Lacroix M & Leclercq G (2004) Relevance of breast cancer cell lines as models for breast tumours: an update. *Breast cancer research and treatment* 83(3):249-289.
26. Levenson AS & Jordan VC (1997) MCF-7: the first hormone-responsive breast cancer cell line. *Cancer research* 57(15):3071-3078.
27. Lai H & Singh NP (1995) Selective cancer cell cytotoxicity from exposure to dihydroartemisinin and holotransferrin. *Cancer letters* 91(1):41-46.
28. Chen HH, Zhou HJ, Wang WQ, & Wu GD (2004) Antimalarial dihydroartemisinin also inhibits angiogenesis. *Cancer chemotherapy and pharmacology* 53(5):423-432.
29. He Y, et al. (2011) The anti-malaria agent artesunate inhibits expression of vascular endothelial growth factor and hypoxia-inducible factor-1alpha in human rheumatoid arthritis fibroblast-like synoviocyte. *Rheumatology international* 31(1):53-60.
30. Posner GH, et al. (2004) Anticancer and antimalarial efficacy and safety of artemisinin-derived trioxane dimers in rodents. *Journal of medicinal chemistry* 47(5):1299-1301.
31. Efferth T, et al. (2003) Molecular modes of action of artesunate in tumor cell lines. *Molecular pharmacology* 64(2):382-394.
32. Zetterberg A, Larsson O, & Wiman KG (1995) What is the restriction point? *Current opinion in cell biology* 7(6):835-842.
33. Araki K, Nakajima Y, Eto K, & Ikeda MA (2003) Distinct recruitment of E2F family members to specific E2F-binding sites mediates activation and repression of the E2F1 promoter. *Oncogene* 22(48):7632-7641.
34. Bonin S, Brunetti D, Benedetti E, Gorji N, & Stanta G (2006) Expression of cyclin-dependent kinases and CDC25a phosphatase is related with recurrences and

- survival in women with peri- and post-menopausal breast cancer. *Virchows Archiv : an international journal of pathology* 448(5):539-544.
35. Wang CH, Chang HC, & Hung WC (2006) p16 inhibits matrix metalloproteinase-2 expression via suppression of Sp1-mediated gene transcription. *Journal of cellular physiology* 208(1):246-252.
 36. Garcia HH, Brar GA, Nguyen DH, Bjeldanes LF, & Firestone GL (2005) Indole-3-carbinol (I3C) inhibits cyclin-dependent kinase-2 function in human breast cancer cells by regulating the size distribution, associated cyclin E forms, and subcellular localization of the CDK2 protein complex. *The Journal of biological chemistry* 280(10):8756-8764.
 37. Hung WC & Chang HC (2009) Indole-3-carbinol inhibits Sp1-induced matrix metalloproteinase-2 expression to attenuate migration and invasion of breast cancer cells. *Journal of agricultural and food chemistry* 57(1):76-82.
 38. Sieuwerts AM, *et al.* (2006) Which cyclin E prevails as prognostic marker for breast cancer? Results from a retrospective study involving 635 lymph node-negative breast cancer patients. *Clinical cancer research : an official journal of the American Association for Cancer Research* 12(11 Pt 1):3319-3328.
 39. Zhang SY, *et al.* (2000) E2F-1: a proliferative marker of breast neoplasia. *Cancer epidemiology, biomarkers & prevention : a publication of the American Association for Cancer Research, cosponsored by the American Society of Preventive Oncology* 9(4):395-401.
 40. Sundar SN, Marconett CN, Doan VB, Willoughby JA, Sr., & Firestone GL (2008) Artemisinin selectively decreases functional levels of estrogen receptor-alpha and ablates estrogen-induced proliferation in human breast cancer cells. *Carcinogenesis* 29(12):2252-2258.
 41. Chen H, *et al.* (2010) Growth inhibitory effects of dihydroartemisinin on pancreatic cancer cells: involvement of cell cycle arrest and inactivation of nuclear factor-kappaB. *Journal of cancer research and clinical oncology* 136(6):897-903.
 42. Riganti C, *et al.* (2008) Activation of nuclear factor-kappa B pathway by simvastatin and RhoA silencing increases doxorubicin cytotoxicity in human colon cancer HT29 cells. *Molecular pharmacology* 74(2):476-484.
 43. Wang Y, *et al.* (2011) The anti-malarial artemisinin inhibits pro-inflammatory cytokines via the NF-kappaB canonical signaling pathway in PMA-induced THP-1 monocytes. *International journal of molecular medicine* 27(2):233-241.
 44. Antalis CJ, Uchida A, Buhman KK, & Siddiqui RA (2011) Migration of MDA-MB-231 breast cancer cells depends on the availability of exogenous lipids and cholesterol esterification. *Clinical & experimental metastasis* 28(8):733-741.
 45. Ferguson AT, *et al.* (1997) Role of estrogen receptor gene demethylation and DNA methyltransferase.DNA adduct formation in 5-aza-2'deoxyctidine-induced cytotoxicity in human breast cancer cells. *The Journal of biological chemistry* 272(51):32260-32266.
 46. Worsham MJ, *et al.* (2006) High-resolution mapping of molecular events associated with immortalization, transformation, and progression to breast cancer in the MCF10 model. *Breast cancer research and treatment* 96(2):177-186.

47. Soule HD, *et al.* (1990) Isolation and characterization of a spontaneously immortalized human breast epithelial cell line, MCF-10. *Cancer research* 50(18):6075-6086.
48. Lai H, Sasaki T, Singh NP, & Messay A (2005) Effects of artemisinin-tagged holotransferrin on cancer cells. *Life sciences* 76(11):1267-1279.
49. Jiao Y, *et al.* (2007) Dihydroartemisinin is an inhibitor of ovarian cancer cell growth. *Acta pharmacologica Sinica* 28(7):1045-1056.

Chapter IV

Conclusion and Future Directions

CONCLUSION AND FUTURE DIRECTIONS

Breast cancer is such a complex disease to diagnose, study, and treat because it manifests with multiple distinct phenotypes, each with its own set of symptoms and respond to therapeutic treatments with varying levels of success. For example, selective estrogen receptor modulators (SERMs) are more effective at targeting estrogen sensitive breast cancers while immunotherapies may be used to target HER2 overexpressing breast cancers. This makes characterizing the phenotype of each distinct breast cancer subset ever more important to develop prognostic markers for better treatment alternatives and reach the end goal of personalized medicine.

In the rapidly evolving field of cancer stem cell biology, the characterization of cancer stem cells as a subset of a tumor population with unique biological and genetic properties will profoundly impact the convention of diagnosing, treating, and preventing cancer. The very idea of the existence of cancer stem cells has changed the way chemotherapeutic and radiation therapies are used to target cancer cells. It is important however to keep in mind that the field is still in its infancy. It is too early to take much of what has been hypothesized and determined for a single cancer and use it as a dogma.

With regards to breast cancer stem cells, full and proper characterization still remains a hurdle that must be overcome. The ectopic expression of HER2 in MCF-10AT cells resulted in the phenotypic expression of surface markers CD44⁺/CD24⁻ and maintained active ALDH-1 and nucleostemin. Furthermore, these cells are capable of forming tumorspheres in suspension cultures as well as tumors xenografts of athymic NIH III mice. While these traits may not be the only criteria necessary for the stable expression of breast cancer stem cells, it certainly provides distinguishable characteristics for a population highly enriched in breast cancer stem cells. Also, it is still unclear as to the role of HER2 signaling and expression in mediating the genetic and epigenetic changes necessary to generate breast cancer stem cells.

The identification of breast cancer stem cells sets up an interesting therapeutic question as to the potential targets that can disrupt breast cancer stem cell maintenance, viability, and proliferation. This research demonstrates that I3C selectively targets breast cancer stem cells through the disruption of nucleostemin activation and signaling. I3C promotes the interaction and sequestration of MDM2 by nucleostemin. Also, this alters the steady state equilibrium between MDM2 and p53 to induce apoptosis. I3C represents a powerful therapeutic as a small molecule phytochemical because it is cheap to produce and patients have a high tolerance to I3C given that it is already a component in the human diet. While I3C targets nucleostemin it is still unclear as to how nucleostemin activity is modulated. For example, I3C may disrupt a kinase or phosphatase that targets nucleostemin thereby altering its activation. Other potential targets of nucleostemin may be regulated by I3C as well. For example, it has been shown that nucleostemin and telomerase, a known target of I3C, can form a complex and the cellular consequence of I3C inhibition on both telomerase and nucleostemin remains unknown.

Other areas of potential investigation are predicated on the ability of I3C to inhibit estrogen receptor alpha (ER α). Previous studies have shown that the downregulation of ER α by I3C disrupts telomerase activity. Furthermore, estradiol (E2) the ligand for ER α has been shown to upregulate nucleostemin levels. Elucidating if and how I3C regulates ER α , telomerase, and nucleostemin signaling may lead to further potential therapeutic targets against breast cancer stem cells. Finally, one area of study that needs to be addressed is the role of HER2 on breast cancer stem cells. It is still unclear if constitutive HER2 overexpression is required for cancer stem cells maintenance. For example, an unexplored area would be to investigate the effects of commercially available inhibitors of HER2 on breast cancer stem cells. Given that HER2 overexpression induced the breast cancer stem cell phenotype, an area of interest would be to investigate the breast cancer stem cell phenotype with 10AT-Her2 cells treated with immunotherapy inhibitors such as Trastuzumab (Herceptin). An open question to be discovered is if HER2 induces permanent genetic and epigenetic changes or if its constitutive expression is necessary for breast cancer stem cells. Furthermore, looking at other HER2 regulated pathways such as the MAPK pathway will become more important with increased study of breast cancer stem cells.

Determining the molecular mechanism of action for I3C induced proteolytic degradation of Akt1 in 10AT-Her2 cells will help identify biomarkers that may be useful for characterizing the true nature of breast cancer stem cells. I3C dependent downregulation of Akt1 only occurred at the protein level indicating an alteration in protein stability. While data presented only examines the effects of Akt1 on MDM2 phosphorylation, there are numerous targets of Akt1 phosphorylation such as FOXO transcription factors, mTOR, B-Raf, BRCA1, and Bcl-xL. These downstream effector targets have not been studied in the 10AT-Her2 model system and many of them may also directly impact apoptotic response we observe. Furthermore, nucleostemin activation can also lead to many downstream genetic changes. Nucleostemin has multiple binding partners such as p14^{ARF} and telomerase and it is highly probably that I3C will alter the interactions of nucleostemin with its other binding partners as well. It will be especially interesting to see how I3C may affect nucleostemin and telomerase interaction, as I3C is known to directly alter the signaling of both proteins. In addition, what functional consequence I3C has on nucleostemin and telomerase remains to be seen.

The small molecule phytochemical artemisinin has been extensively used as a potent antimalarial agent. As an antimalarial agent, the mechanism of action of artemisinin is to initiate a series of redox reaction and to a certain extent this same mechanism is thought to inhibit cancer cell proliferation. Chapter III of this thesis begins to elucidate previously unknown mechanisms in which artemisinin functions. Artemisinin has been shown to transcriptionally downregulate E2F1 and as a result of the loss of the E2F1 transcription factor, decrease promoter activity in both cyclin E as well as CDK2. Furthermore, E2F1 is capable of autoregulation where the E2F1 transcription factor promotes the transcription of more E2F1. Thus, following the initial loss of E2F1 by artemisinin, E2F1 may downregulate itself; however, at present it is still unclear how artemisinin induces the initial loss of E2F1. As a cancer therapy, it will be critical to establish at what level is E2F1 initially regulated by artemisinin. Another area that has not

been addressed is how artemisinin regulates other G1 cell cycle regulators such as cyclin D1 and CDK4. There are no known E2F1 binding sites regulating the transcription and translation of cyclin D1 and CDK4 suggesting there are other signaling pathways regulated by artemisinin. Once these signaling pathways are characterized, novel prognostic biomarkers may be identified that artemisinin may be well suited to treat as an effective anticancer therapy.

Taken together, the small molecule phytochemicals I3C and artemisinin represent an emerging class of chemicals with extensive clinical relevance. Each of these respective phytochemicals have shown to tightly regulate model systems representing breast cancer stem cells and luminal A, estrogen sensitive breast cancer. Finally, the establishment of the 10AT-Her2 cancer stem cell model system provides a direct way to test stable populations of cells highly enriched with tumor initiating cells. Creating a unique system to study breast cancer stem cells has profound implications for the diagnosis and treatment of breast cancer. This thesis highlights the significance of breast cancer stem cells as well as provides direct evidence for which two small molecule phytochemicals exert their anticancer properties.